MULTI-USER MULTI-ANTENNA COOPERATIVE CELLULAR SYSTEMS

by

Yi Zheng

A thesis submitted to the
Department of Electrical and Computer Engineering
in conformity with the requirements
for the degree of Doctor of Philosophy

Queen's University
Kingston, Ontario, Canada
June, 2013

Abstract

To meet the very high data rate requirements for wireless Internet and multimedia services, cooperative systems with multiple antennas have been proposed for future generation wireless systems. In this thesis, we focus on multiple antennas at the source, relay and destination.

We study both downlink and uplink cooperative systems with single antenna relays. For downlink systems, the optimal precoder to minimize the sum transmit power subject to quality of service (QoS) constraints with fixed relay weights is derived. We also study the optimization of relay weights with a fixed precoder. An iterative algorithm is developed to jointly optimize the precoder and relay weights. The performance of the downlink system with imperfect CSI as well as multiple receive antennas is also studied.

For the uplink system, we similarly derive the optimum receiver as in the downlink with fixed relay weights. The optimization of relay weights for a fixed receiver is then studied. An iterative algorithm is developed to jointly optimize the receiver and relay weights in the uplink. Systems with imperfect channel estimation are also considered.

The study of cooperative MIMO systems is then extended to a multi-cell scenario. In particular, two scenarios are studied. In the first, the cells coordinate their beamformers to find the most suitable cell to serve a specific user. In the second, each base station selectively transmits to a fixed group of users, and the cells coordinate to suppress mutual interference.

Finally, our investigation culminates with a study of an uplink cooperative system equipped with multi-antenna relays under a capacity maximization criterion. The specific scheme that users access the base station through a single multi-antenna relay are studied. Iterative capacity maximization algorithm are proposed and shown to converge to local maxima. Numerical results are presented to highlight that the algorithms are able to come close to these bounds after only a few iterations.

Acknowledgments

I can never thank my thesis advisor Prof. Steven D. Blostein enough for his guidance, technical advice, encouragement, kindness, great patience and considerations as well as financial support during my Ph.D. study. Without Prof. Blostein's tremendous efforts and help, I would not be able to accomplish my Ph.D study.

I would like to thank Prof. Fady Alajaji and Prof. Glen Takahara of Department of Mathematics and Statistics for their kind help, support and great considerations.

I would like to thank Dr. Jinsong Wu, for his consistent support and kind help.

I would like to thank Prof. Il-Min Kim, for his teaching and suggestions.

I would like to thank my friends Prof. Qingguo Li, Pastor Xiaofeng Zhang, Mrs. Xiaohui Zhang, Dr. Tong Jin, Dr. Huayong Chen, Mr. Shiqi Chen, Pastor. Lo Kong at Kingston Chinese Alliance Church and other friends in Kingson Chinese Allicance Church.

I would like to thank Pastor Mitchell Persaud, Nathen Kidd and other friends in New Horizon Christian Church.

I thank all my lab-mates Dr. Yu Cao, Dr. Hani Mehrpouyan and Dr. Minhua Ding for their friendship and all the good time we had together.

In particular I can never thank my wife and parents enough for their patience and encouragements through all these years.

Above all, I would praise God for his work on me and leading me through this journey with all

the lessons for me.

This work is in part sponsored by Defense R & D Canada through the Defense Research Program at the Communications Research Centre Canada, Graduate Awards from Queen's University. Their financial support is greatly appreciated.

Contents

List of Figures

Acronyms

SDMA	Spatial Division Multiple Access
AWGN	Additive White Gaussian Noise
SDP	Semi-definite Programming
CSI	Channel State Information
i.i.d.	independent and identically distributed
MIMO	Multiple-Input Multiple-Output
MLE	Maximum-Likelihood Estimator
LLF	Log-Likelihood Function
LMMSE	Least Minimum Mean-Square Error
DRBF	Dirstributed Relay Beam Former
AF	Amplify and Forward
DF	Decode and Forward
LTE	Long Term Evolution
SINR	Signal-to-Interference Noise Ratio
SPW	Scheduling Priority Weight
GBR	Guaranteed Bit Rate
Qos	Quality of Service
SVD	Singular Value Decomposition

LTE-A	Long Term Evolution-Advanced
AP	Access point

List of Important Symbols

$(\cdot)^T$	Matrix or vector transpose
$(\cdot)^*$	Complex conjugate
$(\cdot)^\dagger$	Matrix of vector conjugate transpose
$\otimes$	Kronecker product
$*$	Signal convolution
$\Gamma(x)$	Gamma function
$\boldsymbol{\Lambda}_N$	Temporal interference correlation matrix
C	Channel information capacity
$\det(\cdot)$	Determinant of a matrix
$\mathrm{E}\{\cdot\}$	Expectation of random variables
$\boldsymbol{H}$	MIMO channel matrix of the desired user
$\mathscr{H}(\cdot)$	Entropy
$\boldsymbol{I}_N$	$N \times N$ identity matrix
$\mathfrak{I}(\cdot)$	Imaginary part of a complex number
$\mathscr{I}(\cdot;\cdot)$	Mutual information
$\mathfrak{R}(\cdot)$	Real part of a complex number
$\mathrm{Tr}(\cdot)$	Trace of a matrix

Chapter 1

Introduction

Communication over a wireless channel is highly challenging due to the complex propagation medium. The major impairments of a wireless channel are fading and cochannel interference. Due to ground irregularities and typical wave propagation phenomena such as diffraction, scattering, and reflection, when a signal is radiated into the wireless environment, it arrives at the receiver along a number of distinct paths, and is referred to as a multi-path signal. Each of these paths has a distinct and time-varying amplitude, phase and angle of arrival. These multi-paths may add up constructively or destructively at the receiver. Hence, the received signal parameters may vary over frequency, time, and space. These variations are collectively referred to as fading and deteriorate link quality. Moreover, in cellular systems, to maximize the spectral efficiency and accommodate more users while maintaining minimum quality of service, frequencies have to be reused in different cells that are sufficiently separated. Therefore, a desired user's signal may be corrupted by the interference generated by other users operating at the same frequency.

Multiple users that access the same time-frequency-space resources may achieve signal separation in the spatial domain. In multi-user beamforming, each user's stream is precoded with beamforming weights at the transmitter using some form of user channel state information in order to optimize each user's signal-to-interference and noise ratio (SINR) and, in the process, reduce co-user interference

[2]. Space-division multiple access (SDMA) emerged as a popular technique for next-generation communication systems and has appeared in standards such as IEEE 802.16x and 3GPP LTE.

Array gain [3] is achieved in MIMO systems through the enhancement of average signal-to-noise ratio (SNR) owing to transmission and reception by multiple antennas. Availability of channel state information (CSI) at the transmitter/receiver is necessary to realize transmit/receive array gains.

Diversity [4] is a powerful technique to mitigate fading and increase robustness to interference. Diversity techniques rely on transmitting a data-bearing signal over multiple (ideally) independently fading paths over time/frequency/space. Spatial (i.e., antenna) diversity is particularly attractive when compared to time/frequency diversity since it does not incur an expenditure in transmission time/bandwidth. Space-time coding to exploit spatial diversity gain in point-to-point MIMO channels has been studied extensively [5] [6].

Considering the rapidly increasing demand for high data rate and reliable wireless communications, bandwidth efficient transmission schemes are of great importance. In recent years, user cooperation has attracted increased research interest and has been widely studied. By relaying messages for each other, mobile terminals can provide the final destination receiver with multiple replicas of a signal arriving via different paths. These techniques, known as cooperative diversity [7] [8], are shown to significantly improve network performance through mitigating the detrimental effects of signal fading. Various schemes have been proposed to achieve spatial diversity through user cooperation [7] [9]. The most popular schemes are amplify-and-forward (AF), decode-and-forward (DF), and coded cooperation [10]. A distributed beamforming system with a single transmitter and receiver and multiple relay nodes are studied in [11], and second order statistics of the channel are employed to design the optimal beamforming weights at the relays.

In the communication industry, spectrum efficiency is a critical performance metric due to its high cost for operators and its availability. The use of MIMO concepts has the potential to significantly

increase spectrum efficiency in close range portions of the communication system. In frequency division duplex long term evolution (FDD LTE), four-by-four antenna MIMO products has been deployed in commercial network (Canadian operators like Bell, Telus etc). Base stations are being equipped with more antennas as hardware cost becomes less of a concern for operators compared with spectrum. An obvious trend in the communication industry is to increase spectrum efficiency by deploying more antennas at the base station as well as at user terminals. However, spectrum efficiency decreases with the increase of distance between user terminals and the base station. To mitigate this effect, high transmission power is needed at user terminals. However, high transmission power is not achievable at user terminals due to radiation limits and battery life. In this thesis we propose the application of multiple antenna relays to reduce propagation distances to the user terminals and enable MIMO communication between user terminals and relays and between relays and the base station.

1.1 Motivation and Thesis Overview

The role of the relays discussed above is to establish wireless connections between sources with their respective destinations. If the sources, destinations, and relays are distributed in space, relaying offers multiplexing that allows for multiple source-destination pairs to efficiently share communication resources. A straightforward approach to establish such connections is to have sources transmit their data over orthogonal channels. The relays are then required to receive signals transmitted over each of these channels, and then amplify and forward on the same channel. Each destination then tunes in to its corresponding channel to retrieve data. There are, however, two disadvantages in these orthogonal schemes. The first disadvantage is inefficient use of communication resources: at any time instant, each orthogonal channel is needed to establish the connection between source and

destination. Therefore, if any channel from that source to the relays or those from the relays to the corresponding destination go into deep fade, that specific connection cannot be established. As a result, the corresponding resources including (bandwidth, time slot, code, and power) are being wasted as no other connection in the network can access these resources. The second disadvantage of orthogonal schemes is that the relays would require significant complexity, as for example, in case of orthogonal frequency division multiple access (OFDMA) or code division multiple access (CDMA) schemes. To avoid these disadvantages, in this thesis, we rely on the fact that the different sources and destinations are located at physically different locations and we instead propose a space division multiplexing scheme.

The cooperative scheme in this thesis consists of two phases. In the first phase, sources transmit their data to the relays simultaneously over orthogonal channels. In the second phase, each relay transmits an amplified and phase-adjusted version of its received signal. With perfect or imperfect channel state information, in Chapter 3-5 we calculate the complex gains of the relays such that the total power dissipated by the relays is minimized, and at the same time, SINRs at all destinations are kept above predefined thresholds. In Chapter 6, we instead maximize capacity under power constraints.

Herein a fully synchronous system is considered: for all sources, relays and destinations, time and frequency synchronization is assumed.

In the existing literature, cooperative systems based on a single-antenna source, relay and destination are well studied, but multiple antenna relay system research is less complete. In this thesis, a multiple antenna single-source single-destination system is first studied, with single-antenna relays providing phase-shifting of the signal received at the relays. Previous work [11] [12] studied distributed beamforming systems with multiple source-destination pairs where relays were each

equipped with a single antenna. In this thesis, practical considerations of current cellular wireless communication systems also motivates the proposed uplink distributed beamforming system and downlink distributed system. The uplink system investigated considers single or multi-antenna sources which are mobile users, single or multiple antenna relays, and a multiple-antenna destination which is the base station. The downlink systems investigated consider a multiple-antenna source which is the base station, single-antenna relays and multiple destinations/users where both single-antenna and multiple-antenna mobile users are considered. We remark that it is becoming common for the handsets to be equipped with two antennas. To make our investigation more realistic, the effect of imperfect channel state information (CSI) for both uplink and downlink systems is studied. In this thesis, we study the wireless link between relays and base station because in many actual deployments, either high cost or the requirements of civic regulations preclude wireline transmission between relays and base station. Considering deployment changes and future re-deployment strategies, operators would normally prefer wireless links rather than fixed lines.

Recently, multi-cell cooperative systems attract increased research interest. In this thesis, multi-cell cooperative system coordination is studied in two practical scenarios: 1) There are mobile users and there is a need to choose the best cell, and 2) Due to interference from other cells, each cell with multiple mobile users becomes an interference-limited system and base stations coordinate transmission to suppress interference to users in other cells.

1.2 Thesis Organization

The organization of this thesis is as follows:

In Chapter 2, basic concepts of MIMO data processing and convex optimization are first reviewed, followed by a brief description of cooperative system capacity upper bound and the imperfect channel

model which are used later in this thesis.

In Chapter 3, a downlink cooperative system with multiple single-antenna relays is proposed. We first derive the optimal precoder for fixed relay weights. An iterative algorithm to jointly optimize the precoder and relay weights is proposed and shown to converge to a sub-optimal point. The study is further extended to the case of imperfect CSI case as well as to multi-antenna destinations.

In Chapter 4, an uplink cooperative system with single-antenna relays is proposed. The optimum decoder at the receiver for fixed relay weights is first derived. Then with a fixed decoder, the relay weights are optimized. An iterative algorithm for joint optimization of the relay weights and the decoder is proposed and proven to converge. Extension to imperfect CSI is studied. Numerical results demonstrate the performance of the iterative algorithm.

In Chapter 5, two schemes for multi-cell coordination are studied. In the first scheme, multiple cells transmit the same signal to a user and in the second scheme, each user receives a signal from only one cell. Numerical results are presented for the first scheme.

In Chapter 6, an uplink cooperative system with multiple antennas at the relay is proposed. A specific scenario is studied: users access the base station through a single multi-antenna relay. Numerical results are presented to demonstrate the performance of the proposed iterative algorithms. Capacity maximization criterion is used for the system optimization. Optimal user beamformers are derived with fixed relay beamformer and then the optimal relay beamformer is derived with fixed user beamformers. Iterative algorithms are developed to jointly optimize user beamformers and relay beamformer/beamformers. The performance results are compared with upper bounds on system capacity.

Chapter 7 concludes this thesis and suggests future work.

1.3 Thesis Contributions

The primary contributions of this thesis are briefly summarized as follows:

- In Chapter 3, we proposed a downlink multi-antenna cooperative system. In this system, a multiple-antenna base station transmits to multiple destinations through multiple relays, and the objective is to jointly determine the BS and relay beamformer parameters to minimize the BS transmitter and relay power with quality of service (QoS) constraints. An iterative algorithm is developed to jointly optimize the precoder at the BS and relay weights and is proven to converge. When the CSI is not perfect, a new design method is proposed that takes statistical information about CSI uncertainly into account and is evaluated by comparing the performance to that of a design that assumes perfect CSI. The scheme is further extended to the case of multiple receive antennas at destinations with linear minimum mean square error (LMMSE) receivers.

- In Chapter 4, we proposed an uplink multi-antenna cooperative system. In this system, multiple single-antenna sources access the multi-antenna BS through a group of single-antenna relays, and the objective is to jointly determine the decoder at the BS and minimize the relay power with QoS constraints. An iterative algorithm is developed to jointly optimize the decoder at the BS and the relay weights and is proven to converge. When the CSI is not perfect, the design method takes into account the statistical information about CSI uncertainty and is evaluated by comparing the performance to that of a design that assumes perfect CSI.

- In Chapter 5, we propose a multi-cell cooperative system. In this system, multi-cells each with a multi-antenna BS coordinate the data transmission to a group of users through a group of single-antenna relays. Two schemes are proposed for the following scenarios: 1) multiple cells that send the same signal to a specific user, with weighted sum power minimization as

objective and QoS constraints, the best cell to serve a given user is found, and 2) each specific user is only served by one of the cells to support as many users as possible with weighted sum power minimization as the objective under QoS constraints. Numerical results show that the best serving cell can be found to serve a given user.

- A capacity maximization scheme for uplink cooperative systems is proposed in Chapter 6. In this scheme, multiple users access a BS through a multi-antenna relay. An iterative algorithm to jointly optimize the user beamformers and relay beamformer is derived and proven to converge, which is typically achieved in few iterations. Numerical results show that the performance of the iterative algorithm is very close to the user-relay MIMO-MAC channel upper bound and the relay-BS MIMO upper bound.

Chapter 2

Background

2.1 MIMO Data Processing

Consider a MIMO link with N_t transmit and N_r receive antennas, denoted as (N_t, N_r). The baseband model of the received signal vector **y** is expressed as [13]

$$\boldsymbol{y} = \boldsymbol{H}\boldsymbol{s} + \boldsymbol{n} \tag{2.1}$$

where $\boldsymbol{H}$ is the $N_r \times N_t$ channel matrix, and $\boldsymbol{s}$ is the $N_t \times 1$ transmitted signal vector. The $N_r \times 1$ noise vector $\boldsymbol{n}$ is assumed to be circularly symmetric complex Gaussian with zero-mean and covariance matrix $\boldsymbol{R}$. We note here that the noise vector $\boldsymbol{n}$ is independent of input $\boldsymbol{s}$ and channel $\boldsymbol{H}$.

In this section it is assumed that the receiver has perfect knowledge of channel matrix $\boldsymbol{H}$ and spatial noise covariance matrix $\boldsymbol{R}$. This assumption only holds when perfect channel state information (CSI) is considered. In Chapters 3, 4 and 5, cooperative systems with both perfect CSI and imperfect CSI are considered. If the transmitted signal $\boldsymbol{s}$ is chosen from a signal constellation with equal probability, the optimum receiver is a maximum-likelihood (ML) receiver that selects the most probable transmitted signal vector $\boldsymbol{s}$ given the received signal vector $\boldsymbol{y}$. More specifically, the optimum ML

receiver selects a transmitted signal vector that maximizes the conditional PDF

$$\Pr(\boldsymbol{y}|\boldsymbol{x}) = \frac{1}{\pi^{N_r}\det(\boldsymbol{R})}\exp\Big\{-(\boldsymbol{y}-\boldsymbol{H}\boldsymbol{s})^{\dagger}\boldsymbol{R}^{-1}(\boldsymbol{y}-\boldsymbol{H}\boldsymbol{s})\Big\}. \tag{2.2}$$

Assuming the signal transmitted on each antenna is drawn from an M-ary signal constellation, there are M^{N_t} possible choices of the transmitted signal vector. The optimum receiver computes the conditional PDF for each possible transmitted signal vector, and selects the one that yields the largest conditional PDF. Hence, the complexity of the optimum ML receiver grows exponentially with the number of transmitting antennas, N_t.

Due to the high complexity of the optimum receiver, various suboptimal receivers which yield a reasonable tradeoff between performance and complexity have been investigated. Examples of nonlinear suboptimal detectors are the sphere detector [14] and detectors which combine linear processing with local ML search [15]. The linear suboptimal detectors usually used in practice are zero-forcing (ZF) and minimum mean-squared error (MMSE) detectors [13, 16, 17]. Data detection for MIMO systems is similar to multiuser detection for synchronous users [15], where in MIMO systems we consider one user having multiple transmitting antennas and in multi-user detection we consider multiple users each having one transmitting antenna. The ZF and MMSE MIMO detectors are akin to the decorrelating and MMSE multiuser detectors, respectively.

In the following, we briefly derive MMSE detectors which include the detection algorithms in [13, 16, 17] as special cases of spatially white noise. We assume that $N_t \leq N_r$. Note that these two detectors are valid even for non-Gaussian noise.

2.1.1 MMSE detector

We seek linear estimate $\tilde{\boldsymbol{s}} = \boldsymbol{A}\boldsymbol{y}$ such that the mean square error (MSE)

$$J(\boldsymbol{A}) = \mathrm{tr}\Big\{E\big[(\boldsymbol{s}-\boldsymbol{A}\boldsymbol{y})(\boldsymbol{s}-\boldsymbol{A}\boldsymbol{y})^{\dagger}\big]\Big\} \tag{2.3}$$

is minimized. Without loss of generality, we assume that the transmitted signal vector is zero-mean and with covariance matrix $E\{\boldsymbol{s}\boldsymbol{s}^\dagger\} = \boldsymbol{I}_{N_t}$. It is also assumed that the transmitted signal vector is uncorrelated of the noise vector, i.e., $E\{\boldsymbol{s}\boldsymbol{n}^\dagger\} = \boldsymbol{0}$. Substituting (2.1) into (2.3), the MSE becomes

$$J(\boldsymbol{A}) = \mathrm{tr}\left\{\boldsymbol{I}_{N_t} - \boldsymbol{A}\boldsymbol{H} - \boldsymbol{H}^\dagger\boldsymbol{A}^\dagger + \boldsymbol{A}\left(\boldsymbol{H}\boldsymbol{H}^\dagger + \boldsymbol{R}\right)\boldsymbol{A}^\dagger\right\}. \tag{2.4}$$

By setting $\partial J(\boldsymbol{A})/\partial \boldsymbol{A} = \boldsymbol{0}$, we obtain

$$\begin{aligned} \boldsymbol{A} &= \boldsymbol{H}^\dagger\left(\boldsymbol{H}\boldsymbol{H}^\dagger + \boldsymbol{R}\right)^{-1} && (2.5)\\ &= \left(\boldsymbol{I}_{N_t} + \boldsymbol{H}^\dagger\boldsymbol{R}^{-1}\boldsymbol{H}\right)^{-1}\boldsymbol{H}^\dagger\boldsymbol{R}^{-1} && (2.6) \end{aligned}$$

where the second equality is due to the matrix identity in [18, p528, D.11]. Hence, the soft MMSE estimate is

$$\tilde{\boldsymbol{s}}_{\mathrm{MMSE}} = \left(\boldsymbol{I}_{N_t} + \boldsymbol{H}^\dagger\boldsymbol{R}^{-1}\boldsymbol{H}\right)^{-1}\boldsymbol{H}^\dagger\boldsymbol{R}^{-1}\boldsymbol{H}\boldsymbol{s} + \tilde{\boldsymbol{n}} \tag{2.7}$$

where

$$\tilde{\boldsymbol{n}} = \left(\boldsymbol{I}_{N_t} + \boldsymbol{H}^\dagger\boldsymbol{R}^{-1}\boldsymbol{H}\right)^{-1}\boldsymbol{H}^\dagger\boldsymbol{R}^{-1}\boldsymbol{n}. \tag{2.8}$$

Again, the detected signal vector is obtained by quantizing the soft estimate $\tilde{\boldsymbol{s}}_{\mathrm{MMSE}}$ to the nearest point in the signal constellation.

Substituting (2.5) into the matrix of the trace operation in (2.4), we obtain the covariance matrix of the estimation error

$$\begin{aligned} E\left\{(\boldsymbol{s} - \tilde{\boldsymbol{s}}_{\mathrm{MMSE}})(\boldsymbol{s} - \tilde{\boldsymbol{s}}_{\mathrm{MMSE}})^\dagger\right\} &= \boldsymbol{I}_{N_t} - \boldsymbol{H}^\dagger\left(\boldsymbol{H}\boldsymbol{H}^\dagger + \boldsymbol{R}\right)^{-1}\boldsymbol{H} \\ &= \boldsymbol{I}_{N_t} - \left(\boldsymbol{I}_{N_t} + \boldsymbol{H}^\dagger\boldsymbol{R}^{-1}\boldsymbol{H}\right)^{-1}\boldsymbol{H}^\dagger\boldsymbol{R}^{-1}\boldsymbol{H} \\ &= \left(\boldsymbol{I}_{N_t} + \boldsymbol{H}^\dagger\boldsymbol{R}^{-1}\boldsymbol{H}\right)^{-1} && (2.9) \end{aligned}$$

where the second equality is due to the alternative expression of $\boldsymbol{H}^\dagger(\boldsymbol{H}\boldsymbol{H}^\dagger + \boldsymbol{R})^{-1}$ in (2.6), and the last equality comes from the fact that $\boldsymbol{I}_{N_t} = (\boldsymbol{I}_{N_t} + \boldsymbol{H}^\dagger\boldsymbol{R}^{-1}\boldsymbol{H})^{-1}(\boldsymbol{I}_{N_t} + \boldsymbol{H}^\dagger\boldsymbol{R}^{-1}\boldsymbol{H})$. It is easy to see that soft MMSE estimate $\tilde{\boldsymbol{s}}_{\mathrm{MMSE}}$ is a biased estimate of $\boldsymbol{s}$ from (2.7).

For spatially white noise with $\boldsymbol{R} = \boldsymbol{I}_{N_r}$, the estimate in (2.7) is reduced to $\tilde{\boldsymbol{s}}_{\mathrm{MMSE}} = \left(\boldsymbol{I}_{N_t} + \boldsymbol{H}^{\dagger}\boldsymbol{H}\right)^{-1}\boldsymbol{H}^{\dagger}\boldsymbol{y}$ [19].

2.2 MIMO Channel Capacity

Consider a Gaussian MIMO channel whose input-output relationship is given by (2.1). In coherent communications, assuming the channel $\mathbf{H}$ is perfectly known at the receiver. Given $\mathbf{H}$, the capacity is expressed as [20]

$$C(\mathbf{H}) = \max_{p(\mathbf{s})} I(\mathbf{s};\mathbf{y}) = \max_{\mathbf{Q}\succeq 0, tr\{\mathbf{Q}\}\leq P_T} \log_2 \det(\mathbf{I}_{n_R} + \frac{1}{\sigma^2}\mathbf{H}\mathbf{Q}\mathbf{H}^H), \tag{2.10}$$

where $p(\mathbf{s})$ denotes the input distribution, $I(\cdot;\cdot)$ denotes the mutual information between channel input and channel output, P_T is the total transmit power, and $\mathbf{Q} \triangleq E(\mathbf{s}\mathbf{s}^H)$ is the transmit signal covariance matrix. $\mathbf{Q} \succeq 0$ means that $\mathbf{Q}$ is positive semidefinite. Here the transmitted signal vector is assumed to be zero-mean.

If the channel is unknown to the transmitter, uniform power allocation is used at the transmitter, i.e., $\mathbf{Q} = \frac{P_T}{n_T}\mathbf{I}_{n_T}$, and

$$C_{uni}(\mathbf{H}) = \log_2 \det(\mathbf{I}_{n_R} + \frac{P_T}{n_T\sigma_n^2}\mathbf{H}\mathbf{H}^H) \tag{2.11}$$

where σ_n^2 is the noise variance at the receiver. On the other hand, if the channel state information is perfectly known at the transmitter (CSIT), the matrix channel can be decoupled into a set of parallel scalar Gaussian channels by means of singular value decomposition (SVD) [21]. Specifically, let $\breve{r} = \mathrm{rank}(\mathbf{H})$ and let $\mathbf{H}$ be represented by its SVD:

$$\mathbf{H} = \breve{\mathbf{U}}\breve{\Lambda}^{1/2}\breve{\mathbf{V}}^H \tag{2.12}$$

where $\breve{\mathbf{U}}, \breve{\Lambda}, \breve{\mathbf{V}}$ are $n_R \times \breve{r}$,$\breve{r} \times \breve{r}$ and $n_T \times \breve{r}$ matrices, respectively, $\breve{\mathbf{U}}$ *and* $\breve{\mathbf{V}}$ are unitary matrices. $\breve{\Lambda} = \text{diag}(\breve{\lambda}_1, \ldots, \breve{\lambda}_{\breve{r}})$ denotes a diagonal matrix composed of the non-zero eigenvalues of $\mathbf{H}\mathbf{H}^H$ arranged in decreasing order. Then we have

$$\breve{y}_i = \begin{cases} \sqrt{\breve{\lambda}_i}\breve{y}_i + n_i, & i = 1, \ldots, \breve{r}; \\ \breve{n}_i, & i = \breve{r}+1, \ldots, n_R, \end{cases} \tag{2.13}$$

where $\breve{\mathbf{y}} = \breve{\mathbf{U}}^H \mathbf{y}, \breve{\mathbf{s}} = \breve{\mathbf{V}}^H \mathbf{s}$ and $\breve{\mathbf{n}} = \breve{\mathbf{U}}^H \mathbf{n}$ are the transformed receive signal vector, transmit signal vector and noise vector. The transmit power is optimally allocated among the effective $\breve{r}$ scalar channels using the well-known water-filling procedure [22]. As a result,

$$\breve{P}_i^{opt} = (\breve{\mu} - \sigma_n^2/\breve{\lambda}_i)_+, \;\; i = 1, \ldots, \breve{r}, \tag{2.14}$$

where

$$\begin{aligned} \breve{\mathbf{Q}} &= \breve{\mathbf{V}} \cdot \text{diag}(\breve{P}_1^{opt}, \ldots, \breve{P}_{\breve{r}}^{opt}) \breve{\mathbf{V}}^H \\ &= \breve{\mathbf{V}}(\breve{\mu})(\breve{\mu}\mathbf{I}_{\breve{r}} - \sigma_n^2 \breve{\Lambda}^{-1})_+ \breve{\mathbf{V}}^H \end{aligned} \tag{2.15}$$

and the capacity is given by

$$C_{wf}(\mathbf{H}) = \sum_{i=1}^{\breve{r}} \log_2(1 + \frac{(\breve{\lambda}\breve{\mu} - \sigma_n^2)_+}{\sigma_n^2}). \tag{2.16}$$

It is important to note that, due to CSIT, $C_{wf}(\mathbf{H})$ is larger than $C_{uni}(\mathbf{H})$, especially in the low to medium SNR region. For full-rank channels, $C_{uni}(\mathbf{H})$ approaches $C_{wf}(\mathbf{H})$ when P_T goes to infinity.

The ergodic capacity of a coherent MIMO fading channel is the capacity $C(\mathbf{H})$ averaged over different channel realizations:

$$C = E_{\mathbf{H}} \left[\max_{\mathbf{Q}, \text{tr}(\mathbf{Q}) \le P_T} \log_2 \det(\mathbf{I}_{n_R} + \frac{1}{\sigma_n^2} \mathbf{H}\mathbf{Q}\mathbf{H}^H). \right] \tag{2.17}$$

In [20], it has been shown that if $\mathbf{H}$ is random, with its entries forming an independent and identically distributed (i.i.d.) Gaussian collection with zero-mean, independent real and imaginary

parts, each with unit variance, then the capacity as expressed in this formula scales linearly with the number of antennas via $\min(n_T, n_R)$.

2.3 Convex Optimization

Many communication problems can either be cast as or be converted into convex optimization problems, which greatly facilitate their analytical and numerical solutions. Convex optimization refers to the minimization of a convex objective function subject to convex constraints.

2.3.1 Basic Optimization Concepts

Convex Sets: A set $S \subseteq \mathbf{R}^n$ is said to be affine if for any two points $x, y \in S$, the line segment joining and also lies in S. Mathematically, it is defined by the following property:

$$\theta x + (1-\theta)y \in S, \quad \forall \theta \ in \ [0,1] \text{ and } x, y \in S. \tag{2.18}$$

In general, a convex set must be a solid body, containing no holes, and always curves outward. Other examples of convex sets include ellipsoids, hypercubes, polyhedral sets, and so on. The most important property about a convex set is the fact that the intersection of any number (possibly uncountable) of convex sets remains convex. The union of two convex sets, however, is typically nonconvex.

Convex Cones: A convex cone $\mathbb{K}$ is a special type of convex set which is closed under positive scaling: for each $x \in \mathbb{K}$ and each $\alpha \geq 0, \alpha x \in \mathbb{K}$. Define n as the dimension, the most common convex cones are the following:

1) *Nonnegative orthant*: $\Re_+^n$.

2) *Second-order cone*:

$$\mathbb{K} = SOC(n) = \{(t,x) |\ t \geq ||x||\}. \tag{2.19}$$

3) *Positive semidefinite matrix cone*:

$$\mathbb{K} = S_+^n = \{X | \, X \; symmetric \; and \; X \succeq 0\}. \tag{2.20}$$

where S_+^n denotes the set of n by n positive semidefinite real symmetric matrices. For any convex cone $\mathbb{K}$, its dual cone is defined as

$$\mathbb{K}^* = \{x | \, \langle x, y \rangle \geq 0, \forall \, y \in \mathbb{K}\} \tag{2.21}$$

where $\langle \cdot, \cdot \rangle$ denotes the inner product operation. In other words, the dual cone $\mathbb{K} = \mathbb{K}^*$, which is always convex [23]. It can be shown that the nonnegative orthant cone, the second-order cone and the symmetric positive semidefinite matrix cone are all self-dual (an object has the property that it is equal to its own dual, then is said to be self-dual).

Convex Functions: A function $f(x) : \Re^n \to \Re$ is said to be convex if for any two points x,y $\in \Re^n$

$$f(\theta x + (1-\theta)y) \leq \theta f(x) + (1-\theta) f(y), \quad \theta \in \, [0,1]. \tag{2.22}$$

Convex Optimization Problems: Consider a generic optimization problem (in the minimization form)

$$\begin{aligned} & \min \quad f_0(x) \\ \text{subject to} \quad & f_i(x) \leq 0, \;\; i = 1,2,\ldots,m \\ & h_j(x) = 0, \;\; j = 1,2,\ldots,r, \\ & x \in S \end{aligned} \tag{2.23}$$

where f_0 is called the objective function, $\{f_i\}_{i=1}^m$ and $\{h_j\}_{j=1}^r$ are called inequality and equality constraint functions, respectively, and S is called a constraint set. In practice, S can be implicitly defined by user-supplied software. The optimization variable $x \in \Re^n$ is said to be feasible if $x \in S$ and it satisfies all the inequality and equality constraints in (2.23). A feasible solution x^* is said to

be globally optimal if there exists some $\varepsilon > 0$ such that $f_0(x^*) \leq f_0(x)$ for all feasible x satisfying $||x - x^*|| \leq \varepsilon$.

The optimization problem (2.23) is said to be convex if 1) the functions $f_i(i = 0, 1, 2, \ldots, m)$ are convex; 2) $h_j(x)$ are affine functions; and 3) the set S is convex. Violating any one of these three conditions results in a nonconvex problem. For any convex optimization problem, the set of global optimal solutions is always convex. Moreover, every locally optimal solution is also a globally optimal solution. For one thing, there exist highly efficient interior-point optimization algorithms whose worst-case complexity (i.e., the total number of arithmetic operations required to find an ε-optimal solution, where ε is any chosen positive value) grows gracefully as a polynomial function of the problem data length and $\log(1/\varepsilon)$ [23]. Well-designed software for solving convex optimization problems typically returns either an optimal solution, or a certificate (in the form of a dual vector) that establishes the infeasibility of the problem. That is due to the existence of an extensive duality theory for convex optimization problems, a consequence of which is the existence of a computable mathematical certificate for infeasible convex optimization problems.

2.4 Imperfect Channel State Model

2.4.1 Channel State Estimation and Error Model

In this section we present a general model for imperfect CSI model which will be used in later chapters. Channel estimation is not perfect but is estimated from orthogonal training sequences. This model is applicable to four types of channels, namely 1) MIMO channels, 2) channels from multiple-antenna source to single antenna relays, 3) channels from multiple single-antenna relays to multiple single-antenna destinations, 4) channels from a multiple single-antenna relays to multi-antenna destination. First we consider a slow-varying flat-fading MIMO model i.e., (2.1), and then

extend it to other types of channels. Considering antenna correlation on both the transmitter side and receiver side, $\mathbf{H}$ can be written as

$$\mathbf{H} = \mathbf{R}_R^{1/2}\mathbf{H}_w\mathbf{R}_T^{1/2}. \tag{2.24}$$

Here $\mathbf{H}_w$ is a spatially white matrix whose entries are i.i.d. Gaussian with zero mean and unit variance denoted as $N(0,1)$. The matrices $\mathbf{R}_T$ and $\mathbf{R}_R$ represent normalized transmit and receive correlation, respectively. Both $\mathbf{R}_T$ and $\mathbf{R}_R$ are assumed to be *full-rank*. Since $\mathbf{R}_T$ and $\mathbf{R}_R$ are full-rank and assumed to be known, channel estimation is performed on $\mathbf{H}_w$ using the well-established orthogonal training method described in [24] [25] [26] [27] [28] . At the receive antennas, the received signal matrix $\mathbf{Y}_{tr}$ with dimension $N_r \times T_{tr}$, received in n_T time slots,

$$\mathbf{Y}_{tr} = \mathbf{H}\mathbf{S}_{tr} + \mathbf{N}_{tr} = \mathbf{R}_R^{1/2}\mathbf{H}_w\mathbf{R}_T^{1/2}\mathbf{S}_{tr} + \mathbf{N}_{tr} \tag{2.25}$$

where $\mathbf{S}_{tr}$ is the transmitted $T_{tr} \times T_{tr}$ training signal matrix and $\mathbf{N}_{tr}$ is the collection of noise vectors. Let $P_{tr} = \mathrm{Tr}(\mathbf{S}_{tr}\mathbf{S}_{tr}^H)$ denote the total source training power. To obtain orthogonality, $\mathbf{S}_{tr} = \mathbf{R}_T^{-1/2}\mathbf{S}_0$, where $\mathbf{S}_0$ is a unitary matrix scaled by $\sqrt{P_{tr}/\mathrm{Tr}(\mathbf{R}_T^{-1})}$. Pre-multiplying both sides of (2.25) by $\mathbf{R}_R^{-1/2}$ and then post-multiplying the resultant formula by $\mathbf{S}_0^{-1}$, we obtain

$$\begin{aligned}\tilde{\mathbf{H}}_w &= \mathbf{R}_R^{-1/2}\mathbf{Y}_{tr}\mathbf{S}_0^{-1} \\ &= \mathbf{H}_w + \mathbf{R}_R^{-1/2}\mathbf{N}_{tr}\mathbf{S}_0^{-1} \\ &= \mathbf{H}_w + \mathbf{R}_R^{-1/2}\mathbf{N}_0.\end{aligned} \tag{2.26}$$

In the above expression, we define $\mathbf{N}_0 \triangleq \mathbf{N}_{tr}\mathbf{S}_0^{-1}$, whose entries are i.i.d.. $N(0,\sigma_{ce}^2)$ with $\sigma_{ce}^2 = \mathrm{tr}(\mathbf{R}_T^{-1}\dot{\sigma}_n^2)/P_{tr}$. To obtain better estimation performance, minimum MSE (MMSE) channel estimation of $\mathbf{H}_w$ is performed based on (2.26) [25] [26] [27] [28], which yields

$$\hat{\mathbf{H}}_w = \mathbf{H}_w + \mathbf{R}_R^{-1/2}[\mathbf{I}_{n_R} + \sigma_{ce}^2 \cdot \mathbf{R}_R^{-1}]^{-1/2}\mathbf{E}_w \tag{2.27}$$

where the entries of $\mathbf{E}_w$ are i.i.d. $N(0,\sigma_{ce}^2)$, and are independent from those of $\hat{\mathbf{H}}_w$. A derivation of (2.27) is in Appendix A. Let

$$\mathbf{R}_{e,R} = \left[\mathbf{I}_{n_R} + \sigma_{ce}^2 \mathbf{R}_R^{-1}\right]. \tag{2.28}$$

The CSI model is described by

$$\mathbf{H} = \hat{\mathbf{H}} + \mathbf{E} \tag{2.29}$$

where $\mathbf{H}$ is the true channel matrix, $\hat{\mathbf{H}} = \mathbf{R}_R^{1/2}\hat{\mathbf{H}}_w\mathbf{R}_T^{1/2}$ is the estimated channel matrix (i.e., the channel mean), and $\mathbf{E} = \mathbf{R}_R^{1/2}\mathbf{E}_w\mathbf{R}_T^{1/2}$ is the channel estimation error matrix.

In summary, the imperfect CSI model is given by (2.26) (2.27) (2.29). In subsequent sections, we assume that $\hat{\mathbf{H}}, \mathbf{R}_R, \mathbf{R}_T, \sigma_{ce}^2$ and σ_n^2 are known to both ends of the link, which is refered to as the channel mean as well as both transmit and receive correlation information.

We note that the imperfect channel model can be easily applied to different types of channels as follows:

- The channel from a multi-antenna source to multiple single-antenna relays can use the above model by setting $\mathbf{R}_R = \mathbf{I}_R$.
- The channel from multiple single-antenna relays to a multi-antenna destination can use the above model by setting $\mathbf{R}_T = \mathbf{I}_T$.
- The channel from multiple single-antenna relays to multiple single-antenna destinations (or the channel from multiple single-antenna sources to multiple single-antenna relays) can use the above mode by setting $\mathbf{R}_T = \mathbf{I}_T$, *and* $\mathbf{R}_R = \mathbf{I}_R$.

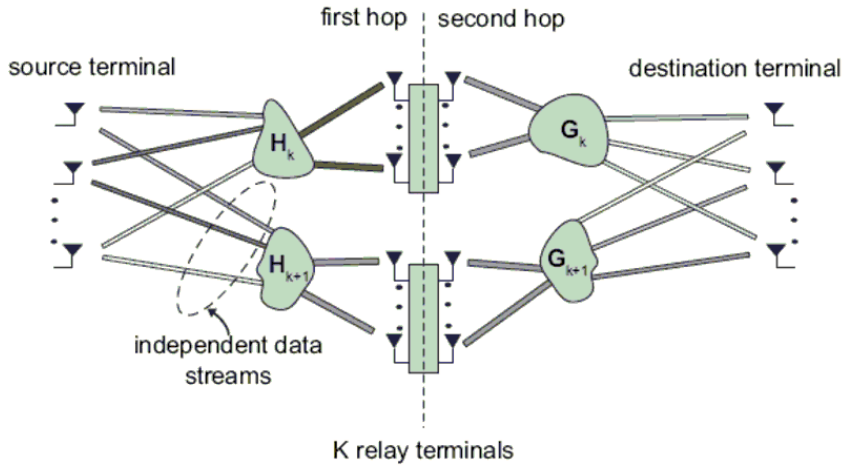

Figure 2.1. MIMO relay system [1] with K relays each equipped with N antennas.

2.5 MIMO Relay Channel Capacity bound

Channel capacity for cooperative systems has been studied in the literature. In [29], a cooperative system with one relay between source and destination and direct link between source and destination is studied, with corresponding upper and lower bounds derived. In [1], both an asymptotic upper-bound and lower-bound was derived for multiple relay MIMO systems for perfect CSI at relays and receiver and no CSI at the source as follows:

A cooperative system consists of a source with M antennas, a destination with M antennas and K relays each with $N \geq 1$ antennas, two time slots are employed with the first time slot to transmit data from the source to the relays and the second time slot forward data from the relays to the destination as described in Figure 2.1.

The link between the source and the relays is described as:

$$\mathbf{r}_k = \sqrt{\frac{E_k}{M}}\mathbf{H}_k\mathbf{s} + \mathbf{n}_k, \quad ,k = 1,2,\ldots,K \tag{2.30}$$

where $\mathbf{r}_k$ denotes the $N \times 1$ received vector signal, E_k is the average energy of the transmitted

signal received at the kth relay terminal over one symbol period through the source-relay link. $\mathbf{H}_k = [\mathbf{h}_{k,1} \ \mathbf{h}_{k,2} \ \ldots \ \mathbf{h}_{k,M}]$ is the $N \times M$ random channel matrix corresponding to link from the source to the kth relay, consisting of i.i.d. $\mathscr{CN}(0,1)$ entries, $\mathbf{s} = [s_1 \ s_2 \ldots \ s_M]^T$ with $E\{\mathbf{s}\mathbf{s}^H\} = \mathbf{I}_M$ and $\mathbf{n}_k$ as spatio-temporally white circularly symmetric complex Gaussian noise vector sequence, independent across k, with covariance matrix $E\{\mathbf{n}_k\mathbf{n}_k^H\} = \sigma_n^2\mathbf{I}_M$. The link from the relays to the destination is described by

$$\mathbf{y} = \sum_{k=1}^{K} \sqrt{\frac{P_k}{N}}\mathbf{G}_k\mathbf{r}_k + \mathbf{z} \tag{2.31}$$

where P_k is the average signal energy over one symbol period contributed by the kth relay terminal, $\mathbf{G}_k = [\mathbf{g}_{k,1} \ \mathbf{g}_{k,2} \ldots \ \mathbf{g}_{k,M}]^T$ is the corresponding $M \times N$ channel matrix with i.i.d. $\mathscr{CN}(0,1)$ entries and $\mathbf{z} = [z_1 \ z_2 \ \ldots \ z_M]$ denotes an $M \times 1$ spatio-temporally white circularly symmetric complex Gaussian noise vector sequence satisfying $E(\mathbf{z}\mathbf{z}^H) = \sigma_n^2\mathbf{I}_M$.

It is proven in [1] that the capacity of the coherent MIMO relay network under two-hop relaying satisfies

$$C \leq C_{upper} = \frac{M}{2}\log\left(1 + \frac{N}{M\sigma_n^2}\sum_{k=1}^{K} E_k\right) \xrightarrow{w.p.1} C_{upper}^{\infty} = \frac{M}{2}log(K) + O(1) \tag{2.32}$$

and for a fixed number of source-destination antenna pairs M and fixed N, in the $K \to \infty$ limit such that $|\chi_1| = |\chi_2| = \ldots = |\chi_M| = K/M$. Here w.p.1 denotes with probability 1. χ_i is denoted as the set of relays assigned to the ith transmit-receive antenna pair, $|\chi|$ denotes the cardinality of set χ, assuming perfect knowledge of $E_k, P_k, \mathbf{H}_k, \mathbf{G}_{k\,k=1}^{K}$ at each of the receive antennas, the relay network capacity scales at least as

$$C_{lower}^{\infty} = \frac{M}{2}log(K) + O(1). \tag{2.33}$$

However, [1] does not provide a design to achieve the capacity.

Chapter 3

Cooperative MIMO System Downlink

3.1 Introduction

In this chapter, we study the multi-user downlink cooperative system. Providing cellular coverage for high-rate multimedia leads to increased transmission power, which in turn increases inter-cell interference. Alternatively, cell-splitting leads to frequent handovers. A recent approach which increase coverage and capacity while limits transmission power is cooperative communication involving relaying. Relay system based on orthogonal frequency division multiplexing access (OFMDA) has been in LTE Advanced [30] [31] [32]. To limit in-band interference, it is important to limit the transmission power at both base stations and relays, which is the topic to be addressed in this chapter.

In [33], the design of linear precoders broadcasting to given MIMO receivers using signal-to-noise plus interference (SINR) constraints is considered. Linear minimum mean-squared error (LMMSE) precoding/decoding design has been studied for the uplink in [27], and for the downlink in [34] [35]. Transceiver design that takes imperfect channel state information into account has also been studied [27] [36] [37]. To date, the design problems concerning relay assignment have been examined mainly for single-user scenarios with focus on the outage probability analysis of the best

relay for transmission or for reception and bottleneck link [38] [39]. Multi-user multi-relay wireless networks with single-carrier frequency division multiple access (SC-FDMA) at the terminals is studied in [40]. Joint relay selection and power allocation for cooperative system has been studied in [41].

Transmission techniques for broadcast channels have been extended to cooperative networks. Relays cooperatively transmit to a receiver [42], where amplitudes and phases of transmitted signals are coherently combined. In [43], rate maximization for a parallel relay network with noise correlation is studied. A distributed beamforming system with a single transmitter and receiver and multiple relay nodes is studied in [11], and second order statistics of the channel are employed to design the optimal distributed relay beamformer (DRBF). Single-antenna source-destination pairs that communicate peer-to-peer through a relay network are considered in [44], and the DRBF problem is formulated in terms of semi-definite programming (SDP) and solved through semi-definite relaxation. Unfortunately, the requirement for accurate channel state information (CSI) and the distributed nature of wireless sensor/relay networks complicate transmit beamforming. A distributed beamforming scheme with two relays is proposed in [45] that has the advantages of limited feedback and improved diversity. The problem of quantized CSI feedback in multiple-input multiple output (MIMO) AF relay systems has been addressed in [46] using beamforming code books designed based on Grassmanian manifolds, perfect CSI is also assumed at the receiver.

As overall precoder-DBRF optimization to achieve minimum-power objectives is complex if not intractable, it is proposed in this chapter that optimization of the linear precoder for a given DRBF be iterated with DRBF optimization for a given linear precoder. A proposed iterative algorithm successively minimizes the transmission power at the base station and sum power at the relays. The approach is then generalized to take imperfect CSI into account. As studied in [47], for cooperative multi-relay systems, synchronization is a real challenge for narrow-band single carrier systems as the

transmitters and receivers are distributed in space due to propagation delay and multi-path. However, in the LTE system which is based on OFDMA with cyclic prefix (CP), any multi-path arrival of signals can be coherently combined at the receiver. The propagation delay (0.1us for typical dense urban scenarios with inter-site distance of 500m) is negligible compared with CP. What is more, there is primary synchronization channel and secondary synchronization channel to guarantee that the synchronization error is less than 3us which is less than the CP length (4.76us) for regular commercial system setting. For network elements distributed in space, synchronization is achieved through GPS with high accuracy symbol-wise. The frequency synchronization accuracy for LTE is less than 0.05PPM, considering the 2.6GHz carrier frequency, the allowable frequency offset mismatch is less than 0.13kHz, which is significantly less than the 15kHz subcarrier frequency. This means that the impact from the possible carrier frequency offset deviation on performance is negligible for LTE system. Hence, the synchronization is not a concern for OFDMA based wide-band systems. In this and following chapters, perfect synchronization across the system is assumed [48] [49] [50]. We also assume full CSI except in sections that focus on imperfect CSI.

The remainder of the chapter is organized as follows: In Section 3.2, we present the system model. Linear precoder optimization is presented in Section 3.4.4, followed by DRBF optimization in Section 3.4.4. Precoding and distributed beamforming with imperfect CSI is presented in Section 3.5, downlink system with multiple antennas at receives is presented in Section 3.6 and numerical results are discussed in Section 3.7.

3.2 System Model

Consider a broadcast channel as shown in Fig. 3.1. As explained above, data is transmitted from the source to multiple users through the relays successively over two time slots. There is an N_{dl}-antenna

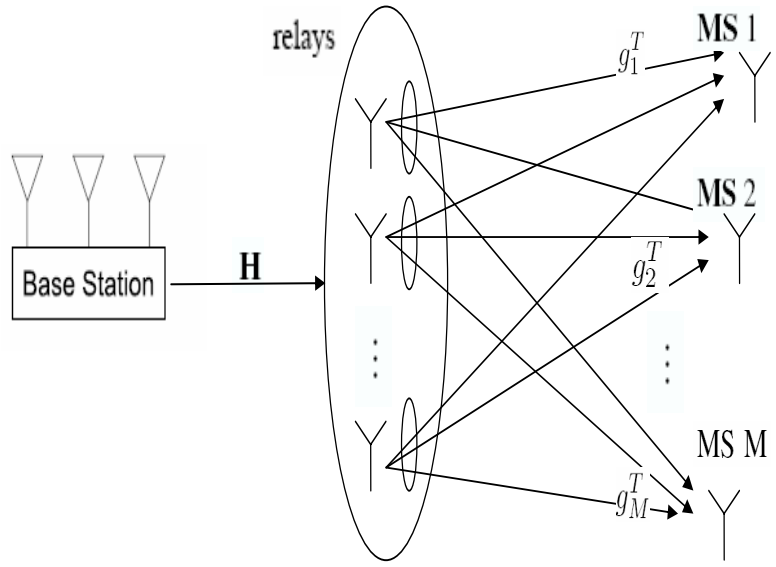

Figure 3.1. Downlink distributed beamforming system.

source, a relay network of n_R^{dl} single-antenna relays, and M_{dl} distributed single-antenna destinations, where $M_{dl} \leq N_{dl}$. The n_R^{dl} relays form the infrastructure of the cooperative relay system. It is assumed that the N_{dl} channels from the source to the relays are estimated at the relays and fed back to the source. Similarly, the n_R^{dl} channels from the relays to the destinations are estimated at the destinations and fed back to the relays, which then forward the estimates back to the source. The relaying operates in a half-duplex mode: in the first time slot, the source uses transmit beamforming, or *precoding* to broadcast to the relays. In the second time slot, the relays cooperatively form a distributed relay beamformer (DRBF) to amplify and forward the M_{dl} relay signals to the destinations. It is assumed that since range extension is an intended application, there are no direct links between the source and the destinations. The $N_{dl} \times 1$ vector $\mathbf{h}_{dl,r}$ represents the link from the source to the rth relay, $1 \leq r \leq n_R^{dl}$, which receives symbols

$$x_{dl,r} = \mathbf{h}_{dl,r}^T \sum_{i=1}^{M_{dl}} \mathbf{t}_{dl,i} s_{dl,i} + v_{dl,r} \tag{3.1}$$

where $\mathbf{t}_{dl,i}$ denotes $N_{dl} \times 1$ transmit beamforming vector corresponding to signal $s_{dl,i}$ intended for the ith destination and the $n_R^{dl} \times 1$ vector $\nu_{dl} = [\nu_{dl,1}, \ldots, \nu_{dl,n_R^{dl}}]^T$ represents i.i.d. Gaussian noise terms at the relays with noise powers of $\sigma^2_{dl,\nu}$,.

To model distributed beamforming, the ith relay multiplies its received signal by complex coefficient $w_{dl,i}$. The vector $\mathbf{u}_{dl}$ representing the signal vector transmitted from the relays to the destinations is

$$\mathbf{u}_{dl} = \mathbf{W}_{dl}^H \mathbf{x}_{dl} \tag{3.2}$$

where diagonal DBRF matrix $\mathbf{W}_{dl} = \text{diag}(w_{dl,1}, w_{dl,2}, \ldots, w_{dl,n_R^{dl}})$ and $\mathbf{x}_{dl} = [x_{dl,1}\ x_{dl,2}\ \ldots\ x_{dl,n_R^{dl}}]^T$. Using (3.1), the received signal at the ith destination is

$$\begin{aligned} y_{dl,i} &= \mathbf{g}_{dl,i}^T \mathbf{u}_{dl} + n_{dl,i} \\ &= \underbrace{\mathbf{g}_{dl,i}^T \mathbf{W}_{dl}^H \mathbf{H}_{dl} \mathbf{t}_{dl,i} s_{dl,i}}_{Desired\ Signal} + \underbrace{\mathbf{g}_{dl,i}^T \mathbf{W}_{dl}^H \mathbf{H}_{dl} \sum_{j=1, j\neq i}^{M_{dl}} \mathbf{t}_{dl,j} s_{dl,j}}_{interference} + \underbrace{\mathbf{g}_{dl,i}^T \mathbf{W}_{dl}^H \nu_{dl} + n_{dl,i}}_{noise} \end{aligned} \tag{3.3}$$

where the $n_R^{dl} \times N_{dl}$ matrix $\mathbf{H}_{dl} = [\mathbf{h}_{dl,1} \ldots \mathbf{h}_{dl,n_R^{dl}}]^T$ represents the combined channel from the source to the relays, $1 \times n_R^{dl}$ row vector $\mathbf{g}_{dl,i}^T$ represents the channel from the relays to the ith destination, and $n_{dl,i}, i = 1, \ldots, M_{dl}$ represents the i.i.d. Gaussian noise terms at the destinations with noise powers of $\sigma^2_{dl,\mathbf{n}}$.

3.3 Transmit Precoder Optimization

First, the optimal minimum source power transmit precoder is determined under the constraints that for $1 \leq k \leq M_{dl}$, the kth destination node's quality of service (QoS), expressed in terms of its signal-to-interference plus noise ratio, $\text{SINR}_{dl,k}$, which is kept above pre-defined threshold $\gamma_{dl,k}$ for a given DRBF. This leads to the following optimization problem that has already been presented

in the generic form of (2.23) in Section 2.3 with fixed relay weights:

$$\min_{\mathbf{t}_{dl,1},\mathbf{t}_{dl,2},\ldots,\mathbf{t}_{dl,M_{dl}}} P_{dl,T}$$
$$s.t. \quad \text{SINR}_{dl,k} \geq \gamma_{dl,k}, \quad \text{for} \quad k = 1,2,\ldots,M_{dl} \tag{3.4}$$

where $P_{dl,T}$ is the transmission power at the source,

$$\text{SINR}_{dl,k} = \frac{P^k_{dl,s}}{P^k_{dl,i} + P^k_{dl,n}} \tag{3.5}$$

and s.t. stands for *subject to*. In (3.5), $P^k_{dl,s}, P^k_{dl,i}$ and $P^k_{dl,n}$ denote desired signal power, interference power, and noise power at the kth destination, respectively. Average transmission power $P_{dl,T}$ is given by

$$\begin{aligned} P_{dl,T} &= E\{(\sum_{i=1}^{M_{dl}} \mathbf{t}_{dl,i} s_{dl,i})^H (\sum_{j=1}^{M_{dl}} \mathbf{t}_{dl,j} s_{dl,j})\} \\ &= \sum_{i=1}^{M_{dl}} \mathbf{t}^H_{dl,i} \mathbf{t}_{dl,i} = \sum_{i=1}^{M_{dl}} \text{Tr}\{\mathbf{t}_{dl,i} \mathbf{t}^H_{dl,i}\} \end{aligned} \tag{3.6}$$

where $\text{Tr}(\cdot)$ stands for $\text{trace}(\cdot)$. The signal, interference and noise powers in (3.5) are

$$\begin{aligned} P^k_{dl,s} &= E\{(\mathbf{g}^T_{dl,k} \mathbf{W}^H_{dl} \mathbf{H}_{dl} \mathbf{t}_{dl,k} s_{dl,k})^H (\mathbf{g}^T_{dl,k} \mathbf{W}^H_{dl} \mathbf{H}_{dl} \mathbf{t}_{dl,k} s_{dl,k})\} \\ &= \mathbf{t}^H_{dl,k} \mathbf{H}^H_{dl} \mathbf{W}_{dl} \mathbf{g}^*_{dl,k} \mathbf{g}^T_{dl,k} \mathbf{W}^H_{dl} \mathbf{H}_{dl} \mathbf{t}_{dl,k} E(s^*_{dl,k} s_{dl,k}), \end{aligned} \tag{3.7}$$

$$\begin{aligned} P^k_{dl,i} &= E\{(\mathbf{g}^T_{dl,k} \mathbf{W}^H_{dl} \mathbf{H}_{dl} \sum_{j=1, j\neq k}^{M_{dl}} \mathbf{t}_{dl,j} s_{dl,j})^H (\mathbf{g}^T_{dl,k} \mathbf{W}^H_{dl} \mathbf{H}_{dl} \sum_{l=1, l\neq k}^{M_{dl}} \mathbf{t}_{dl,l} s_{dl,l})\} \\ &= \sum_{j=1, j\neq k}^{M_{dl}} \mathbf{t}^H_{dl,j} \mathbf{H}^H_{dl} \mathbf{W}_{dl} \mathbf{g}^*_{dl,k} \mathbf{g}^T_{dl,k} \mathbf{W}^H_{dl} \mathbf{H}_{dl} \mathbf{t}_{dl,j}, \quad \text{and} \end{aligned} \tag{3.8}$$

$$\begin{aligned} P^k_{dl,n} &= E\{(\mathbf{g}^T_{dl,k} \mathbf{W}^H_{dl} \nu_{dl} + n_{dl,k})^H (\mathbf{g}^T_{dl,k} \mathbf{W}^H_{dl} \nu_{dl} + n_{dl,k})\} \\ &= \text{Tr}\{\mathbf{W}_{dl} \mathbf{g}^*_{dl,k} \mathbf{g}^T_{dl,k} \mathbf{W}^H_{dl} \sigma^2_{dl,\nu}\} + \sigma^2_{dl,n}, \end{aligned} \tag{3.9}$$

where $\sigma^2_{dl,n}$ and $\sigma^2_{dl,\nu}$ represent noise powers at the destinations and relays, respectively. It is assumed, without loss of generality, that all destinations and all relays each have the same noise powers.

Combining (3.6)-(3.9), (3.4) can be expressed as

$$\min_{\mathbf{t}_{dl,1},\mathbf{t}_{dl,2},\ldots,\mathbf{t}_{dl,M_{dl}}} \sum_{i=1}^{M_{dl}} \mathrm{Tr}\{\mathbf{t}_{dl,i}\mathbf{t}_{dl,i}^H\}$$

$$s.t. \quad \frac{\mathbf{t}_{dl,k}^H \mathbf{H}_{dl}^H \mathbf{W}_{dl} \mathbf{g}_{dl,k}^* \mathbf{g}_{dl,k}^T \mathbf{W}_{dl}^H \mathbf{H}_{dl} \mathbf{t}_{dl,k}}{\sum_{j=1,j\neq k}^{M_{dl}} \mathbf{t}_{dl,j}^H \mathbf{H}_{dl}^H \mathbf{W}_{dl} \mathbf{g}_{dl,k}^* \mathbf{g}_{dl,k}^T \mathbf{W}_{dl}^H \mathbf{H}_{dl} \mathbf{t}_{dl,j} + P_{dl,n}^k} \geq \gamma_{dl,k} \quad \text{for} \quad k = 1,2,\ldots,M_{dl}. \tag{3.10}$$

Problem (3.10) can be transformed as follows [51] [44] [11] [52] [53]: defining matrices

$$\mathbf{T}_{dl,i} = \mathbf{t}_{dl,i}\mathbf{t}_{dl,i}{}^H, \quad i = 1,2,\ldots,M_{dl} \tag{3.11}$$

and dropping the rank-one constraints of the $\mathbf{T}_{dl,i}$, (3.10) becomes

$$\min_{\mathbf{T}_{dl,1},\mathbf{T}_{dl,2},\ldots,\mathbf{T}_{dl,M_{dl}}} \sum_{k=1}^{M_{dl}} \mathrm{Tr}(\mathbf{T}_{dl,k})$$

$$s.t. \quad \mathrm{Tr}(\mathbf{U}_{dl,k}(\mathbf{T}_{dl,k} - \gamma_{dl,k} \sum_{j=1,j\neq k}^{M_{dl}} \mathbf{T}_{dl,j})) \geq \gamma_{dl,k} P_{dl,n}^k,$$

$$\mathbf{T}_{dl,k} \succeq 0 \quad \text{for } k = 1,2,\ldots,M_{dl} \tag{3.12}$$

where $\mathbf{U}_{dl,k} = \mathbf{H}_{dl}^H \mathbf{W}_{dl} \mathbf{g}_{dl,k}^* \mathbf{g}_{dl,k}^T \mathbf{W}_{dl}^H \mathbf{H}_{dl}$. The solution to problem (3.12) establishes a lower bound to (3.10), which is only achieved in the case when (3.12) has a solution with the $\mathbf{T}_{dl,i}, i = 1,\ldots,M_{dl}$ all rank one. Problem (3.12) can be solved via semi-definite programming. Interestingly, it was proven in [51] with a similar problem formulation that there always exists at least one solution to (3.12) with $\mathrm{rank}(\mathbf{T}_{dl,k}) = 1, k = 1,\ldots,M_{dl}$:

Remark 1: The precoding problem of (3.10) can be reformulated in the form of Eq. (18.17) in [51], it is proven in [51] that *If the relaxed problem of* (3.10) *is feasible, (3.12) always has at least one minimum power solution where all* $\mathbf{T}_{dl,i}$ *are rank-one.*

3.4 Distributed Relay Beamforming (DRBF) Optimization

In this section, for a fixed source precoder, which can be obtained from the previous section, we first consider the general problem of minimum power DRBF optimization for multiple destinations. Individual power constraints at the relays are also considered. We then remark on the special case of a single destination.

3.4.1 Sum Relay Power Minimization for Multiple Destinations

As in Section 3.3, full CSI at the source is assumed, and (3.3) is rewritten as

$$y_{dl,k} = \underbrace{\mathbf{w}_{dl}^H \mathrm{diag}\{\mathbf{g}_{dl,k}^T\}\mathbf{H}_{dl}\mathbf{t}_{dl,k}s_{dl,k}}_{Desired\ Signal} + \underbrace{\mathbf{w}_{dl}^H \mathrm{diag}\{\mathbf{g}_{dl,k}^T\}\mathbf{H}_{dl}\sum_{j=1,j\neq k}^{M_{dl}}\mathbf{t}_{dl,j}s_{dl,j}}_{Interference} + \underbrace{\mathbf{w}_{dl}^H \mathrm{diag}\{\mathbf{g}_{dl,k}^T\}\nu + n_{dl,k}}_{Colored\ noise} \tag{3.13}$$

where DRBF column vector $\mathbf{w}_{dl} = diag\{\mathbf{W}_{dl}\}$. We aim to solve:

$$\min_{\mathbf{w}_{dl}} \quad P_{dl,R} \tag{3.14}$$

$$s.t. \quad \mathrm{SINR}_{dl,k} \geq \gamma_{dl,k} \ \text{ for } \ k = 1,\ldots,M_{dl}$$

where $P_{dl,R}$ is the average sum transmission power at the relays given as

$$\begin{aligned} P_{dl,R} &= E\{\mathbf{u}_{dl}^H\mathbf{u}_{dl}\} \\ &= \mathrm{Tr}\{\mathbf{W}_{dl}^H E\{\mathbf{x}_{dl}\mathbf{x}_{dl}^H\}\mathbf{W}_{dl}\} \\ &= \mathbf{w}_{dl}^H\mathbf{D}_{dl}\mathbf{w}_{dl}, \end{aligned} \tag{3.15}$$

where

$$\mathbf{D}_{dl} \triangleq \mathrm{diag}([\mathbf{R}_{dl,\mathbf{x}}]_{1,1}, [\mathbf{R}_{dl,\mathbf{x}}]_{2,2}, \ldots, [\mathbf{R}_{dl,\mathbf{x}}]_{n_R^{dl},n_R^{dl}}), \tag{3.16}$$

with *correlation* terms

$$\mathbf{R}_{dl,\mathbf{x}} \triangleq \mathbf{H}_{dl}(\sum_{k=1}^{M_{dl}} \mathbf{t}_{dl,k}\mathbf{t}_{dl,k}^H)\mathbf{H}_{dl}^H + \sigma_{dl,v}^2 \mathbf{I}_{n_R^{dl}}. \tag{3.17}$$

The SINR constraints for the kth user can be expressed as

$$\frac{\mathbf{w}_{dl}^H \mathbf{E}_{dl,k} \mathbf{w}_{dl}}{\mathbf{w}_{dl}^H \mathbf{F}_{dl,k} \mathbf{w}_{dl} + \sigma_{dl,n}^2} \geq \gamma_{dl,k} \tag{3.18}$$

where

$$\begin{aligned} \mathbf{E}_{dl,k} &= \mathrm{diag}(\mathbf{g}_{dl,k}^T)\mathbf{H}_{dl}\mathbf{t}_{dl,k}\mathbf{t}_{dl,k}^H\mathbf{H}_{dl}^H\mathrm{diag}(\mathbf{g}_{dl,k}^*), \\ \mathbf{F}_{dl,k} &= \mathrm{diag}(\mathbf{g}_{dl,k}^T)\left(\mathbf{H}_{dl}(\sum_{j=1,j\neq k}^{M_{dl}} \mathbf{t}_{dl,k}\mathbf{t}_{dl,k}^H)\mathbf{H}_{dl}^H + \sigma_{dl,v}^2\mathbf{I}\right)\mathrm{diag}(\mathbf{g}_{dl,k}^*). \end{aligned} \tag{3.19}$$

Using (3.15) and (3.18) we can rewrite (3.14) as

$$\begin{aligned} &\min_{\mathbf{w}_{dl}} \quad \mathbf{w}_{dl}^H \mathbf{D}_{dl} \mathbf{w}_{dl} \\ s.t. \quad &\mathbf{w}_{dl}^H \left(\mathbf{E}_{dl,k} - \gamma_{dl,k}\mathbf{F}_{dl,k}\right)\mathbf{w}_{dl} \geq \gamma_{dl,k}\sigma_{dl,n}^2 \text{ for } k = 1,2,\ldots,M_{dl}. \end{aligned} \tag{3.20}$$

We remark that with the above definitions, problem (3.14) has been reformulated into the equivalent problem of Eq. (17) in [44]. As these problems are equivalent, the discussion regarding Eq. (18) of [44] applies and semi-definite relaxation can be employed by solving a relaxed version of (3.20). It is noted here that in general cases, rank-1 solution does not always exists. However, in particular case when $M_{dl} \leq 3$, it is proven in [54] that the relaxed problem has optimal rank-1 solution. That is, by defining $\mathbf{Z}_{dl} \triangleq \mathbf{w}_{dl}\mathbf{w}_{dl}^H$, and dropping constraint $\mathrm{rank}(\mathbf{Z}_{dl}) = 1$, (3.20) becomes

$$\begin{aligned} &\min_{\mathbf{Z}_{dl}} \quad \mathrm{Tr}(\mathbf{Z}_{dl}\mathbf{D}_{dl}) \\ s.t. \quad &\mathrm{Tr}\left(\mathbf{Z}_{dl}(\mathbf{E}_{dl,k} - \gamma_{dl,k}\mathbf{F}_{dl,k})\right) \geq \gamma_{dl,k}\sigma_{dl,n}^2 \\ &\qquad\qquad \textit{and} \quad \mathbf{Z}_{dl} \succeq 0 \\ &\text{for} \quad k = 1,2,\ldots,M_{dl}. \end{aligned} \tag{3.21}$$

3.4.2 Individual Power Constraints at Relays

In this subsection, we consider additional power constraints that arises in practice. More specifically, each relay is restricted in its transmission power. This constraints are needed as some of the relays may end up with significantly high transmit powers which is impractical due to the power limitations of their transmit amplifiers. In this case, we add constraints to (3.20) and solve the following problem:

$$\begin{aligned} \min_{\mathbf{w}_{dl}} \quad & \mathbf{w}_{dl}^H \mathbf{D}_{dl} \mathbf{w}_{dl} \\ s.t. \quad & \mathbf{w}_{dl}^H \left(\mathbf{E}_{dl,k} - \gamma_{dl,k} \mathbf{F}_{dl,k} \right) \mathbf{w}_{dl} \geq \gamma_{dl,k} \sigma_{dl,n}^2 \text{ for } k = 1,2,\ldots,M_{dl} \\ & [\mathbf{D}_{dl}]_{i,i} |w_{dl,i}|^2 \leq P_{dl,i} \quad i = 1,\ldots,n_R^{dl} \end{aligned} \tag{3.22}$$

where $[\mathbf{D}_{dl}]_{i,i}$ denotes the ith diagonal term of matrix $\mathbf{D}_{dl}$, $w_{dl,i}$ denotes the ith relay weight, and $P_{dl,i}$ denotes the individual power constraint on the ith relay.

Using the semi-definite relaxation technique, (3.22) can be written as

$$\begin{aligned} \min_{\mathbf{Z}_{dl}} \quad & \text{Tr}(\mathbf{Z}_{dl} \mathbf{D}_{dl}) \\ s.t. \quad & \text{Tr}\left(\mathbf{Z}_{dl} (\mathbf{E}_{dl,k} - \gamma_{dl,k} \mathbf{F}_{dl,k}) \right) \geq \gamma_{dl,k} \sigma_{dl,n}^2 \quad \text{for} \quad k = 1,2,\ldots,M_{dl} \\ & \textit{and} \quad \mathbf{Z}_{dl} \succeq 0 \\ & \mathbf{Z}_{dl,i,i} \leq P_{dl,i} / [\mathbf{D}_{dl}]_{i,i} \quad i = 1,\ldots,n_R^{dl} \end{aligned} \tag{3.23}$$

3.4.3 The Case of a Single Destination

In the case $M_{dl} = 1$, the signal model in (3.3) reduces to

$$y_{dl} = \underbrace{\mathbf{w}_{dl}^H \text{diag}\{\mathbf{g}_{dl}^T\} \mathbf{H}_{dl} \mathbf{t}_{dl} s_{dl}}_{\textit{Desired Signal}} + \underbrace{\mathbf{w}_{dl}^H \text{diag}\{\mathbf{g}_{dl}^T\} v_{dl} + n_{dl}}_{\textit{Colored noise}} \tag{3.24}$$

where $\mathbf{t}_{dl}$ is the linear precoder vector at the source and $\mathbf{g}_{dl}$ is the channel vector from the relays to the user. We remark that the problem considered in [11] is a special case of (3.24) since in [11] there

is one source antenna ($N_{dl} = 1$) and the use of statistical channel information does not change the overall problem formulation.

3.4.3.1 Sum Relay Power Minimization

Using the derivations in the last subsection, the problem of sum power minimization at the relays with SINR constraints for a fixed linear precoder becomes:

$$\begin{aligned} & \min_{\mathbf{w}_{dl}} \ \mathbf{w}_{dl}^H \mathbf{D}_{dl} \mathbf{w}_{dl} \\ s.t. \quad & \frac{\mathbf{w}_{dl}^H \text{diag}(\mathbf{g}_{dl}^T) \mathbf{H}_{dl} \mathbf{t}_{dl} \mathbf{t}_{dl}^H \mathbf{H}_{dl}^H \text{diag}(\mathbf{g}_{dl}^*) \mathbf{w}_{dl}}{\sigma_{dl,v}^2 \mathbf{w}_{dl}^H \text{diag}(\mathbf{g}_{dl}^T) \text{diag}(\mathbf{g}_{dl}^*)^H \mathbf{w}_{dl} + \sigma_{dl,n}^2} \geq \gamma_{dl}. \end{aligned} \tag{3.25}$$

As there is one destination, here $\mathbf{R}_x$ in (3.16) becomes

$$\mathbf{R}_{dl,\mathbf{x}} = \mathbf{H}_{dl}^H \mathbf{t}_{dl} \mathbf{t}_{dl}^H \mathbf{H}_{dl}^H + \sigma_{dl,v}^2 \mathbf{I}_{n_R^{dl}}. \tag{3.26}$$

By transforming the optimization vector variable to $\hat{\mathbf{w}}_{dl} = \mathbf{D}_{dl}^{1/2} \mathbf{w}_{dl}$, (3.25) can be written as

$$\begin{aligned} & \min_{\hat{\mathbf{w}}_{dl}} \ \|\hat{\mathbf{w}}_{dl}\|^2 \\ s.t. \quad & \hat{\mathbf{w}}_{dl}^H \mathbf{D}_{dl}^{-1/2} (\mathbf{C}_{dl} - \gamma \mathbf{E}_{dl}) \mathbf{D}_{dl}^{-1/2} \hat{\mathbf{w}}_{dl} \geq \gamma \sigma_n^2 \end{aligned} \tag{3.27}$$

where $\mathbf{C}_{dl} = \text{diag}(\mathbf{g}_{dl}^T) \mathbf{H}_{dl} \mathbf{t}_{dl} \mathbf{t}_{dl}^H \mathbf{H}_{dl}^H \text{diag}(\mathbf{g}_{dl}^*)$ and $\mathbf{E}_{dl} = \sigma_{dl,v}^2 \text{diag}(\mathbf{g}_{dl}^T) \text{diag}(\mathbf{g}_{dl}^*)$.

We note that problem (3.27) is equivalent to that in [11], Eq. (12). The optimum solution to (3.27) appears as [11], Eq. (19), and the corresponding transmit power is given by [11], Eq. (20).

3.4.4 Joint Determination of Linear Precoder and Relay Weights

To achieve the objective of low-power linear precoding and relay beamforming, the following iterative algorithm is proposed:

1. Initialize the DRBF vector as $\mathbf{w}_{dl} = c_{dl}\ \mathrm{vec}(\mathbf{v}_{dl})$, where constant c_{dl} is chosen to be large relative to $\sigma^2_{dl,n}$, and $\mathbf{v}_{dl,i} = e^{j\theta_i}$, where θ_i is a random variable uniformly distributed over $[0, 2\pi]$.

2. Solve (3.12) using semi-definite programming to optimize the precoder with the current relay weights fixed. Use the rank-one matrices to obtain the precoder vectors (as discussed in Remark 1, the problem 3.12 has at least one rank-one matrix solution, so the rank-one solution can be used to obtain the precoder vectors through eigen decomposition).

3. If a solution to Step 2 exists, then continue on to Step 4. Otherwise, loosen the SINR constraints of (3.12) and go back to Step 2.

4. Solve (3.21) using semi-definite programming. If there is a rank-one solution, e.g., when $M_{dl} \leq 3$, then the relay weights can be obtained as the eigenvector corresponding to the largest eigenvalue of the rank-one matrix. Otherwise apply the randomization method in [55] to obtain the DRBF vector (See Appendix B or details).

5. If the relay sum power is sufficiently close to a fixed point, or else if a predetermined number of iterations is exceeded, then stop. Otherwise go back to Step 3.

We remark that since the transmission power of the source and relays are both lower-bounded, and that in each of Steps 3 and 4 the power is non-increasing, the algorithm hence converge (Lemma 3.1 below). This is apparent by observing that the optimizations in Steps 3 and 4 each have the same SINR constraints.

Lemma 3.1: Provided a feasible solution exists, the iterative algorithm stated above converges.

Proof: See Appendix C.

3.5 Problem formulation for Imperfect Channel State Information

In previous sections, we study the design of precoder and relay weights with perfect CSI. In practice, however, perfect CSI is unattainable due to channel estimation errors. Consequently, it is necessary to design a system robust to imperfect CSI. In this section, we will study how to incorporate the statistics of channel estimation error into the design of the precoder and relay weights of the downlink cooperative MIMO system. The imperfect CSI model for the link from the base station (BS) to the relays is

$$\mathbf{H}_{dl} = \hat{\mathbf{H}}_{dl} + \mathbf{E}_{\mathbf{H}_{dl}} \tag{3.28}$$

with $\hat{\mathbf{H}}_{dl}$ as the estimated channel gain from source to the relays and $\mathbf{E}_{\mathbf{H}_{dl}}$ as the channel estimation error which are i.i.d. Gaussian with variance $\sigma^2_{\mathbf{E}_{\mathbf{H}_{dl}}}$. and the imperfect CSI model for the link from the relays to the jth destination is

$$\mathbf{g}_{dl,j} = \hat{\mathbf{g}}_{dl,j} + \mathbf{e}^T_{\mathbf{g}_{dl,j}} \tag{3.29}$$

with $\hat{\mathbf{g}}_{dl,j}$ as the estimated channel gain from relays to the jth destination and $\mathbf{e}^T_{\mathbf{g}_{dl,j}}$ as the channel estimation error which are i.i.d. Gaussian with variance $\sigma^2_{\mathbf{e}_{\mathbf{g}_{dl}}}$.

3.5.1 Precoder with Imperfect Channel State Information

With the imperfectly estimated CSI model above, the precoder design for perfect CSI can be generalized to the imperfect CSI case. Combining (3.28) and (3.29), the received signal (3.3) at the jth destination can be rewritten as

$$y_{dl,j} = \underbrace{\hat{\mathbf{g}}^T_{dl,j}\mathbf{W}^H_{dl}\hat{\mathbf{H}}_{dl}\mathbf{t}_{dl,j}s_{dl,j}}_{desired\ signal} + \underbrace{\hat{\mathbf{g}}^T_{dl,j}\mathbf{W}^H_{dl}\hat{\mathbf{H}}_{dl}\sum_{i=1,i\neq j}^{M_{dl}}\mathbf{t}_{dl,i}s_{dl,i}}_{Interference} + \underbrace{\xi_{dl,j}}_{noise} \tag{3.30}$$

where the noise term

$$\xi_{dl,j} = \hat{\mathbf{g}}_{dl,j}^T \mathbf{W}_{dl}^H \mathbf{E}_{\mathbf{H}_{dl}} \sum_{i=1}^{M_{dl}} \mathbf{t}_{dl,i} s_{dl,i} + \mathbf{e}_{\mathbf{g}_{dl,j}}^T \mathbf{W}_{dl}^H (\hat{\mathbf{H}}_{dl} + \mathbf{E}_{\mathbf{H}_{dl}}) \sum_{i=1}^{M_{dl}} \mathbf{t}_{dl,i} s_{dl,i} + (\hat{\mathbf{g}}_{dl,j}^T + \mathbf{e}_{\mathbf{g}_{dl,j}}^T) \mathbf{W}_{dl}^H \nu_{dl,r} + n_{dl,j},$$

Using (3.30) and (3.31), the signal power $P_{dl,s}$, interference power $P_{dl,i}$ and noise power $P_{dl,n}$ in SINR constraints (3.4) and (3.5) become

$$\hat{P}_{dl,s}^j = \mathbf{t}_{dl,j}^H \hat{\mathbf{H}}_{dl}^H \mathbf{W}_{dl} \hat{\mathbf{g}}_{dl,j}^* \hat{\mathbf{g}}_{dl,j}^T \mathbf{W}_{dl}^H \hat{\mathbf{H}}_{dl} \mathbf{t}_{dl,j}, \tag{3.31}$$

$$\hat{P}_{dl,i}^j = \sum_{i=1, i\neq j}^{M_{dl}} \mathbf{t}_{dl,i}^H \hat{\mathbf{H}}_{dl}^H \mathbf{W}_{dl} \hat{\mathbf{g}}_{dl,j}^* \hat{\mathbf{g}}_{dl,j}^T \mathbf{W}_{dl}^H \hat{\mathbf{H}}_{dl} \mathbf{t}_{dl,i}, \text{ and} \tag{3.32}$$

$$\hat{P}_{dl,n}^j = \hat{P}_{dl,n_1}^j + \hat{P}_{dl,n_2}^j + \hat{P}_{dl,n_3}^j + \hat{P}_{dl,n_4}^j, \tag{3.33}$$

where

$$\begin{aligned}
\hat{P}_{dl,n_1}^j &= \sum_{i=1}^{M_{dl}} \frac{\sigma_{dl,ce}^2}{1+\sigma_{dl,ce}^2} \mathrm{Tr}(\mathbf{W}_{dl} \hat{\mathbf{g}}_{dl,j}^* \hat{\mathbf{g}}_{dl,j}^T \mathbf{W}_{dl}^H) \mathbf{t}_{dl,i}^H \mathbf{t}_{dl,i}, \\
\hat{P}_{dl,n_2}^j &= \sum_{i=1}^{M_{dl}} \mathbf{t}_{dl,i}^H \hat{\mathbf{H}}_{dl}^H \mathbf{W}_{dl} \mathbf{R}_{\mathbf{e}_{g_{dl}}}^j \mathbf{W}_{dl}^H \hat{\mathbf{H}}_{dl} \mathbf{t}_{dl,i}, \\
\hat{P}_{dl,n_3}^j &= \sum_{i=1}^{M_{dl}} \frac{\sigma_{dl,ce}^2}{1+\sigma_{dl,ce}^2} \mathrm{Tr}(\sigma_{\mathbf{e}_{\mathbf{g}_{dl}}}^2 \mathbf{W}_{dl} \mathbf{W}_{dl}^H) \mathbf{t}_{dl,i}^H \mathbf{t}_{dl,i}, \\
\hat{P}_{dl,n_4}^j &= \sigma_{dl,\nu}^2 \mathrm{Tr}(\mathbf{W}_{dl}^H \left(\hat{\mathbf{g}}_{dl,j}^* \hat{\mathbf{g}}_{dl,j}^T + \sigma_{\mathbf{e}_{\mathbf{g}_{dl}}}^2 \mathbf{I}_{n_R^{dl}} \right) \mathbf{W}_{dl}) + \sigma_{dl,n}^2,
\end{aligned} \tag{3.34}$$

and with $\mathbf{R}_{\mathbf{e}_{\mathbf{g}_{dl}}}^j = E(\mathbf{e}_{\mathbf{g}_{dl,j}} \mathbf{e}_{\mathbf{g}_{dl,j}}^H) = \sigma_{\mathbf{e}_{\mathbf{g}_{dl}}}^2 \mathbf{I}_{n_R^{dl}}$. Following similar procedures as in Section 3.3 using the above expressions, the precoder optimization of (3.4) can be reformulated as

$$\min_{\mathbf{t}_{dl,1}, \mathbf{t}_{dl,2}, \ldots, \mathbf{t}_{dl,M_{dl}}} \sum_{j=1}^{M_{dl}} \mathbf{t}_{dl,j}^H \mathbf{t}_{dl,j}$$

$$\mathbf{t}_{dl,j}^H \mathbf{Q}_{j,j}^{dl} \mathbf{t}_{dl,j} \geq \gamma_{dl,j} \sum_{i=1, i\neq j}^{M_{dl}} \mathbf{t}_{dl,i}^H \mathbf{Q}_{i,j}^{dl} \mathbf{t}_{dl,i} + \gamma_{dl,j} P_{dl,n_4}^j, j = 1, \ldots, M_{dl} \tag{3.35}$$

where

$$\mathbf{Q}_{j,j}^{dl} = \hat{\mathbf{H}}_{dl}^H \mathbf{W}_{dl} \hat{\mathbf{g}}_{dl,j}^* \hat{\mathbf{g}}_{dl,j}^T \mathbf{W}_{dl}^H \hat{\mathbf{H}}_{dl} - \gamma_{dl,j} \sigma_{\mathbf{e}_{\mathbf{g}_{dl}}}^2 \hat{\mathbf{H}}_{dl}^H \mathbf{W}_{dl} \mathbf{W}_{dl}^H \hat{\mathbf{H}}_{dl} - \tag{3.36}$$
$$\gamma_{dl,j} \frac{\sigma_{dl,ce}^2}{1+\sigma_{dl,ce}^2} \mathrm{Tr}(\mathbf{W}_{dl} \hat{\mathbf{g}}_{dl,j}^* \hat{\mathbf{g}}_{dl,j}^T, \mathbf{W}_{dl}^H) \mathbf{I} - \gamma_{dl,j} \frac{\sigma_{dl,ce}^2}{1+\sigma_{dl,ce}^2} \sigma_{\mathbf{e}_{\mathbf{g}_{dl}}}^2 \mathrm{Tr}(\mathbf{W}_{dl} \mathbf{W}_{dl}^H) \mathbf{I},$$

and where for $i \neq j$,

$$\mathbf{Q}_{i,j}^{dl} = \mathbf{H}_{dl}^H \mathbf{W}_{dl} \hat{\mathbf{g}}_{dl,j}^* \hat{\mathbf{g}}_{dl,j}^T \mathbf{W}_{dl}^H \hat{\mathbf{H}}_{dl} + \frac{\sigma_{dl,ce}^2}{1+\sigma_{dl,ce}^2} \mathrm{Tr}(\mathbf{W}_{dl} \hat{\mathbf{g}}_{dl,j}^* \hat{\mathbf{g}}_{dl,j}^T \mathbf{W}_{dl}^H) + \tag{3.37}$$
$$\sigma_{\mathbf{e}_{\mathbf{g}_{dl}}}^2 \hat{\mathbf{H}}_{dl}^H \mathbf{W}_{dl} \mathbf{W}_{dl}^H \hat{\mathbf{H}}_{dl} + \frac{\sigma_{dl,ce}^2}{1+\sigma_{dl,ce}^2} \sigma_{\mathbf{e}_{\mathbf{g}_{dl}}}^2 \mathrm{Tr}(\mathbf{W}_{dl} \mathbf{W}_{dl}^H).$$

We remark that if the conditions of Remark 1 are satisfied for the imperfect CSI case, and following a similar approach to Section 3.3, the optimum precoder can be obtained. The proof follows similarly to that of Remark 1.

3.5.2 Distributed Beamforming with Imperfect Channel State Information

We now consider the minimum power DRBF optimization with the imperfect CSI model for a given precoder. Using results from Section 3.2, the received signal (3.13) at the jth destination can be written as

$$y_{dl,j} = \underbrace{\mathbf{w}_{dl}^H \mathrm{diag}(\hat{\mathbf{g}}_{dl,j}^T) \hat{\mathbf{H}}_{dl} \mathbf{t}_{dl,j} s_{dl,j}}_{desired\ \ signal} + \underbrace{\mathbf{w}_{dl}^H \mathrm{diag}(\hat{\mathbf{g}}_{dl,j}^T) \hat{\mathbf{H}}_{dl} \sum_{i=1, i\neq j}^{M_{dl}} \mathbf{t}_{dl,i} s_{dl,i}}_{Interference} + \underbrace{\varsigma_{dl,j}}_{noise} \tag{3.38}$$

where the noise term

$$\varsigma_{dl,j} = \mathbf{w}_{dl}^H \mathrm{diag}(\hat{\mathbf{g}}_{dl,j}^T) \mathbf{E}_{\mathbf{H}_{dl}} \textstyle\sum_{i=1}^{M_{dl}} \mathbf{t}_{dl,i} s_{dl,i} + \mathbf{w}_{dl}^H \mathrm{diag}(\hat{\mathbf{g}}_{dl,j}^T + \mathbf{e}_{\mathbf{g}_{dl,j}}^T) \nu_{dl,r} \tag{3.39}$$
$$+ \mathbf{w}_{dl}^H \mathrm{diag}(\mathbf{e}_{\mathbf{g}_{dl,j}}^T) (\hat{\mathbf{H}}_{dl} + \mathbf{E}_{\mathbf{H}_{dl}}) \textstyle\sum_{i=1}^{M_{dl}} \mathbf{t}_{dl,i} s_{dl,i} + n_{dl,j}.$$

Similar to the previous section, the DRBF optimization can also be generalized to the case of imperfect CSI. With (3.38) and (3.39), following a similar approach as in Section 3.4.1, the optimization

of the relay weights (3.14) can be formulated as:

$$\min_{\mathbf{w}} \quad \mathbf{w}_{dl}^H \hat{\mathbf{D}} \mathbf{w}_{dl} \tag{3.40}$$

$$s.t. \quad \mathbf{w}_{dl}^H \left(\hat{\mathbf{U}}_{dl,j} - \gamma_{dl,j} \hat{\mathbf{V}}_{dl,j} \right) \mathbf{w}_{dl} \geq \gamma_{dl,j} \sigma_{dl,n}^2$$

$$\text{for} \quad j = 1, 2, \ldots, M_{dl},$$

where for imperfect CSI $\mathbf{R}_x$ in (3.16) becomes

$$\hat{\mathbf{R}}_{dl,\mathbf{x}} = \hat{\mathbf{H}}_{dl} \left(\sum_{k=1}^{M_{dl}} \mathbf{t}_{dl,k} \mathbf{t}_{dl,k}^H \right) \hat{\mathbf{H}}_{dl}^H + \frac{\sigma_{dl,ce}^2}{1+\sigma_{dl,ce}^2} \mathrm{Tr} \left(\sum_{k=1}^{M_{dl}} \mathbf{t}_{dl,k} \mathbf{t}_{dl,k}^H \right) \mathbf{I}_{n_R^{dl}} + \sigma_{dl,v}^2 \mathbf{I}_{n_R^{dl}}, \tag{3.41}$$

$$\hat{\mathbf{U}}_{dl,j} = \mathrm{diag}(\hat{\mathbf{g}}_{dl,j}^T) \hat{\mathbf{H}}_{dl} \mathbf{t}_{dl,j} \mathbf{t}_{dl,j}{}^H \hat{\mathbf{H}}_{dl}^H \mathrm{diag}(\hat{\mathbf{g}}_{dl,j}^*), \ \textit{and} \tag{3.42}$$

$$\begin{aligned} \hat{\mathbf{V}}_{dl,j} = {} & \mathrm{diag}(\hat{\mathbf{g}}_{dl,j}^T) \hat{\mathbf{H}}_{dl} \left(\sum_{i=1, i\neq j}^{M_{dl}} \mathbf{t}_{dl,i} \mathbf{t}_{dl,i}^H \right) \hat{\mathbf{H}}_{dl}^H \mathrm{diag}(\hat{\mathbf{g}}_{dl,j}^*) \\ & + \frac{\sigma_{dl,ce}^2}{1+\sigma_{dl,ce}^2} \mathbf{w}_{dl}^H \mathrm{diag}(\hat{\mathbf{g}}_{dl,j}^T) \hat{\mathbf{H}}_{dl} \left(\sum_{i=1, i\neq j}^{M_{dl}} \mathbf{t}_{dl,i} \mathbf{t}_{dl,i}^H \right) \hat{\mathbf{H}}_{dl}^H \mathrm{diag}(\hat{\mathbf{g}}_{dl,j}^*) \mathbf{w}_{dl} \\ & + \sigma_{dl,v}^2 \mathbf{w}_{dl}^H (\mathrm{diag}(\hat{\mathbf{g}}_{dl,j}^T) \mathrm{diag}(\hat{\mathbf{g}}_{dl,j}^*) + \sigma_{\mathbf{e}_{\mathbf{g}_{dl}}}^2 \mathbf{I}_{n_R^{dl}}) \mathbf{w}_{dl} \\ & + \sigma_{\mathbf{e}_{\mathbf{g}_{dl}}}^2 \mathbf{w}_{dl}^H \mathrm{diag}(\hat{\mathbf{H}}_{dl} (\sum_{i=1}^{M_{dl}} \mathbf{t}_{dl,i} \mathbf{t}_{dl,i}^H) \hat{\mathbf{H}}_{dl}^H)) \mathbf{w}_{dl} + \frac{\sigma_{dl,ce}^2}{1+\sigma_{dl,ce}^2} \sigma_{\mathbf{e}_{\mathbf{g}_{dl}}}^2 \mathbf{w}_{dl}^H \mathrm{diag}(\sum_{i=1}^{M_{dl}} \mathbf{t}_{dl,i} \mathbf{t}_{dl,i}^H) \mathbf{w}_{dl}. \end{aligned} \tag{3.43}$$

We note here that joint iteration of the precoder and DRBF similarly applies to the imperfect CSI case with similar convergence properties.

3.6 Multiple receive antennas at the terminals

3.6.1 Multiple Data Streams for Each User

In this section, we consider the case where each user has multiple antennas that also support multiple data streams. Assume that the ith user terminal has l_i antennas and supports l_i data streams. Here

we make the assumption that the assumption that $\sum_{i=1}^{M_{dl}} l_i \leq N_{dl}$. For the ith user, the corresponding precoder vectors and transmitted signals are $[\mathbf{t}_{dl,i,1} \dots \mathbf{t}_{dl,i,l_i}]$ and $\mathbf{S}_{dl,i} = [s_{dl,i,1} \dots s_{dl,i,l_i}]'$, respectively,

$$\mathbf{y}_{dl,i} = \mathbf{G}_{dl,i}\mathbf{W}_{dl}^H\mathbf{H}_{dl}\sum_{j=1}^{l_i}\mathbf{t}_{dl,i,j}s_{dl,i,j} + \mathbf{G}_{dl,i}\mathbf{W}_{dl}^H\mathbf{H}_{dl}\sum_{k=1,k\neq i}^{M_{dl}}\sum_{j=1}^{l_k}\mathbf{t}_{dl,k,j}s_{dl,k,j} + \mathbf{G}_{dl,i}\mathbf{W}_{dl}^H\nu_{dl} + \mathbf{n}_{dl,i}, \quad i = 1,\dots,M_{dl} \tag{3.44}$$

where $\mathbf{G}_{dl,i}$ denotes the channel from the relays to the ith receiver. The linear minimum mean square error (LMMSE) receiver for the ith user with given precoder and relay weights is derived according to Section 2.1.1 as follows:

$$\Xi_i = (\mathbf{G}_{dl,i}\mathbf{W}_{dl}^H\mathbf{H}_{dl}\sum_{j=1}^{l_i}\mathbf{t}_{dl,i,j})^H\left(\mathbf{G}_{dl,i}\mathbf{W}_{dl}^H\mathbf{H}_{dl}(\sum_{j=1}^{l_i}\sum_{k=1}^{l_i}\mathbf{t}_{dl,i,j}\mathbf{t}_{dl,i,k}^H)\mathbf{H}_{dl}^H\mathbf{W}_{dl}\mathbf{G}_{dl,i}^H + \Psi_i\right)^{-1} \tag{3.45}$$

where Ψ_i is the covariance of the interference and the colored noise as

$$\Psi_i = \mathbf{G}_{dl,i}\mathbf{W}_{dl}^H\mathbf{H}_{dl}\left(\sum_{k=1,k\neq i}^{M_{dl}}\sum_{m=1}^{l_k}\sum_{n=1}^{l_k}\mathbf{t}_{dl,k,j}\mathbf{t}_{dl,k,n}^H\right)\mathbf{H}_{dl}^H\mathbf{W}_{dl}\mathbf{G}_{dl,i}^H + \sigma_{dl,\nu}^2\mathbf{G}_{dl,i}\mathbf{W}_{dl}^H\mathbf{W}_{dl}\mathbf{G}_{dl,i}^H \tag{3.46}$$

and the estimate of the signal vector is

$$\hat{\mathbf{S}}_{dl,i} = \Xi_i\mathbf{y}_{dl,i}. \tag{3.47}$$

The decoding vector of the jth data stream for ith user is the jth row of Ξ_i

$$\Xi_{i,j} = [(\Xi_i)^T]_j. \tag{3.48}$$

So the estimate of the jth data stream of ith user can be written as

$$\hat{s}_{dl,i,j} = \underbrace{\Xi_{i,j}^T\mathbf{G}_{dl,i}\mathbf{W}_{dl}^H\mathbf{H}_{dl}\mathbf{t}_{dl,i,j}s_{dl,i,j}}_{signal} + + \underbrace{\Xi_{i,j}^T\mathbf{G}_{dl,i}\mathbf{W}_{dl}^H\nu_{dl} + \mathbf{n}_{dl,i}}_{colored\ \ noise}$$
$$+ \underbrace{\Xi_{i,j}^T\mathbf{G}_{dl,i}\mathbf{W}_{dl}^H\mathbf{H}_{dl}\sum_{j=1,j\neq i}^{M_{dl}}\mathbf{t}_{dl,i,j}s_{dl,i,j} + \Xi_{i,j}^T\mathbf{G}_{dl,i}\mathbf{W}_{dl}^H\mathbf{H}_{dl}\sum_{k=1,k\neq i}^{M_{dl}}\sum_{n=1}^{l_k}\mathbf{t}_{dl,k,n}\mathbf{S}_{dl,k}}_{interference} \tag{3.49}$$

.

Next we can follow the procedures in the precoder optimization, we reformulate the precoder optimization as follows:

$$\begin{aligned} & \sum_{i=1}^{M_{dl}} \sum_{j=1}^{l_i} \mathrm{Tr}\{\mathbf{t}_{dl,i,j}\mathbf{t}_{dl,i,j}^H\} \\ s.t \quad & \frac{\mathbf{t}_{dl,i,j}^H \mathbf{H}_{dl}^H \mathbf{W}_{dl} \mathbf{G}_{dl,i}^H \Xi_{i,j}^* \Xi_{i,j}^T \mathbf{G}_{dl,i} \mathbf{W}_{dl}^H \mathbf{H}_{dl} \mathbf{t}_{dl,i,j}}{\sum_{j=1,j\neq i}^{M_{dl}} \sum_{k=1}^{l_j} \mathbf{t}_{j,k}^H \mathbf{H}_{dl}^H \mathbf{W}_{dl} \mathbf{G}_{dl,j}^H \Xi_{j,k}^* \Xi_{j,k}^T \mathbf{G}_{dl,j} \mathbf{W}_{dl}^H \mathbf{H}_{dl} \mathbf{t}_{j,k} + \varpi_{i,j}} \\ & \geq \gamma_{dl,i,j} \quad for \quad i = 1,2,\ldots,M_{dl}, \ \ , j = 1,\ldots,l_i \end{aligned} \tag{3.50}$$

where

$$\varpi_{i,j} = \mathrm{Tr}\{\mathbf{W}_{dl} \mathbf{G}_{dl,i}^H \Xi_{i,j}^* \Xi_{i,j}^T \mathbf{G}_{dl,i} \mathbf{W}_{dl}^H\} \sigma_{dl,v}^2 + \sigma_{dl,n}^2. \tag{3.51}$$

Define $\Upsilon_{i,j} = \mathbf{t}_{dl,i,j}\mathbf{t}_{dl,i,j}^H$.

After dropping the constraints $\mathrm{rank}(\Upsilon_{i,j}) = 1, i = 1,2,\ldots,M_{dl}, \ \ j = 1,\ldots,l_i$, (3.50) becomes

$$\begin{aligned} & \min_{\Upsilon_{i,j}} \quad \sum_{i=1}^{M_{dl}} \sum_{j=1}^{l_i} \mathrm{Tr}(\Upsilon_{i,j}) \\ s.t. \quad & \mathrm{Tr}(\mathbf{U}_{i,j}(\Upsilon_{i,j} - \gamma_{dl,i,j} \sum_{m=1,m\neq j}^{l_i} \Upsilon_{i,m} - \gamma_{dl,i,j} \sum_{m=1,m\neq i}^{M_{dl}} \sum_{n=1}^{l_m} \Upsilon_{m,n})) \geq \gamma_{dl,i,j} P_n^{i,j}, \\ & \Upsilon_{i,j} \succeq 0 \quad for \ \ i = 1,2,\ldots,M_{dl}, \ \ j = 1,\ldots,l_i \end{aligned} \tag{3.52}$$

where $\mathbf{U}_{i,j} = \mathbf{H}_{dl}^H \mathbf{W}_{dl} \mathbf{G}_{dl,i}^H \Xi_{i,j}^* \Xi_{i,j}^T \mathbf{G}_{dl,i} \mathbf{W}_{dl}^H \mathbf{H}_{dl}$. The optimization of (3.52) follows a similar procedure as that of the precoder optimization in Section 3.3.

The estimated signal (3.49) can be rewritten as

$$\begin{aligned} \hat{s}_{dl,i,j} = & \underbrace{\mathbf{w}_{dl}{}^H \mathrm{diag}(\Xi_{i,j}^T \mathbf{G}_{dl,i}) \mathbf{H}_{dl} \mathbf{t}_{dl,i,j} s_{dl,i,j}}_{signal} \\ & + \underbrace{\mathbf{w}_{dl}{}^H \mathrm{diag}(\Xi_{i,j}^T \mathbf{G}_{dl,i}) \mathbf{H}_{dl} \sum_{j=1,j\neq i}^{M_{dl}} \mathbf{t}_{dl,i,j} s_{dl,i,j} + \mathbf{w}_{dl}{}^H \mathrm{diag}(\Xi_{i,j}^T \mathbf{G}_{dl,i}) \mathbf{H}_{dl} \sum_{k=1,k\neq i}^{M_{dl}} \sum_{n=1}^{l_k} \mathbf{t}_{dl,k,n} \mathbf{S}_k}_{interference} \end{aligned} \tag{3.53}$$

$$+\underbrace{\mathbf{w}_{dl}{}^{H}\mathrm{diag}(\Xi_{i,j}^{T}\mathbf{G}_{dl,i})\nu_{dl}+\mathbf{n}_{dl,i}}_{colored\ \ noise}$$

The relay beamforming weight optimization can be written as

$$\begin{aligned}\min_{\mathbf{w}_{dl}} \quad & \mathbf{w}_{dl}{}^{H}\ddot{\mathbf{D}}_{dl}\mathbf{w}_{dl} \\ s.t. \quad & \mathbf{w}_{dl}{}^{H}\left(\ddot{\mathbf{E}}_{i,j}-\gamma_k\ddot{\mathbf{F}}_{i,j}\right)\mathbf{w}_{dl}\geq\gamma_{dl,i,j}\sigma_{dl,n}^{2} \\ & for \quad i=1,2,\ldots,M_{dl}, \quad j=1,\ldots,l_i\end{aligned} \tag{3.54}$$

where $\ddot{\mathbf{D}}_{dl}=\mathrm{diag}([\mathbf{R}_{dl,\mathbf{x}}]_{1,1},[\mathbf{R}_{dl,\mathbf{x}}]_{2,2},\ldots,[\mathbf{R}_{dl,\mathbf{x}}]_{n_R^{dl},n_R^{dl}}),\mathbf{R}_{dl,\mathbf{x}}=\mathbf{H}_{dl}^{H}(\sum_{i=1}^{M_{dl}}\sum_{j=1}^{l_i}\mathbf{t}_{dl,i,j}\mathbf{t}_{dl,i,j}^{H})\mathbf{H}_{dl}^{H}+\sigma_{dl,v}^{2}\mathbf{I}$ and

$$\begin{aligned}\ddot{\mathbf{E}}_{i,j} &= \mathrm{diag}(\Xi_{i,j}^{T}\mathbf{G}_{dl,i})\mathbf{H}_{dl}\mathbf{t}_{dl,i,j}\mathbf{t}_{dl,i,j}^{H}\mathbf{H}_{dl}^{H}\mathrm{diag}(\Xi_{i,j}^{T}\mathbf{G}_{dl,i})^{*} \\ \ddot{\mathbf{F}}_{i,j} &= \mathrm{diag}(\Xi_{i,j}^{T}\mathbf{G}_{dl,i})\left(\mathbf{H}_{dl}(\sum_{j=1,j\neq i}^{M_{dl}}\sum_{k=1}^{l_i}\mathbf{t}_{dl,j,k}\mathbf{t}_{dl,j,k}^{H}+\sum_{m=1,m\neq j}^{l_i}\mathbf{t}_{dl,i,m}\mathbf{t}_{dl,i,m}^{H})\mathbf{H}_{dl}^{H}+\sigma_{dl,v}^{2}\mathbf{I}\right) \\ & \quad \mathrm{diag}(\Xi_{i,j}^{T}\mathbf{G}_{dl,i}).\end{aligned} \tag{3.55}$$

Denoting $\Lambda=\mathbf{w}_{dl}\mathbf{w}_{dl}{}^{H}$ and follow the same procedures in Section 3.4, the relay weights optimization (3.54) can be written as

$$\begin{aligned}\min_{\Lambda} \quad & \mathrm{Tr}(\Lambda\ddot{\mathbf{D}}_{dl}) \\ s.t. \quad & \mathrm{Tr}\left(\Lambda(\ddot{\mathbf{E}}_{i,j}-\gamma_k\ddot{\mathbf{F}}_{i,j})\right)\geq\gamma_{dl,i,j}\sigma_{dl,n}^{2} \\ & and \quad \Lambda\succeq 0 \\ for \quad & i=1,2,\ldots,M_{dl} \quad ,j=1,\ldots,l_i.\end{aligned} \tag{3.56}$$

The overall iterative algorithm for the cooperative system with multiple receive antennas is as follows:

1. Initialize the relay beamforming vector as $\mathbf{w}_{dl}=c_{dl}*vec(\mathbf{v})_{dl}$, where constant c is chosen to be large relative to $\sigma_{dl,n}^{2}$, and $\mathbf{v}_{dl,i}=e^{j\theta_i}$, where θ_i is a random variable, uniformly distributed over $[0,2\pi]$, $\Xi_{i,j}^{T}=[1\ldots1]$.

2. Check the feasibility of the constraints of (3.52). If not feasible, then modify the SINR constraints and go back to Step 1.

3. Solve (3.52) using semidefinite programming to optimize the precoder with the current relay weights and LMMSE receivers given. Use the rank-one matrices to obtain the precoder vectors.

4. Solve (3.56) using semidefinite programming with given precoder and LMMSE receivers, if there is a rank-one solution, then the relay weights can be obtained through eigenvector of the rank one matrix, otherwise apply the randomization method in [55] to obtain the relay weight vector.

5. Obtain the LMMSE receivers as in (3.48) with given precoder and relay weights.

6. If the relay sum power is sufficiently close to a given point, or else if a predetermined number of iterations is exceeded, then stop. Otherwise go back to Step 3.

3.7 Simulation Results

We study the performance of the proposed cooperation methods under three scenarios: 1) perfect CSI available 2) imperfect CSI with different levels of channel estimation quality which are determined by path loss, and 3) perfect CSI and multi-base-station cooperation. For scenarios 1) and 2), we assume N_{dl} source antennas, n_R^{dl} single-antenna relays and M_{dl} single-antenna destinations. According to Section 3.2, N_{dl} and n_R^{dl} time slots are required for channel estimation from the source BS to relays and relays to destinations, respectively. As explained earlier, CSI is assumed to be available to the BS. The channel coefficient matrix $\mathbf{H}_{dl}$ and vector $\mathbf{g}_{dl,k}$ are assumed to be mutually independent where $\mathbf{H}_{dl}$ represents the set of n_R^{dl} distributed channels from the source to the relays and $n_R^{dl} \times 1$ vector $\mathbf{g}_{dl,k}$ represents the n_R^{dl} channels from the relays to the kth destination. Channel vectors $\mathbf{g}_{dl,k}$ are also assumed to be mutually independent.

Figure 3.2 plots the minimum source sum transmit power to noise ratio versus SINR threshold γ with $M_{dl} = 4$ destinations, n_R^{dl} relays, and N_{dl} source antennas. The cases of $N_{dl} = n_R^{dl} = 4$, $N_{dl} = n_R^{dl} = 6$ and $N_{dl} = n_R^{dl} = 8$ are shown. As can be seen, as the numbers of source antennas and relays increase, minimum sum transmit power required at the relays decreases. This is to be expected, since more source antennas and relays result in greater beamforming gain. Figure 3.3 plots the corresponding relay sum power to noise ratios, where it is similarly observed that as more source antennas and relays are added, relay sum power also decreases. A threshold effect, however, is also noted: when SINR constraints exceed about 6 or 8 dB for the case of $N_{dl} = n_R^{dl} = M_{dl} = 4$, transmission power increases sharply. This is due to tightening of SINR constraints, which is exacerbated as the number of source antennas and relays used are reduced to the minimum required. With further reduction of the numbers of antennas and relays, the optimization problem becomes infeasible.

Figure 3.4 shows the effect of the number of relays on performance, where 4 source antennas and 4 destinations ($M_{dl} = N_{dl} = 4$) are compared using $n_R^{dl} = 6, 8$, and 12 relays. It can be observed that even though more relays are used, network total power consumption decreases. Similarly, though not shown for the sake of brevity, the corresponding total transmission power required at the source also decreases as the number of relays increases.

To consider the effect of individual relay power constraints, a scenario of 4 sources, 6 relays and 6 receive antenna destination system is simulated. The maximum allowable power for each relay is chosen to be 6 dB above the average power consumed by each relay in the unconstrained problem. As can be seen from Figure 3.5, such per-relay power constraints do not affect the performance of our technique significantly for a wide range of up to 15 dB.

Figure 3.6 compares algorithm performance as a function of the number of iterations in joint precoder-DRBF optimization of Section 3.4 for the case of $M_{dl} = N_{dl} = 4$ and $n_R^{dl} = 6$. Note that that after about 5 iterations, a fixed point is approached, and that the first two iterations result in the

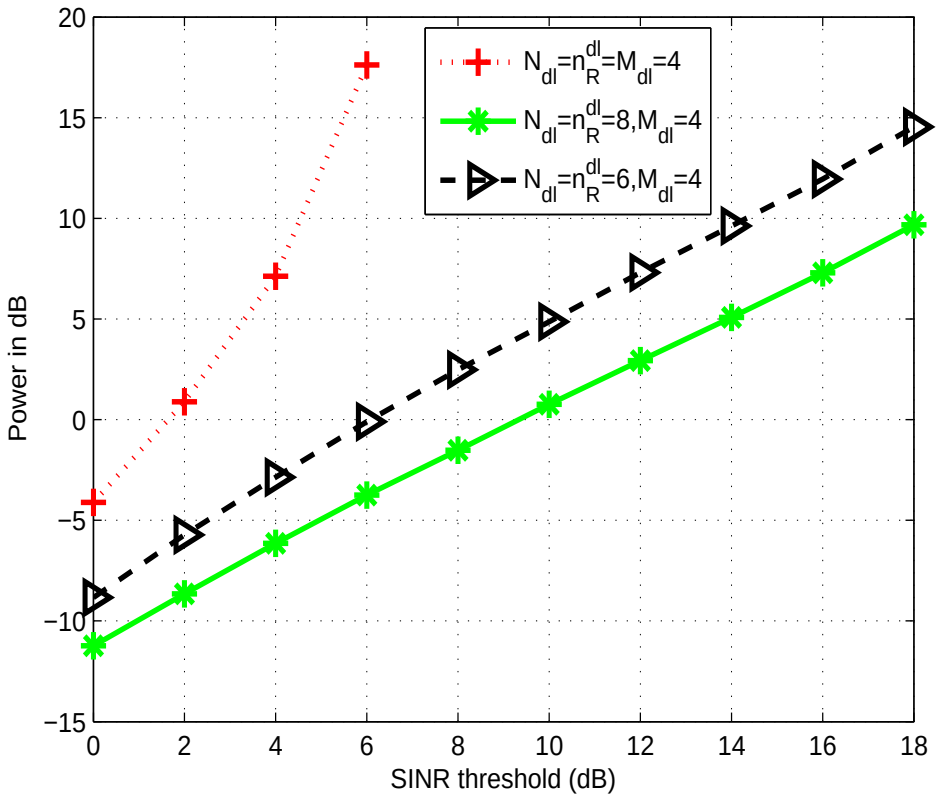

Figure 3.2. Comparison of minimum total source transmit power versus SINR threshold γ as a function of network size for cooperative system with N_{dl} source antennas, n_R^{dl} relays and M_{dl} destinations.

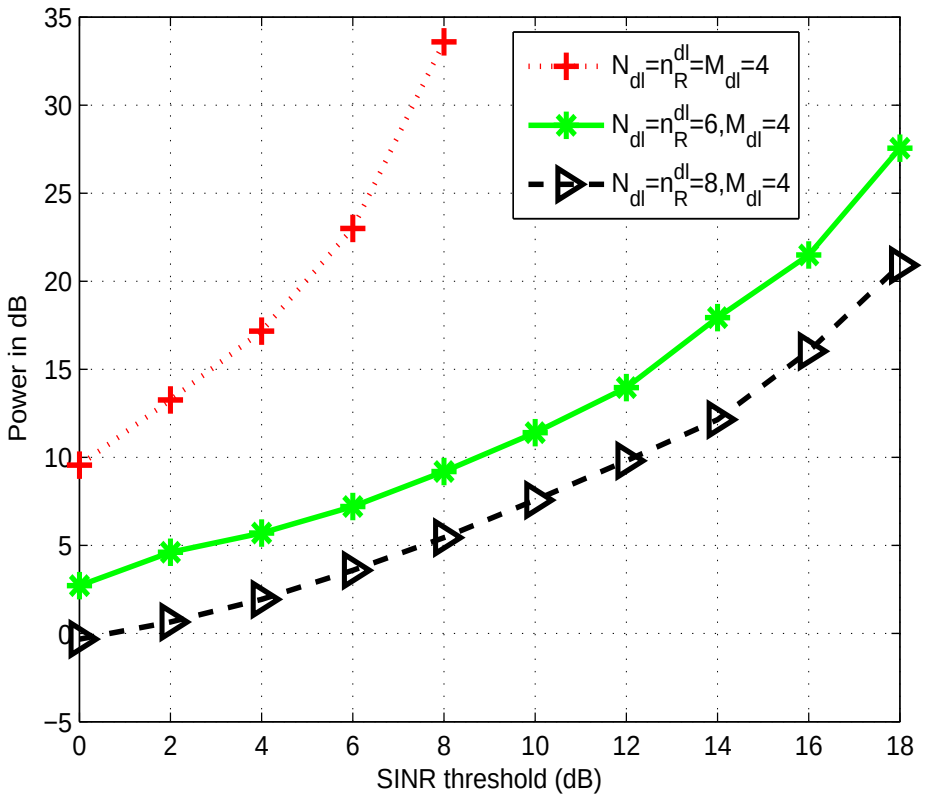

Figure 3.3. Comparison of minimum total relay transmit power versus SINR threshold γ as a function of network size for cooperative system with N_{dl} source antennas, n_R^{dl} relays and M_{dl} destinations.

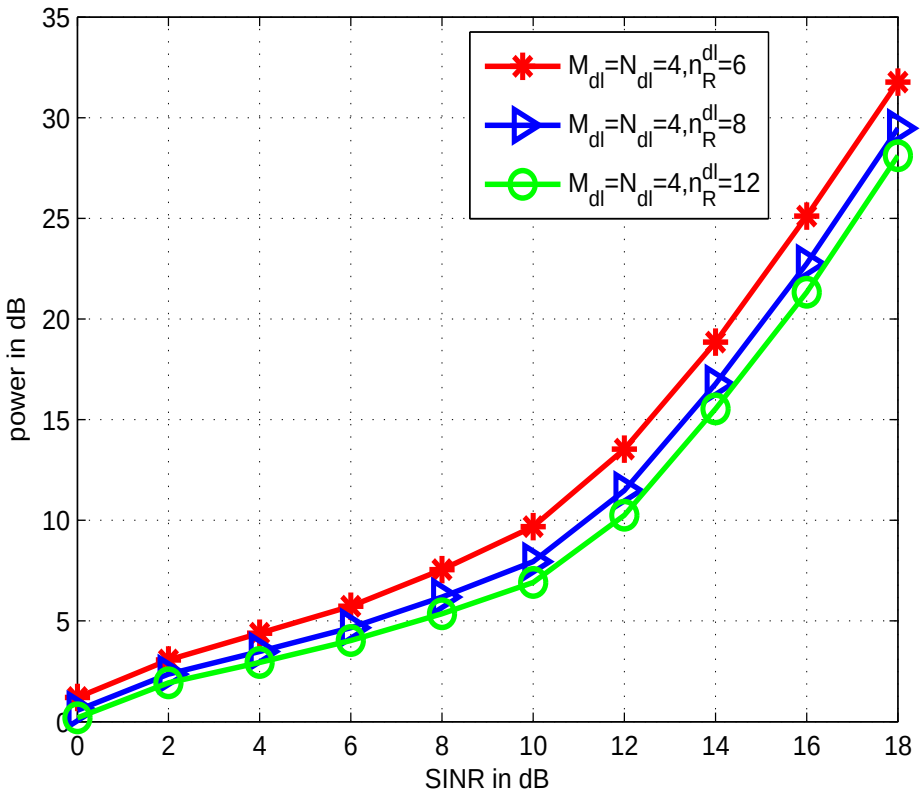

Figure 3.4. Comparison of minimum total relay transmit power versus SINR threshold γ for different numbers of relays for cooperative system with N_{dl} source antennas, n_R^{dl} relays and M_{dl} destinations.

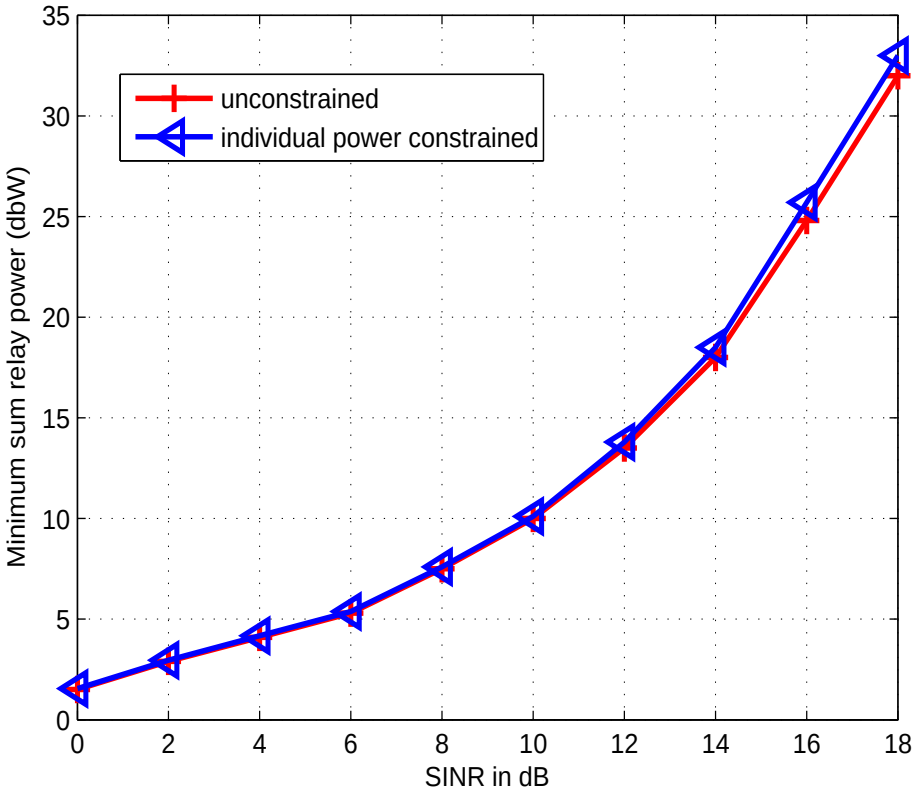

Figure 3.5. Comparison of minimum total relay transmit power with and without power constraints for cooperative system with 4 source antennas, 6 relays and 4 destinations.

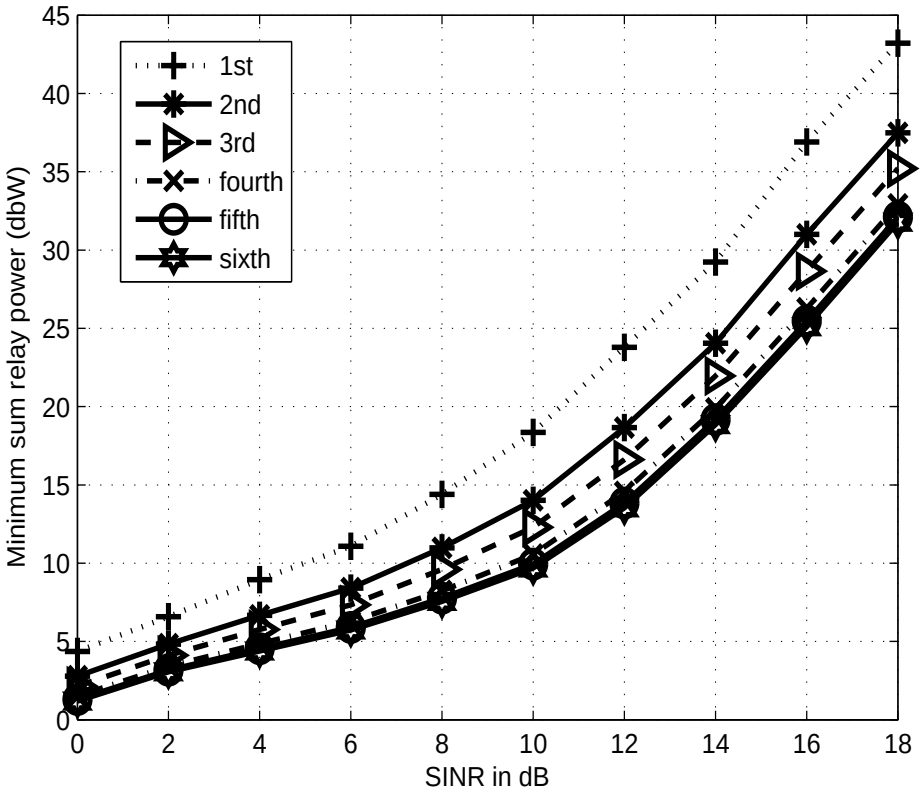

Figure 3.6. Comparison of minimum total relay transmit power versus SINR threshold γ for different numbers of iterations as a function of network size for cooperative system with 4 source antennas, 6 relays and 4 destinations.

largest gain.

Figure 3.7 and 3.8 show the performance of the modified problem formulation of Section 3.5 that takes knowledge of imperfect CSI into account. In the scenario considered, the cooperative system has 6 source antennas, 12 relays and 4 destinations. The matrix

$$\mathbf{R}_{dl,T} = \begin{pmatrix} 1 & \rho_T & \rho_T^2 & \dots & \rho_T^N \\ \rho_T & 1 & \rho_T & \dots & \rho_T^{N-1} \\ \vdots & & \vdots & & \vdots \\ \rho_T^N & \rho_T^{N-1} & \dots & \rho_T^2 & 1 \end{pmatrix} \tag{3.57}$$

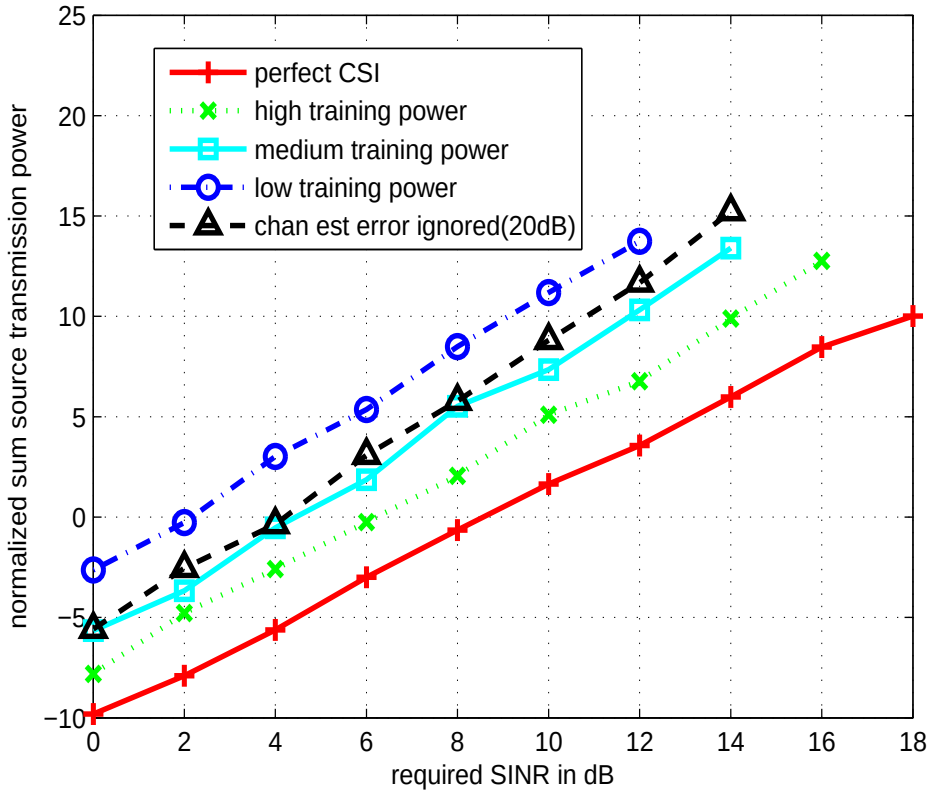

Figure 3.7. Comparison of source transmit sum power versus SINR threshold: effect of imperfect CSI and effect of taking channel estimation error into account.

models correlation for a typical uniform linear array (ULA). In (3.57), we choose the correlation coefficient ρ_T between source antennas to be 0.5. Since the relays are part of the infrastructure of the system, the source to relay distances are fixed and equal. In this case, for channel estimation, we set $\sigma_{ce}^2 = \mathrm{Tr}(\mathbf{R}_{dl,T}^{-1})/P_{tr} = 0.01$. The training power to noise ratio P_{tr}/σ_n^2 is set to 29.7dB.

For channel estimation from relays to destinations, three cases are considered: $P_{tr}/\sigma_{dl,n}^2$ is chosen to be 20 dB (*high* training SNR), 15 dB (*medium* training SNR) and 10 dB (*low* training SNR), corresponding to users at the nominal distance of 250m. The CSI error variances, quantified by the diagonal elements of the $n_R^{dl} \times n_R^{dl}$ matrices $\mathbf{R}_{\mathbf{e}_{dl}}^{j}$ for destinations $j = 1, \ldots M_{dl}$, are determined according to path loss from uniformly distributed users ranging from 250 to 750 meters according to

the lognormal model [56]

$$PL = PL_0 + 10\zeta \log_{10} \frac{d}{d_0} \tag{3.58}$$

where path loss exponent $\zeta = 2.5$, and reference distance $d_0 = 500$m. In (3.58), it is assumed that the effects of small scale fading are averaged out. (The reference power PL_0 is not relevant here due to the normalization.) The additional path loss effects results in CSI estimation error variances in the ranges [20, 31.9], [15, 26.9] and [10, 21.9] dB, corresponding to the cases of *high*, *medium* and *low* training power to noise ratios, respectively. Finally, zero mean independent Gaussian noise is added to the channel estimates with the above CSI error variances.

Figure 3.7 compares source transmission power (normalized to $\sigma^2_{dl,n}$) (i) for perfect CSI, (ii) the formulation in Section 3.5 that takes imperfectly estimated CSI into account for three different channel training SNRs, as well as (iii) a system with imperfectly estimated CSI, for the case of *high* training power, and processed using the formulation from Section 3.3 and Section 3.4 that ignores CSI uncertainly. As shown, for the system formulation based on imperfect CSI, as channel estimation training SNR degrades from high to low, power consumption at the source increases. When channel estimation is perfect, it is noted that in (3.36) and (3.37), $\mathbf{Q}^{dl}_{j,j}$ is positive definite. As CSI estimation quality degrades, eigenvalues of $\mathbf{Q}^{dl}_{j,j}$ decrease while eigenvalues of $\mathbf{Q}^{dl}_{i,j}$ increase, tightening the constraints. As CSI estimation quality degrades further, the constraints tend to become infeasible. As discussed previously, it is clear that the SINR threshold γ_{dl} has a similar effect on the feasibility of the constraints. In the situation where channel estimation error is not taken into account, valid constraints may not be guaranteed. This causes the SINR threshold to degrade to a lower level.

Similar to Figure 3.7, Figure 3.8 compares the sum relay power and shows that as channel estimation quality degrades from high to low, power consumption at the relays increases correspondingly, as expected. As indicated in (3.42) and (3.43), the feasibility of the constraints is determined by the eigenvalues of the matrix $\hat{\mathbf{U}}_{dl,k} - \gamma_{dl,k}\hat{\mathbf{V}}_{dl,k}$. When channel estimation is perfect, the feasibility of

the constraints is mainly affected by the SINR threshold γ_k. As the CSl estimation quality degrades, the eigenvalues of $\hat{\mathbf{U}}_{dl,k} - \gamma_{dl,k}\hat{\mathbf{V}}_{dl,k}$ decrease until $\hat{\mathbf{U}}_{dl,k} - \gamma_{dl,k}\hat{\mathbf{V}}_{dl,k}$ is no longer positive definite. On the other hand, when channel estimation error is not taken account, the precoder matrix and DRBF optimized for the SINR threshold used for the perfect CSI case will no longer result in K valid constraints. To overcome such a situation, the SINR threshold would have to be degraded to a lower level. As shown by these two figures, ignoring the effects of imperfect CSI can result in a loss of performance of approximately 5dB over the range of target SINR QoS values from 0 to 14 dB. When channel estimation quality degrades a lot (for example when the training power is worse than the low training SNR case), the problem easily becomes infeasible.

Figure 3.9 and Figure 3.10 compare source transmission power (normalized to $\sigma^2_{dl,n}$) and sum relay power respectively for a system consisting of 2 users and 6 relays (i) for single antenna at each user ii) MRC with two receive antennas at each user. The figures show that the MRC with two receive antennas has lower power consumption at the source and relays due to the receiver diversity.

Figure 3.11 and Figure 3.12 compares source transmission power and sum relay power respectively for a system consisting of 6 relays for (i) 4 users each with single antenna ii) 2 users each with two receive antennas using LMMSE to receive two data streams at each user. The figures show that the LMMSE has lower power consumption at the source and relays due to interference cancellation of one of the data streams at each user.

3.8 Summary

In this chapter we study the scenario of a downlink broadcast system through a network of relays. For given relay weights, the optimum precoder was derived. For given linear precoder at the base station, the relay weights are optimized using semidefinite programming relaxation. We also proposed an

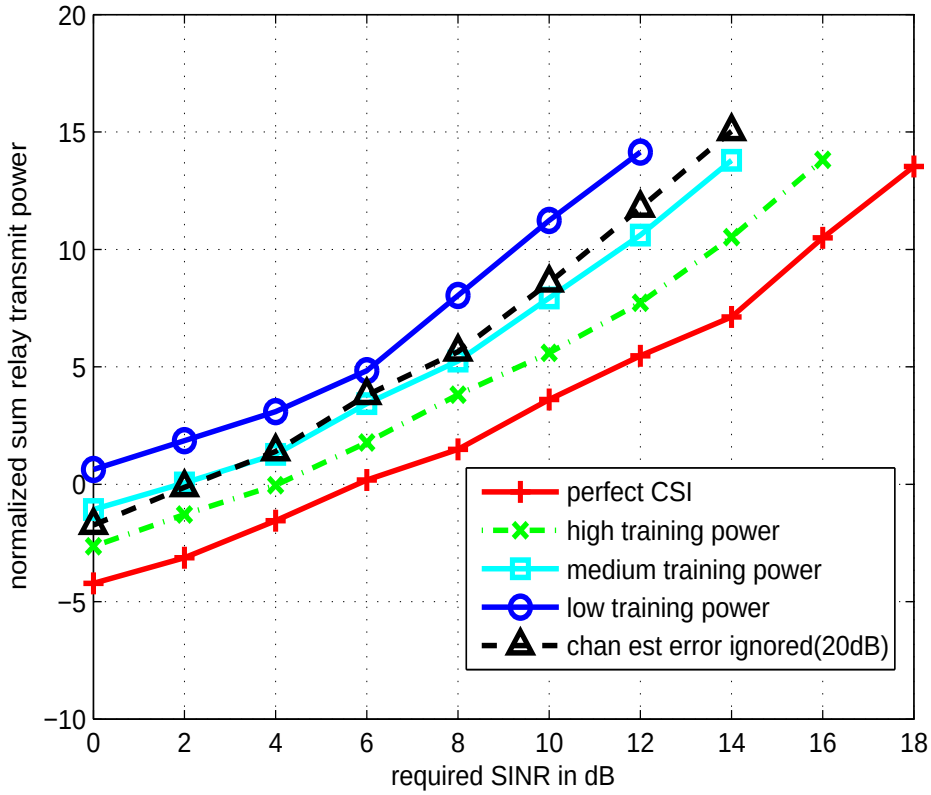

Figure 3.8. Comparison of relay transmit sum power versus SINR threshold: effect of imperfect CSI and effect of taking channel estimation error into account.

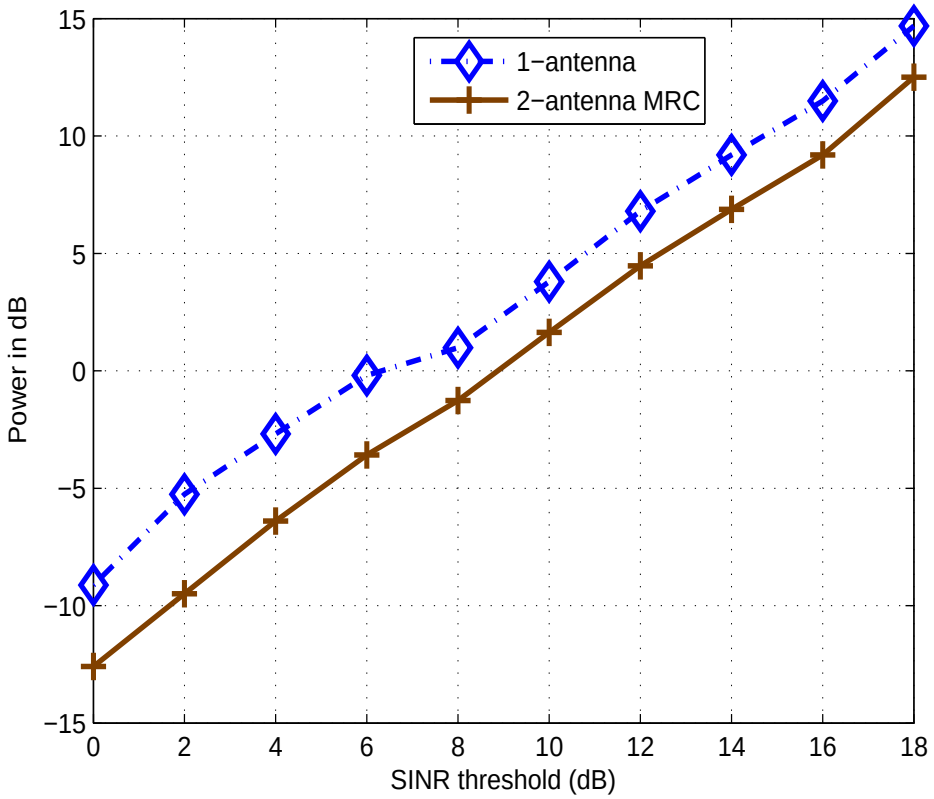

Figure 3.9. Comparison of minimum total source transmit power versus SINR threshold for 2 receivers each with single receive antenna and 2 receivers each with 2 receive antenna MRC.

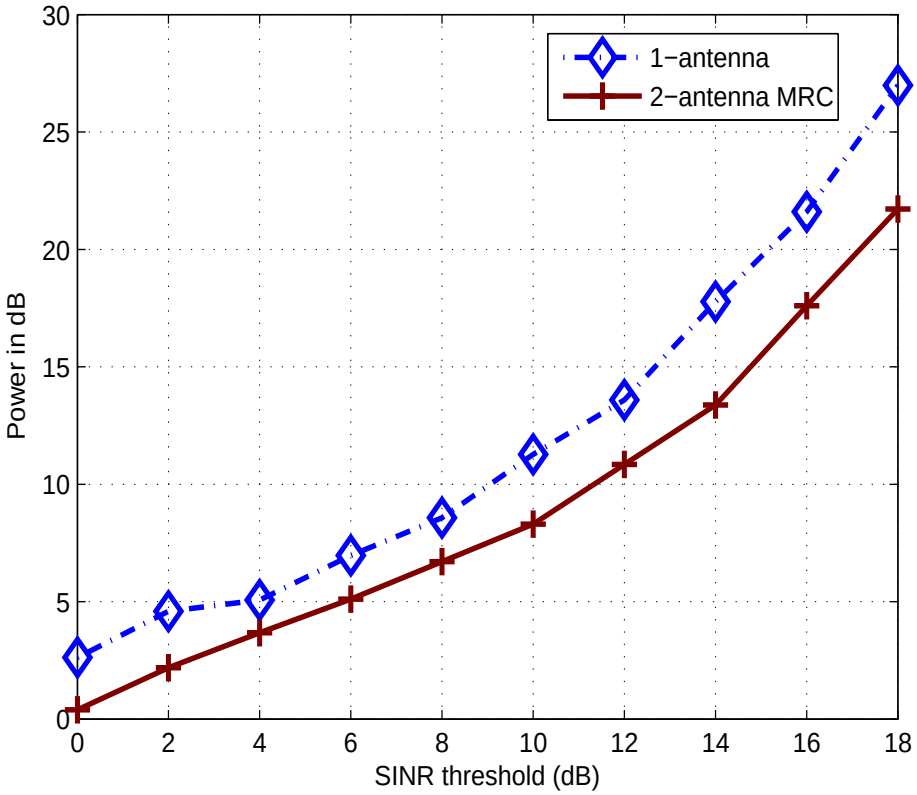

Figure 3.10. Comparison of minimum sum relay power versus SINR threshold for 2 receivers each with single receive antenna and 2 receivers each with 2 receive antenna MRC.

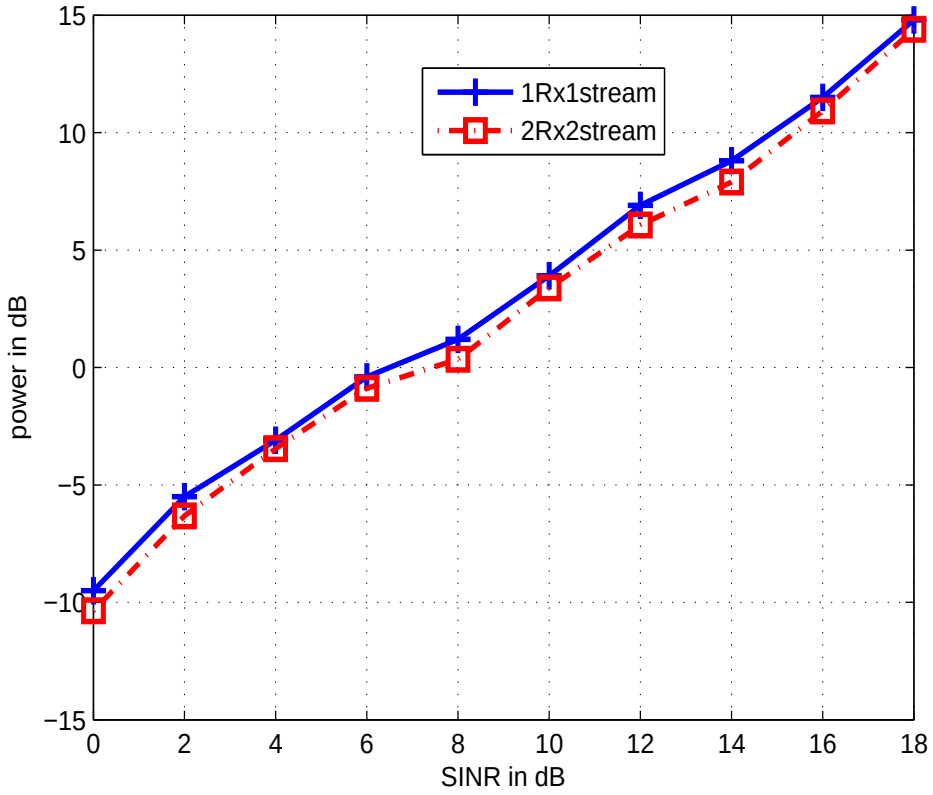

Figure 3.11. Comparison of minimum total source transmit power versus SINR threshold for 4 receivers each with single receive antenna to receive one data stream each and 2 receivers with 2 receive antennas to receive two data streams.

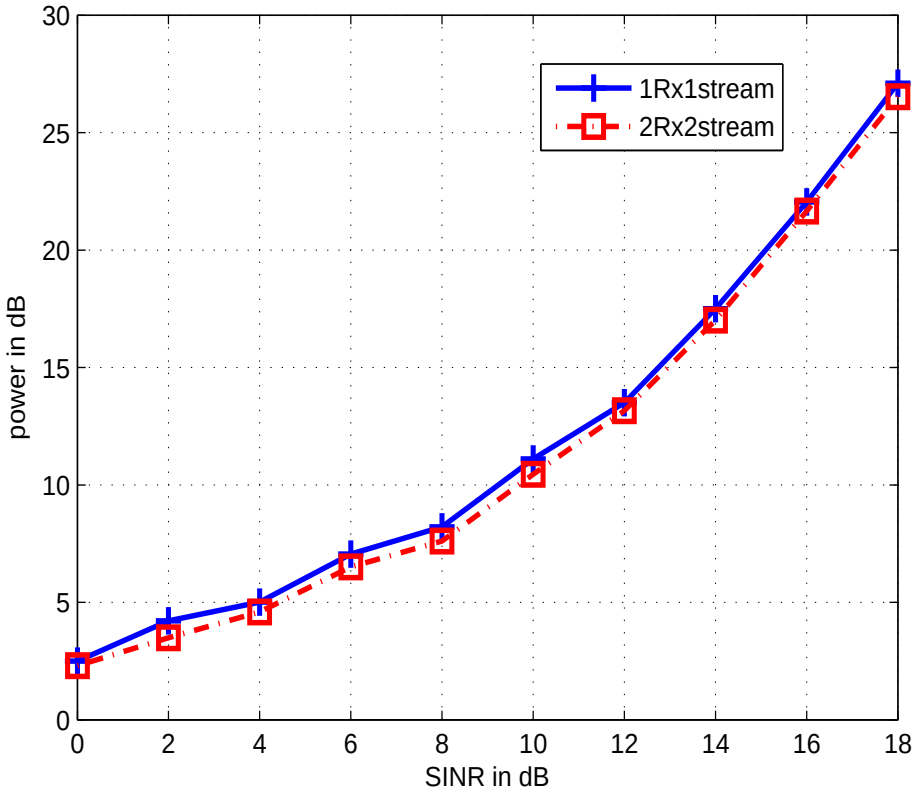

Figure 3.12. Comparison of minimum sum relay power versus SINR threshold for 4 receivers each with single receive antenna to receive one data stream each and 2 receivers with 2 receive antennas to receive two data streams.

iterative algorithm to optimize the decoder at the base station (destination) and the relay weights. The proposed scheme is further extended to the cases of imperfect CSI and multiple receive antennas.

Chapter 4

Cooperative MIMO System Uplink

4.1 Introduction

In Chapter 3, we studied the single-cell multi-user downlink cooperative system with single-antenna relays and a multi-antenna transmitting base station. In this chapter, we study the complimentary problem of uplink cooperative communications where multiple users transmit to a common destination through multiple relays.

Considering the rapidly increasing demand for high data rate and reliable wireless communications, bandwidth efficient transmission schemes are of great importance. In recent years, user cooperation has attracted increased research interest and has been widely studied. By relaying messages for each other, mobile terminals can provide the final receiver with multiple replicas of the message signal arriving via different paths. These techniques, known as cooperative diversity [7] [8], are shown to significantly improve network performance through mitigating the detrimental effects of signal fading. Various schemes have been proposed to achieve spatial diversity through user cooperation [7], [9]. The most popular schemes are amplify-and forward (AF), decode and- forward (DF), and coded cooperation [10]. Recently, the amplify-and-forward approach has been extended to develop space-time coding strategies for relay networks, which opens a new research avenue called

distributed space-time coding [57] [58]. A distributed beamforming system with a single transmitter and receiver and multiple relay nodes are studied in [11], and second order statistics of the channel are employed to design the optimal beamforming weights at the relays. Single antenna source destination pairs communicating through a relay network is studied in [12], where relay weight optimization is formulated in terms of semidefinite programming (SDP) and solved through the semidefinite relaxation technique. A distributed beamforming scheme with two relays nodes is proposed in [45] which has the advantage of limited feedback and improved diversity.

The duality between uplink and downlink multi-hop AF-MIMO relay channels with any number of hops and any number of antennas at each node for single node relaying in each hop was established in [59] for single relay. A study of linear precoding designs for a cellular multi-user system where a multi-antenna base station (BS) conducts bi-directional communications with multiple mobile stations (MSs) via a multi-antenna relay station (RS) with amplify-and-forward relay strategy is developed in [60]. The work in [60] shows that the BS precoding design with the RS precoder fixed can be converted to a standard second order cone programming (SOCP) and the optimal solution is obtained efficiently with the objective of total MSE. Nonlinear precoding design for MIMO amplify-and-forward (AF) two-way relay systems is studied in [61], where nonlinear minimal mean square error (MMSE) decision feedback equalizers (DFEs) are used in two destinations, and linear transmit precoding is applied at the source and relay nodes.

In the literature, the multiple access channel has been studied in depth. The joint optimization of transmitter and receiver for a multiuser MIMO multi-access channel with sum MSE as the objective was studied in [27]. A distributed beamforming strategy has been developed for the case where the relaying nodes cooperate to form a beam towards the receiver under individual relay power constraints in [62]. In this scheme, the amplitude and the phase of the transmitted signals are properly adjusted such that they constructively add at the receiver. A parallel relay network with noise correlation with

rate maximization is studied in [43].

In this chapter, we study the cooperative system with multiple single-antenna sources, multiple single-antenna relays and a multi-antenna destination. More specifically, we study 1) optimization of a linear decoder for given relay weights, 2) optimization of relay weights for given decoder and 3) an iterative algorithm to minimize the sum power at the relays with SINR constraints on the received signals. Full channel state information (CSI) from relays to the base station and full CSI from sources to relays are assumed at the base station is assumed at the base station. Perfect synchronization across the system is assumed [48] [49] [50].

The remainder of the chapter is organized as follows: In Section 4.2, we present the system model. Linear decoder optimization assuming known relay weights is developed in Section 4.3, followed by relay weights optimization in Section 4.4. Numerical results are provided in Section 4.5, and a summary is provided in Section 4.6.

4.2 System Model

We consider a multi-access channel through a relay network to the base station as shown in Figure 4.1. We assume a multi-relay network with n_R^{ul} single-antenna relays, with M_{ul} sources that are distributed in space each with single antenna. In order to communicate to the destination, each source transmits its data to the relay network. The relay network then delivers the data to the base station. The channel from the source to the jth relay is represented as

$$x_{ul,j} = \sum_{i=1}^{M_{ul}} b_{j,i} s_{ul,i} + v_{ul,j}, \tag{4.1}$$

where $x_{ul,j}$ is the received signal at the jth relay, $b_{j,i}$ is the channel from the ith source to the jth relay, and $v_{ul,j}$ is the noise at the jth relay. Each source uses power $P_j, P_j \leq P_{s,max}$, i.e., $E|s_{ul,j}|^2 = P_j$ for $j = 1,2,\ldots,n_R^{ul}$, $P_{s,max}$ is the maximum power available at the source. Using vector notation, we

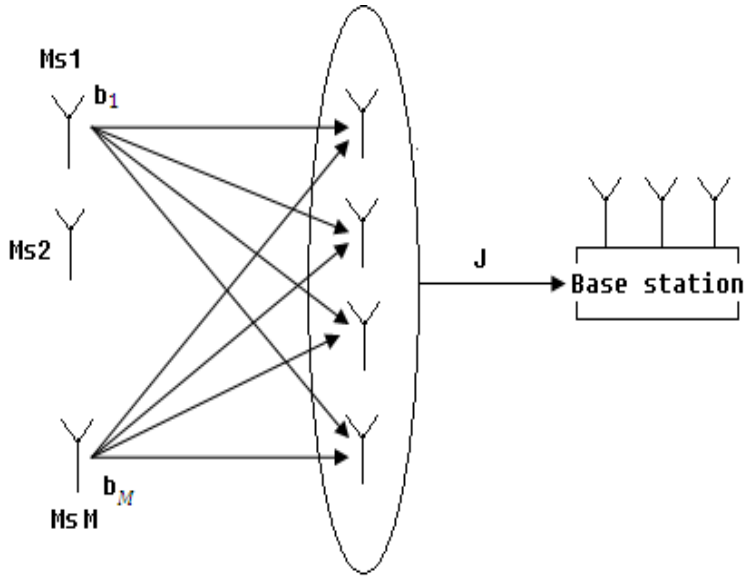

Figure 4.1. Cooperative uplink system diagram.

can rewrite (4.1) as

$$\mathbf{x}_{ul} = \sum_{i=1}^{M_{ul}} \mathbf{b}_i s_{ul,i} + \nu_{ul}, \tag{4.2}$$

where

$$\mathbf{x}_{ul} = [x_{ul,1}\ x_{ul,2}\ \ldots\ x_{ul,n_R^{ul}}]^T,$$

$$\nu_{ul} = [\nu_{ul,1}\ \nu_{ul,2}\ \ldots\ \nu_{ul,n_R^{ul}}]^T, \ \textit{and}$$

$$\mathbf{b}_i = [b_{1,i}\ b_{2,i}\ \ldots\ b_{n_R^{ul},i}]^T.$$

The ith relay multiplies its received signal by a complex weighting coefficient $w_{ul,i}^*$. The vector of the signals $\mathbf{u}_{ul}$ transmitted from the relays is

$$\mathbf{u}_{ul} = \mathbf{W}_{ul}^H \mathbf{x}_{ul}, \tag{4.3}$$

where $\mathbf{W}_{ul} = \text{diag}\{w_{ul,1}, w_{ul,2}, \ldots, w_{ul,n_R^{ul}}\}$. The received signal at the N_{ul}-antenna base station destination is expressed as

$$\mathbf{y}_{ul} = \mathbf{J}\mathbf{u}_{ul} + \mathbf{n}_{ul}, \tag{4.4}$$

where $\mathbf{J}$ is a $N_{ul} \times n_R^{ul}$ matrix representing gains from the relays to the base station. Denote the linear decoder as $\mathbf{F}_{ul}$, the noise items at the destination are i.i.d. Gaussian with noise power of $\sigma^2_{ul,\mathbf{n}}$ and noise power $\sigma^2_{ul,\nu}$ at the relays. The estimated signal vector is denoted as $\hat{\mathbf{s}}_{ul}$ is

$$\hat{\mathbf{s}}_{ul} = \mathbf{F}_{ul}\mathbf{y}_{ul} = \mathbf{F}_{ul}\left(\mathbf{J}\mathbf{W}_{ul}^H\left(\sum_{i=1}^{M_{ul}}\mathbf{b}_i s_{ul,i} + \nu_{ul}\right) + \mathbf{n}_{ul}\right). \tag{4.5}$$

The estimated signal for the kth user is

$$\hat{s}_{ul,k} = \underbrace{\mathbf{f}_{ul,k}^T\mathbf{J}\mathbf{W}_{ul}^H\mathbf{b}_k s_{ul,k}}_{Desired\ \ signal} + \underbrace{\mathbf{f}_{ul,k}^T\mathbf{J}\mathbf{W}_{ul}^H\sum_{j=1,j\neq k}^{M_{ul}}\mathbf{b}_j s_{ul,j}}_{Interference} + \underbrace{\mathbf{f}_{ul,k}^T\mathbf{J}\mathbf{W}_{ul}^H\nu + \mathbf{f}_{ul,k}^T\mathbf{n}_{ul}}_{Colored\ \ noise}, \tag{4.6}$$

where $\mathbf{F}_{ul} = [\mathbf{f}_{ul,1}\ldots\mathbf{f}_{ul,M_{ul}}]^T$.

4.3 Linear Decoder Optimization Assuming Known Relay Weights

First we derive the SINR expression for the ith user,

$$SINR_{ul,k} = \frac{P_{ul,s}^k}{P_{ul,i}^k + P_{ul,n}^k}. \tag{4.7}$$

Here $P_{ul,s}^k$,$P_{ul,i}^k$ and $P_{ul,n}^k$ denotes the desired signal power, the interference power and the noise power at the kth user respectively. The desired signal power is

$$\begin{aligned} P_{ul,s}^k &= \mathbf{f}_{ul,k}^T\mathbf{J}\mathbf{W}_{ul}^H\mathbf{b}_k\mathbf{b}_k^H\mathbf{W}_{ul}\mathbf{J}^H\mathbf{f}_{ul,k}^* E\{|s_{ul,k}|^2\} \\ &= P_k\mathbf{f}_{ul,k}^T\mathbf{J}\mathbf{W}_{ul}^H\mathbf{b}_k\mathbf{b}_k^H\mathbf{W}_{ul}\mathbf{J}^H\mathbf{f}_{ul,k}^*. \end{aligned} \tag{4.8}$$

We assume independence among the different channels from the sources to the relays and the channels from the relays to the base station.

The interference power at the kth user is

$$P_{ul,i}^k = E\left\{\left(\mathbf{f}_{ul,k}^T\mathbf{J}\mathbf{W}_{ul}^H\sum_{j=1,j\neq k}^{M_{ul}}\mathbf{b}_j s_{ul,j}\right)\right.$$

$$\left(\mathbf{f}_{ul,k}^T \mathbf{J} \mathbf{W}_{ul}^H \sum_{j=1, j\neq k}^{M_{ul}} \mathbf{b}_j s_{ul,j} \right)^H \Bigg\}$$
$$= \mathbf{f}_{ul,k}^T \mathbf{J} \mathbf{W}_{ul}^H \left(\sum_{j=1, j\neq k}^{M_{ul}} P_j \mathbf{b}_j \mathbf{b}_j^H \right) \mathbf{W}_{ul} \mathbf{J}^H \mathbf{f}_{ul,k}^*. \tag{4.9}$$

The colored noise power is

$$P_{ul,n}^k = \sigma_{ul,v}^2 \mathbf{f}_{ul,k}^T \mathbf{J} \mathbf{W}_{ul}^H \mathbf{W}_{ul} \mathbf{J}^H \mathbf{f}_{ul,k}^* + \sigma_{ul,n}^2 \mathbf{f}_{ul,k}^T \mathbf{f}_{ul,k}^*. \tag{4.10}$$

Here, for fixed relay weights, the SINR for the kth user is

$$\text{SINR}_{ul,k} = \frac{\mathbf{f}_{ul,k}^T \mathbf{A}_{ul,k} \mathbf{f}_{ul,k}^*}{\mathbf{f}_{ul,k}^T \mathbf{B}_{ul,k} \mathbf{f}_{ul,k}^*}, \tag{4.11}$$

where $\mathbf{A}_{ul,k} = P_k \mathbf{J} \mathbf{W}_{ul}^H \mathbf{b}_k \mathbf{b}_k^H \mathbf{W}_{ul} \mathbf{J}^H$ and

$\mathbf{B}_{ul,k} = \mathbf{J} \mathbf{W}_{ul}^H (\sum_{j=1, j\neq k}^{M_{ul}} P_j \mathbf{b}_j \mathbf{b}_j^H) \mathbf{W}_{ul} \mathbf{J}^H + \sigma_{ul,v}^2 \mathbf{J} \mathbf{W}_{ul}^H \mathbf{W}_{ul} \mathbf{J}^H + \sigma_{ul,n}^2 \mathbf{I}$. $\text{SINR}_{ul,k}$ is maximized when $\mathbf{f}_{ul,k}^*$ is the corresponding principal eigenvector as:

$$\mathbf{f}_{ul,k}^* = \wp\{\mathbf{B}_{ul,k}^{-1} \mathbf{A}_{ul,k}\}, \tag{4.12}$$

and the maximum for $\mathbf{f}_{ul,k}^*$ is the maximum generalized eignevalue by $\lambda_{max}(\mathbf{A}_{ul,k}, \mathbf{B}_{ul,k})$.

4.4 Relay Weight Optimization

4.4.1 Minimization of Sum Power at Relays

Next we consider the problem of relay weights optimization with a given decoder. We rewrite (4.6) as

$$\hat{s}_{ul,k} = \underbrace{\mathbf{w}_{ul}^H \text{diag}\{\mathbf{f}_{ul,k}^T \mathbf{J}\} \mathbf{b}_k s_{ul,k}}_{Desired\ \ Signal} \tag{4.13}$$
$$+ \underbrace{\mathbf{w}_{ul}^H \text{diag}\{\mathbf{f}_{ul,k}^T \mathbf{J}\} \sum_{j=1, j\neq k}^{M_{ul}} \mathbf{b}_j s_{ul,j}}_{Interference} + \underbrace{\mathbf{w}_{ul}^H \text{diag}\{\mathbf{f}_{ul,k}^T \mathbf{J}\} \nu_{ul} + \mathbf{f}_{ul,k}^T \mathbf{n}_{ul}}_{Colored\ \ Noise}$$

where $\mathbf{w}_{ul} \triangleq \text{diag}(\mathbf{W}_{ul})$.

Here we consider the problem of minimizing the sum transmission power of the relay network for a given linear decoder at the base station while the users' quality of service (QoS) are kept above pre-defined thresholds. We use SINR as a measure of QoS. The problem is written in the form of Eq. (2.23) in Section 2.3:

$$\min_{\mathbf{w}_{ul}} \; P_{ul,R} \tag{4.14}$$

$$s.t. \quad SINR_{ul,k} \geq \gamma_{ul,k}, \quad \text{for} \;\; k = 1,2,\ldots,M_{ul}$$

where $P_{ul,R}$ is the sum transmit power at the relays given as

$$\begin{aligned} P_{ul,R} &= E\{\mathbf{u}_{ul}^H \mathbf{u}_{ul}\} \\ &= \text{Tr}\{\mathbf{W}_{ul}^H E\{\mathbf{x}_{ul}\mathbf{x}_{ul}^H\}\mathbf{W}_{ul}\} \\ &= \mathbf{w}_{ul}^H \mathbf{D}_{ul} \mathbf{w}_{ul} \end{aligned} \tag{4.15}$$

and where $\mathbf{D}_{ul} \triangleq \text{diag}\left([\mathbf{R}_{ul,x}]_{1,1}, [\mathbf{R}_{ul,x}]_{2,2}, \ldots, [\mathbf{R}_{ul,x}]_{n_R^{ul},n_R^{ul}}\right)$. $\gamma_{ul,k}$ is the SINR constraint for the kth user. The matrix $\mathbf{R}_{ul,x}$, whose diagonal elements form matrix $\mathbf{D}_{ul}$ is expressed as

$$\mathbf{R}_{ul,x} = \sum_{j=1}^{M_{ul}} P_j \mathbf{b}_j \mathbf{b}_j^H + \sigma_{ul,v}^2 \mathbf{I}. \tag{4.16}$$

The SINR constraints for the kth user can be expressed as

$$\frac{\mathbf{w}_{ul}^H \text{diag}\{\mathbf{f}_{ul,k}^T \mathbf{J}\} \left(P_k \mathbf{b}_k \mathbf{b}_k^H\right) \text{diag}\{\mathbf{f}_{ul,k}^T \mathbf{J}\}^H \mathbf{w}_{ul}}{\mathbf{w}_{ul}^H \mathbf{E}_{ul,k} \mathbf{w}_{ul} + \sigma_{ul,n}^2 \mathbf{f}_{ul,k}^T \mathbf{f}_{ul,k}^*} \geq \gamma_{ul,k} \tag{4.17}$$

where

$$\mathbf{E}_{ul,k} = \text{diag}\{\mathbf{f}_{ul,k}^T \mathbf{J}\} \left(\sum_{j=1, j\neq k}^{M_{ul}} P_j \mathbf{b}_j \mathbf{b}_j^H + \sigma_{ul,v}^2 \mathbf{I} \right) \text{diag}\{\mathbf{f}_{ul,k}^T \mathbf{J}\}^H.$$

Using (4.15) and (4.17) we can rewrite (4.14) as

$$\min_{\mathbf{w}_{ul}} \; \mathbf{w}_{ul}^H \mathbf{D}_{ul} \mathbf{w}_{ul} \tag{4.18}$$

$$s.t. \quad \mathbf{w}_{ul}^H \mathbf{U}_{ul,k} \mathbf{w}_{ul} \geq \gamma_{ul,k} \sigma_{ul,n}^2 \mathbf{f}_{ul,k}^T \mathbf{f}_{ul,k}^*$$

$$\text{for} \quad k = 1, 2, \ldots, M_{ul}$$

where

$$\mathbf{U}_{ul,k} = \text{diag}\{\mathbf{f}_{ul,k}^T \mathbf{J}\} \left(P_k \mathbf{b}_k \mathbf{b}_k^H - \gamma_{ul,k} \sum_{j=1, j\neq k}^{M_{ul}} P_j \mathbf{b}_j \mathbf{b}_j^H - \gamma_{ul,k} \sigma_{ul,v}^2 \mathbf{I} \right) \text{diag}\{\mathbf{f}_{ul,k}^T \mathbf{J}\}^H.$$

There are constraints in Problem (4.18) that are not convex. Therefore convex optimization cannot be applied and (4.18) may not have a solution with affordable computational complexity. We employ a semidefinite relaxation approach to solve a relaxed version of (4.18). Denoting $\mathbf{Z}_{ul} = \mathbf{w}_{ul} \mathbf{w}_{ul}^H$, (4.18) can be rewritten as

$$\min_{\mathbf{Z}_{ul}} \text{Tr}(\mathbf{Z}_{ul} \mathbf{D}_{ul}) \tag{4.19}$$

$$s.t. \quad \text{Tr}(\mathbf{Z}_{ul} \mathbf{U}_{ul,k}) \geq \gamma_{ul,k} \sigma_{ul,n}^2 \mathbf{f}_{ul,k}^T \mathbf{f}_{ul,k}^* \quad \text{for} \quad k = 1, \ldots, M_{ul}$$

$$\mathbf{Z}_{ul} \succeq 0, \quad \text{rank}(\mathbf{Z}_{ul}) = 1.$$

.

Using semidefinite relaxation to remove the non-convex constraints rank-one constraint, Eq (4.19) becomes

$$\min_{\mathbf{Z}_{ul}} \text{Tr}(\mathbf{Z}_{ul} \mathbf{D}_{ul}) \tag{4.20}$$

$$s.t. \quad \text{Tr}(\mathbf{Z}_{ul} \mathbf{U}_{ul,k}) \geq \gamma_{ul,k} \sigma_{ul,n}^2 \mathbf{f}_{ul,k}^T \mathbf{f}_{ul,k}^* \quad \text{for} \quad k = 1, \ldots, M_{ul},$$

$$\mathbf{Z}_{ul} \succeq 0.$$

This optimization problem can be efficiently solved using optimization software, e.g., Sedumi [63] by introducing slack variables $\beta_{ul,k}, k = 1, \ldots, M_{ul}$ to transform (4.20) into standard SDP form

in Sedumi as follows:

$$\min_{\mathbf{Z}_{ul}\in\mathbf{C}^{n_R^{ul}\times n_R^{ul}}} \quad \mathrm{vec}(\mathbf{D}_{ul})^T\mathrm{vec}(\mathbf{Z}_{ul}) \tag{4.21}$$

$$s.t. \quad \mathrm{vec}(\mathbf{U}_{ul,k})\mathrm{vec}(\mathbf{Z}_{ul}) - \beta_{ul,k} = \gamma_{ul,k}\sigma_{ul,n}^2\mathbf{f}_{ul,k}^T\mathbf{f}_{ul,k}^*$$

$$\beta_{ul,k} \geq 0 \quad \text{for } k = 1,\ldots,M_{ul}$$

$$\mathbf{Z}_{ul} \succeq 0$$

It is noted here that in general cases, rank-1 solution does not always exists. However, in particular case when $M_{dl} \leq 3$, it is proven in [54] that the relaxed problem has optimal rank-1 solution. When $M_{ul} \geq 4$ randomization techniques [55] can be applied to obtain a suboptimal rank-one solution. In this later situation, the optimal matrix obtained from (4.21) is used to generate some suboptimal weight vectors χ_{ul} (See Appendix B or details), from which the best solution will be selected [64] [65] [55] .

4.4.2 Feasibility

For a given set of SINR constraints, the feasibility of (4.14) can be tested. It is summarized as follows:

Lemma 4.1: If the number of receive antennas at the base station is larger or equal to the number of relays, the upper bound of the achievable *SINR* of the kth user is

$\lambda_{max}(P_k\mathbf{b}_k\mathbf{b}_k^H, \sum_{j=1,j\neq k}^{M_{ul}} P_j\mathbf{b}_j\mathbf{b}_j^H + \sigma_{ul,v}^2\mathbf{I})$.

Proof: See Appendix D.

4.4.3 Individual Power Constraints at Relays

In this subsection, we consider an additional power constraint that arises in practice. More specifically, each relay is restricted in its transmission power. This constraint is needed as some of the

relays may end up with significantly high transmit powers which is impractical due to the power limitations of their transmit amplifiers. In this case, we add constraints to (4.18) and solve the following problem:

$$\begin{aligned} & \min_{\mathbf{w}_{ul}} \quad \mathbf{w}_{ul}^H \mathbf{D}_{ul} \mathbf{w}_{ul} \\ s.t. \quad & \mathbf{w}_{ul}^H \mathrm{diag}\{\mathbf{f}_{ul,k}^T \mathbf{J}\} \left(P_k \mathbf{b}_k \mathbf{b}_k^H - \gamma_{ul,k} \sum_{j=1, j\neq k}^{M_{ul}} P_j \mathbf{b}_j \mathbf{b}_j^H - \gamma_{ul,k} \sigma_{ul,v}^2 \mathbf{I} \right) \\ & \qquad \mathrm{diag}\{\mathbf{f}_{ul,k}^T \mathbf{J}\}^H \mathbf{w}_{ul} \geq \gamma_{ul,k} \sigma_{ul,n}^2 \mathbf{f}_{ul,k}^T \mathbf{f}_{ul,k}^* \\ & \qquad \text{for} \quad k = 1, 2, \ldots, M_{ul} \\ & [\mathbf{D}_{ul}]_{i,i} |w_{ul,i}|^2 \leq P_i \quad \text{for} \quad i = 1, 2, \ldots, n_R^{ul}, \end{aligned} \tag{4.22}$$

where $[\mathbf{D}_{ul}]_{i,i}$ is the element at ith row and ith column of matrix $[\mathbf{D}_{ul}]$. Using the semi-definite relaxation technique, (4.22) can be written as

$$\begin{aligned} & \min_{\mathbf{Z}_{ul}} \quad \mathrm{Tr}(\mathbf{Z}_{ul} \mathbf{D}_{ul}) \\ s.t. \quad & \mathrm{Tr}\left(\mathbf{Z}_{ul} \mathbf{U}_{ul,k}\right) \geq \gamma_{ul,k} \sigma_{ul,n}^2 \mathbf{f}_{ul,k}^T \mathbf{f}_{ul,k}^* \\ & \mathbf{Z}_{ul,i,i} \leq P_i / [\mathbf{D}_{ul}]_{i,i} \quad \text{for} \quad i = 1, 2, \ldots, n_R^{ul} \\ & \qquad \textit{and} \quad \mathbf{Z}_{ul} \succeq 0. \end{aligned} \tag{4.23}$$

The numerical result in simulation result section shows that per-relay power constraints do not affect the performance of our technique significantly for a wide range of up to 15 dB when the maximum allowable power for each relay is chosen to be 6 dB above the average power consumed by each relay.

4.4.4 Joint Determination of Linear Decoder and Relay Weights

Joint optimization with iterative algorithm has been studied in literature to improve complex system performance. In [27], joint optimization of transmitter and receiver with an iterative algorithm is proposed. In [33], an iterative algorithm to optimize the transmitter with given receiver is proposed. In [37], an iterative algorithm to jointly optimize the transmitter and receiver with imperfect channel state information is studied.

In this section, we study the problem of alternatively optimizating the linear decoder and relay weights as the following algorithm:

1. Initialize the relay weights with $c_{ul} * vec(\mathbf{I})$, where c_{ul} is a large value (e.g. 10^5)

2. Calculate the SINR upper bound for each user according to the results in Lemma 4.1. If the SINR upper bound for each user is larger than the given required SINR criterion, then go to Step 3. Else declare the infeasibility of the problem.

3. Apply the results in Section 4.3 to find the optimal decoder vector for each user.

4. With the decoder obtained from Step 2, apply (4.20) to minimize the relay sum power or apply (4.23) to minimize the relay sum power with individual relay power constraints.

5. Alternate between Step 3 and Step 4 until it reaches a stopping criterion (e.g. the difference of sum power at the relays for the current iteration and the previous iteration is below a certain threshold.).

As the sum power of the relays are lower-bounded and for each alternating Step 3 and 4, the power will reduce monotonically, so it is easy to show the algorithm will converge to a given point, but not necessarily to the globally optimum point.

Lemma 4.2: The iterative algorithm with linear decoder on converges.

Proof: See Appendix E.

4.5 Simulation Results

In our simulations, data is transmitted from users through relays to the base station over two time slots in half-duplex mode. In the first time slot, the users transmit signals to the relay network, in the second time slot, the relays forward signals to the base station. We assume that the second-order statistics of the channel coefficients (rather than their instantaneous values) from the M_{ul} sources to the n_R^{ul} relays are available to the base station and the channel coefficients from the relays to the base station are known at the base station where the beamforming weights for relays are to be determined. This base station then broadcasts the beamforming weights to the relays. The channel coefficients $\mathbf{J}$ and $\mathbf{b}_k, k = 1, \ldots, M_{ul}$ are assumed to be independent where $\mathbf{J}$ represents the channel from relays to the destination and $\mathbf{b}_k$ represents the channel from the kth user to the relays. Here we simulate different scenarios with different numbers of sources, relays and receive antennas and same *SINR* threshold for all users $\gamma = \gamma_1 = \ldots = \gamma_{M_{ul}}$. Figure 4.2 shows the minimum sum transmit power at the relays versus the SINR threshold γ with 6 relays and 6 receive antennas for 2 to 4 sources. It can be seen from Figure 4.2 that as the number of sources increases, the required minimum sum transmit power at the relays increases. This is as expected since more users are generating mutual interference. Figure 4.3 plots the minimum sum transmit power at the relays versus threshold γ with 10 relays and 10 receive antennas. Comparing Figure 4.2 and Figure 4.3 we can see that as the number of relays and receive antennas increases, the required minimum sum transmit power at the relays decreases. This is achieved by the increased diversity at relays and receive antenna arrays. We remark that existing distributed beamforming systems require a larger number of relays (for example 20 relays reported in [11] and [12]) to support a small number of users. As the computational complexity of semidefinite programming is O(n^6) where n is the size of the $\mathbf{W}_{ul}$ matrix, a larger number of relays results in a high cost to compute $\mathbf{W}_{ul}$. In the system proposed in this chapter, with 6-10 relays, the system can

support up to 8 users, reducing computational cost and increasing the number of supported users.

To consider the effect of individual relay power constraints, a scenario of 4 sources, 6 relays and 6 receive antenna destination system is simulated. The maximum allowable power for each relay is chosen to be 6 dB above the average power consumed by each relay in the unconstrained problem. As can be seen from Figure 4.4, such per-relay power constraints do not affect the performance of our technique significantly for a wide range of up to 15 dB.

To consider the effect of imperfect CSI, we consider a cooperative system with 3 sources, 6 relays and 6 receiver antennas. The matrix

$$\mathbf{R}_R = \begin{pmatrix} 1 & \rho_R & \rho_R^2 & \dots & \rho_R^N \\ \rho_R & 1 & \rho_R & \dots & \rho_R^{N-1} \\ \vdots & & \vdots & & \vdots \\ \rho_R^N & \rho_R^{N-1} & \dots & \rho_R^2 & 1 \end{pmatrix} \tag{4.24}$$

models correlation for a typical uniform linear array (ULA). In (4.24), we choose the correlation coefficient ρ_R between source antennas to be 0.5. Since the relays are part of the infrastructure of the system, the distances from the relays to destination are fixed and equal. The training power to noise ratio P_{tr}/σ_n^2 is set to 20dB.

For channel estimation from sources to relays, $P_{tr}/\sigma_{ul,n}^2$ is chosen to be 20 dB (*high* training SNR), corresponding to users at the nominal distance (for example 500m). The CSI error variances, quantified by the diagonal elements of the $n_R^{ul} \times n_R^{ul}$ matrices $\mathbf{R}_{ul,\mathbf{e}_b}^j$ for sources $j = 1,\dots M_{ul}$, are determined according to path loss from uniformly distributed users ranging from 250 to 750 meters according to the log-distance model [56]

$$PL = PL_0 + 10\gamma \log_{10} \frac{d}{d_0} \tag{4.25}$$

where path loss exponent $\gamma = 2.5$ and the path loss unit is dB, and reference distance $d_0 = 500$m.

In (4.25), it is assumed that the effects of small scale fading are averaged out. Finally, zero mean independent Gaussian noise is added to the channel estimates with the above CSI error variances.

Figure 4.5 compares the sum relay power for perfect CSI and imperfect CSI with 20dB channel training SNR and the case without considering the imperfect CSI model. It is noted that when channel estimation is perfect, the performance loss is 4dB loss without considering imperfect CSI while using imperfect CSI model the performance loss is around 1dB.

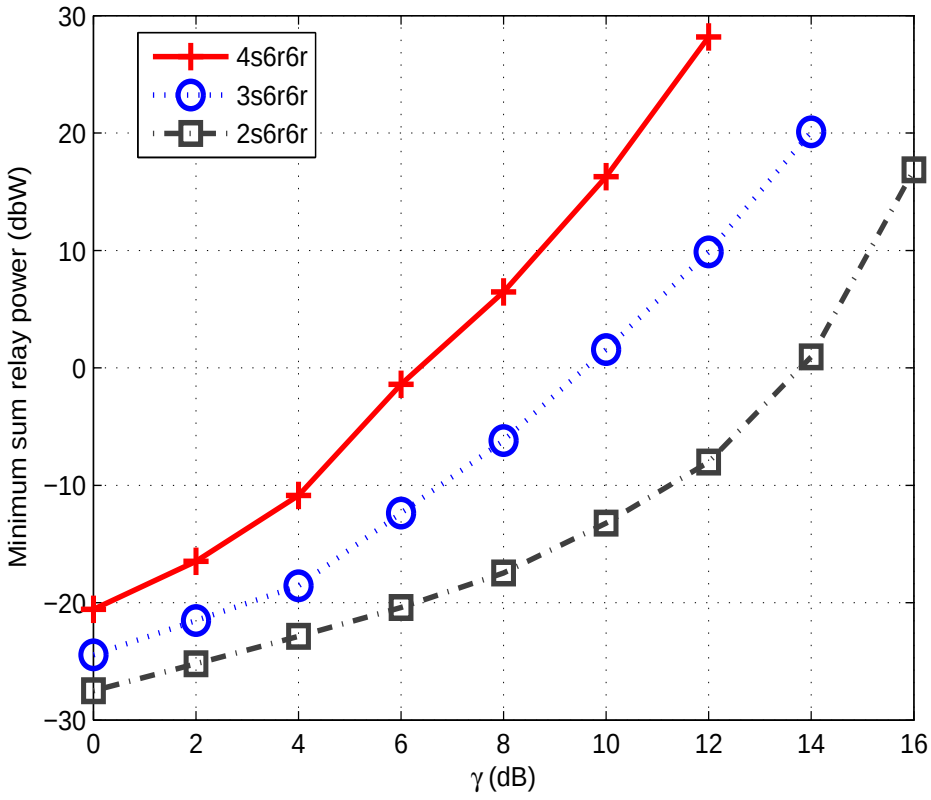

Figure 4.2. Minimum total relay transmit power versus SINR threshold γ_{ul} for 6 relays and 6 receive antennas.

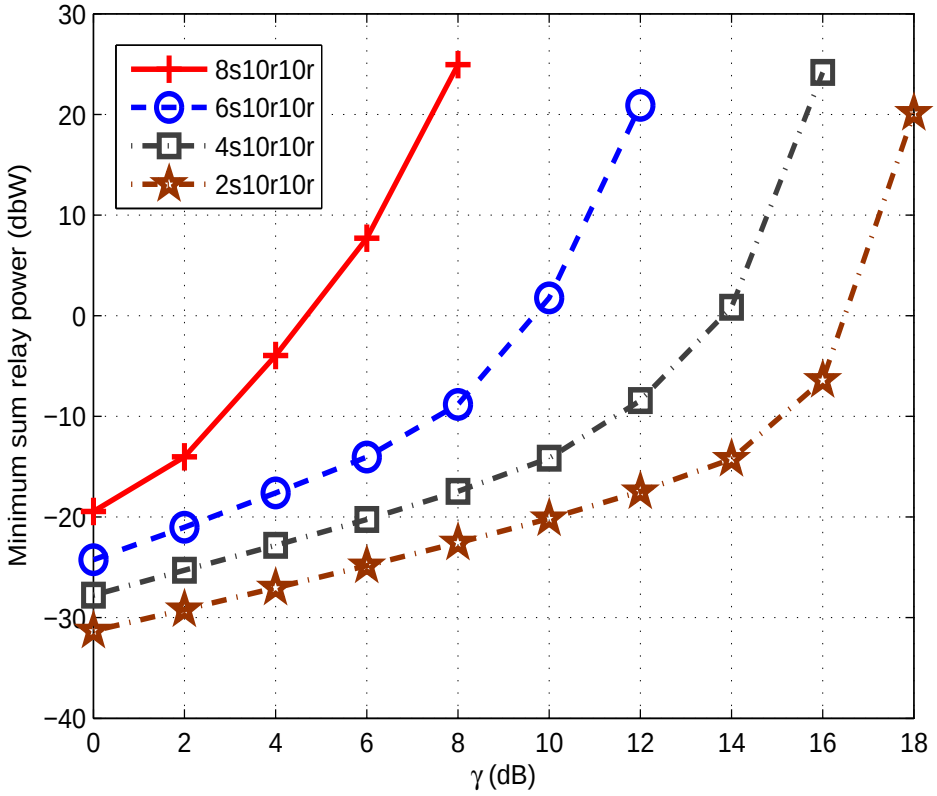

Figure 4.3. Minimum total relay transmit power versus SINR threshold γ_{ul} for 10 relays and 10 receive antennas.

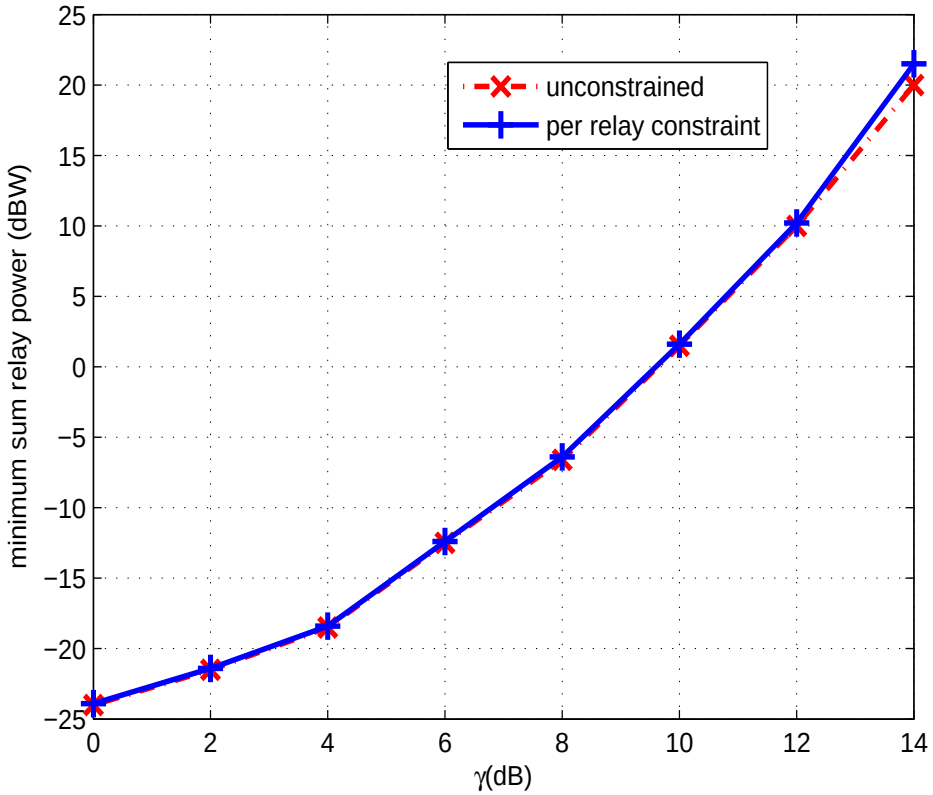

Figure 4.4. Comparison of Minimum total relay transmit power versus SINR threshold γ_{ul} for 3 sources, 6 relays and 6 receive antennas for constrained and unconstrained per relay power.

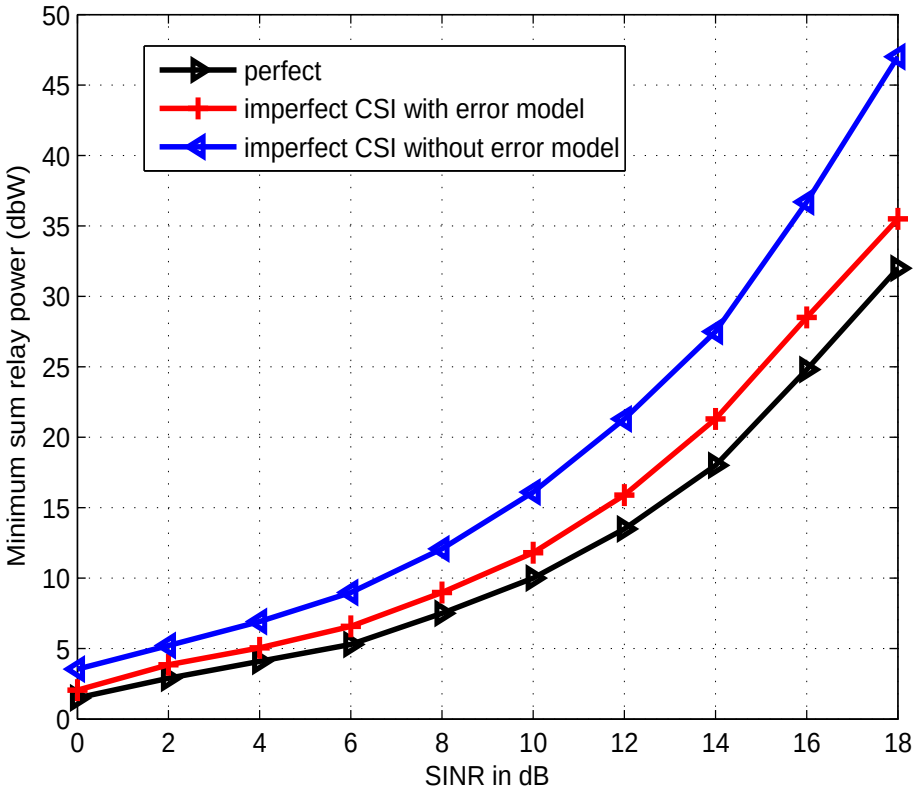

Figure 4.5. Comparison of Minimum total relay transmit power versus SINR threshold γ_{ul} for 3 sources, 6 relays and 6 receive antennas for perfect, imperfect CSI and channel estimation ignored.

4.6 Summary

In this chapter we study the scenario of an uplink multi-access system through a network of relays. For given relay weights, the optimum linear decoder was derived. For given linear decoder at the base station, the relay weights are optimized using semidefinite programming relaxation. We also proposed an iterative algorithm to optimize the decoder at the base station (destination) and the relay weights. We also study the scheme with imperfect CSI scenario.

Chapter 5

Coordinated Multi-cell Transmission

5.1 Introduction

In Chapters 3 and 4, we studied multiple user downlink and uplink cooperative systems for a single cell that utilizes single-antenna relays and multiple antenna base station. In this chapter, we extend some of these results to a multicell downlink scenario.

Downlink beamforming in cellular systems has been an active area of research for many years. Recently, there has been a rapidly growing interest in the area of multicell processing, in which base stations cooperate to provide networkwide, macroscopic beamforming [66] [67].

The conceptual approach to multicell processing is to assume a central coordinating unit, to which the base stations are connected. The central controller's role is to process information from all the base stations and to determine the precoders at each base station to transmit the appropriate signals.

Previous work on multiple cell processing were for the uplink [68] [69]. Both these papers considered a simple linear array model for a cellular network. Wyner [69] also proposed and analyzed a hexagonal array model. Multicell processing is sometimes called "macrodiversity" [70]. In uplink macrodiversity, base stations cooperate to jointly decode a signal from a mobile in the network, taking advantage of the broadcast nature of wireless communications. In downlink macrodiversity,

base stations cooperate to jointly transmit a signal to a mobile, in which the multiple base stations are widely spaced across a geographic area. Theoretically, macrodiversity can eliminate the impact of other cell interference on cellular capacity [71], [68]. The potential capacity gain is, therefore, enormous, as demonstrated in [72], [71], and [73]. A low-complexity physical layer design to introduce cooperation in the downlink of an infrastructure-based multicell MIMO-OFDM is developed in [74], performance insights and analytical upper bounds on the symbol error probability for linear receivers are provided. A novel and practical type of coordination for OFDMA downlink networks relying on multiple antennas at the transmitter and the receiver is proposed in [75]. The transmission ranks, i.e., the number of transmitted streams, and the user scheduling in all cells are jointly optimized in order to maximize a network utility function accounting for fairness among users [75]. Relaying and multi-cell MIMO transmission are investigated in [76] as approaches for improving resource reuse and more flexible organization of cellular networks. Achievable throughput is analyzed under practical constraints using three different normalization approaches: cost-normalization, energy-normalization, and joint cost-energy-normalization [76].

Multicell cooperative systems attract interest as LTE is widely deployed and LTE-Advanced demands new techniques for further improvement on throughput as well as coverage. Multi-cell coordinated shared relay with joint processing (JP) scheme in interference limited network is studied in [77], JP of cooperating BSs and shared relay station (RS) in the relay transmission phase (second phase) using SVD precoding to increase resource usage efficiency was proposed. A comprehensive centralized RRM algorithm for downlink OFDMA cellular fixed relay networks in a way to ensure user fairness with minimal impact on network throughput was proposed in [78], the proposed centralized scheme has improvement in terms of the substantial savings in complexity and feedback overhead compared with traditional centralized schemes. A shared relaying architecture for inter-cell interference mitigation in wireless cellular networks is examined in [79] with focus on resource

allocation and the scheduling of users among the adjacent sectors. A network utility maximization problem was formulated for a realistic shared relaying network, where zero-forcing beamforming is used at the relay to separate users spatially and shown to improve the overall network utility through system level simulation. A heuristic algorithm named integrated radio resource allocation (IRRA) with a mode-aware BS resource-scheduling scheme to find suboptimal solutions was proposed in [80] and shown to have improvement in cell throughput.

The role of the receive antennas in a multi-cell environment is discussed and recently proposed multicell cooperative algorithms and receive antenna techniques for different interference statistics are reviewed in [81]. When the signals from multiple cells are amplified by a group of relays, the interference from other cells becomes mixed and less amenable with the addition of relay noises. In this chapter, the framework and methodology in Chapter 3 are extended to multicell cooperative system.

In Chapter 5, we first present the system model for the multicell cooperative system in Section 5.2.1. Then we studied two multicell cooperative system scenarios, the first is that multicells transmit the same signal to a specific user in Section 5.2.2 and the second is that only one of the cells transmits a signal to a specific user in Section 5.2.3. Numerical results are presented in Section 5.3. Full channel state information (CSI) from relays to the destinations and full CSI from base stations to relays are assumed at the central controller are assumed. Perfect synchronization across the system is assumed [48] [49] [50].

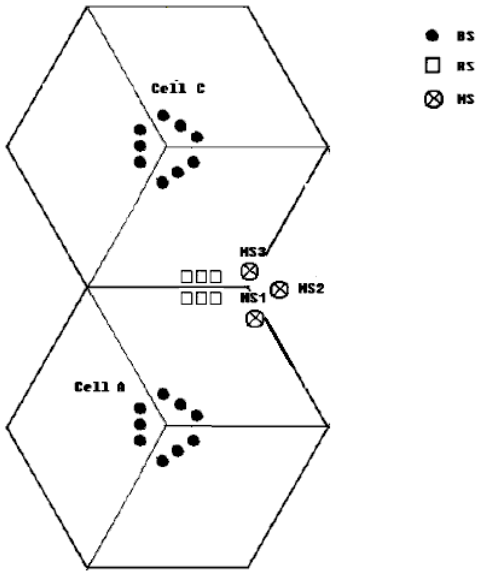

Figure 5.1. BS Scenario: Cell A, C transmit to MS1, MS2, MS3. Multiple cells with shared relays.

5.2 Downlink Multicell Coordination System

5.2.1 System Model

Consider a broadcast channel as shown in Fig. 5.1. As explained above, data is transmitted from multiple multi-antenna sources to multiple users through relays successively over two time slots. There are K_{co} cells, each cell with a N_{co}-antenna base station, a relay network of n_R^{co} single-antenna relays, and M_{co} distributed single-antenna destinations, where $M_{co} \leq N_{co}$. The n_R^{co} relays form the infrastructure of the cooperative relay system. It is assumed that the channels from source to relays are estimated at the relays and fed back to the source. Similarly, the channels from relays to destinations are estimated at the destinations and fed back to the relays, which then forward the estimates back to the source. It is assumed that since range extension is an intended application, there are no direct links between the sources and destinations. Here two different scenarios are considered: 1) each cell transmits the same signal to each subscriber, and one of the base station is selected to transmit to a

specific user. We denote this as the base station selection scenario (BS) and 2) only one cell transmits to a specified subscriber. In this scenario, other cell signals are considered as interference. We denote this as the interference suppression (IS) scenario. With 1), only N_{co} users can be served while with 2), overall $K_{co} \times N_{co}$ users can be served. The two steps can also be regarded as two successive steps for a multicell cooperative system, where 1) is for serving cell selection and 2) is for transmit beamforming optimization. First we consider the BS scenario in which each cell can transmit to each subscriber.

5.2.2 BS scenario: multicell signal broadcast to a user

In this subsection, we study the BS scenario where multiple cells transmit the same signal to a specific user. Let the $N_{co} \times 1$ vector $\mathbf{h}_{co,i,r}(i = 1, \ldots, K_{co})$, represent the link from the ith source to the rth relay, $1 \leq r \leq n_R^{co}$, which receives a symbol

$$x_{co,r} = \sum_{j=1}^{K_{co}} \mathbf{h}_{co,j,r}^T \sum_{i=1}^{M_{co}} \Gamma_{co,j,i} s_{co,i} + \nu_{co,r} \tag{5.1}$$

where $\Gamma_{co,j,i}$ denotes a $N_{co} \times 1$ transmit beamforming vector corresponding to signal $s_{co,i}$ intended for the ith destination from the jth cell, $1 \leq i \leq M_{co}, 1 \leq j \leq K_{co}$.

To model distributed beamforming, the ith relay multiplies its received signal by complex coefficient $w_{co,i}$. The vector $\mathbf{u}_{co}$ representing all signals transmitted from the relays to the destinations is

$$\mathbf{u}_{co} = \mathbf{W}_{co}^H \mathbf{x}_{co} \tag{5.2}$$

where diagonal DBRF matrix

$$\mathbf{W}_{co} = \text{diag}\{w_{co,1}, w_{co,2}, \ldots, w_{co,n_R^{co}}\}$$

$$\mathbf{x}_{co} = [x_{co,1}\ x_{co,2}\ \ldots\ x_{co,n_R^{co}}]^T. \tag{5.3}$$

Using (5.1), the received signal at the ith destination is

$$\begin{aligned} y_{co,i} &= \mathbf{g}_{co,i}^T \mathbf{u}_{co} + n_{co,i} \\ &= \underbrace{\mathbf{g}_{co,i}^T \mathbf{W}_{co}^H \sum_{j=1}^{K_{co}} \mathbf{H}_{co,j}^T \Gamma_{co,j,i} s_{co,i}}_{Desired\ Signal} + \underbrace{\mathbf{g}_{co,i}^T \mathbf{W}_{co}^H \sum_{j=1}^{K_{co}} \mathbf{H}_{co,j}^T \sum_{l=1,l\neq i}^{M_{co}} \Gamma_{j,l} s_{co,l}}_{interference} + \underbrace{\mathbf{g}_{co,i}^T \mathbf{W}_{co}^H \nu_{co} + n_{co,i}}_{noise} \end{aligned} \tag{5.4}$$

where $n_R^{co} \times N_{co}$ matrix $\mathbf{H}_{co,j} = [\mathbf{h}_{co,j,1} \ldots \mathbf{h}_{co,j,n_R^{co}}]^T$ represents the combined channel from the source to relays, $1 \times n_R^{co}$ row vector $\mathbf{g}_{co,i}^T$ represents the channel from the relays to the ith destination, $n_R^{co} \times 1$ vector $\nu_{co} = [\nu_{co,1}, \ldots, \nu_{co,n_R^{co}}]^T$ represents noise at the relays, and $n_{co,i}$ represents $AWGN$ at the ith destination.

5.2.2.1 Transmit Precoder Optimization for BS scenario

The case where multiple base stations coordinate their transmission to serve a coverage area with relaying is shown in Fig. 5.1, where each base station sends the same signal to a specific user through relays. This scheme is applicable to the scenario where the user is located near a cell edge and is able to receive signals from multiple cells. In this case, Eq. (3.10) generalizes to

$$\begin{aligned} &\min_{\Gamma_{1,1},\ldots,\Gamma_{1,M_{co}},\ldots,\Gamma_{K_{co},1},\ldots,\Gamma_{K_{co},M_{co}}} \quad \sum_{i=1}^{K_{co}} \sum_{j=1}^{M_{co}} \alpha_{i,j} \mathrm{Tr}\left(\Gamma_{i,j} \Gamma_{i,j}^H\right) \\ s.t. \quad &\frac{\sum_{m=1}^{K_{co}} \alpha_{m,i} \Gamma_{m,i}^H \mathbf{H}_{co,m}^H \mathbf{W}_{co} \mathbf{g}_{co,i}^T \mathbf{g}_{co,i}^* \mathbf{W}_{co}^H \mathbf{H}_{co,m} \Gamma_{m,i}}{\sum_{n=1,n\neq i}^{M_{co}} \sum_{m=1}^{K_{co}} \alpha_{m,n} \Gamma_{m,n}^H \mathbf{H}_{co,m}^H \mathbf{W}_{co} \mathbf{g}_{co,i}^T \mathbf{g}_{co,i}^* \mathbf{W}_{co}^H \mathbf{H}_{co,m} \Gamma_{m,n} + \mathrm{Tr}\{\mathbf{W}_{co}^H \mathbf{g}_{co,i}^T \mathbf{g}_{co,i}^* \mathbf{W}_{co} \sigma_{co,\nu}^2\} + \sigma_{co,n}^2} \\ &\qquad \geq \gamma_{co,i} \quad \text{for} \quad i = 1, \ldots, M_{co}. \end{aligned} \tag{5.5}$$

The weight factors $\alpha_{i,j}$ are to take into account factors such as path loss from the base station to the relays, cell load, scheduling priority and other physical factors in the multicell scenario as the

minimum power is not the only factor for the determination of the transmit beamforming scheme. Let

$$\mathbf{T}_{co,j,i} = \alpha_{j,i}\Gamma_{co,j,i}\Gamma_{co,j,i}^{H}, \quad \text{for} \quad j = 1,\ldots,K_{co} \quad \text{and} \quad i = 1,\ldots,M_{co} \tag{5.6}$$

and applying semi-definite relaxation by dropping constraints

$$\text{rank}(\mathbf{T}_{co,j,i}) = 1, \tag{5.7}$$

the optimization problem (3.12) generalizes to

$$\begin{aligned}
&\min_{\mathbf{T}_{co,1,1},\ldots,\mathbf{T}_{co,1,M},\ldots,\mathbf{T}_{co,K,1},\ldots,\mathbf{T}_{co,K,M}} \sum_{i=1}^{K_{co}}\sum_{j=1}^{M_{co}} \text{Tr}\left(\mathbf{T}_{co,i,j}\right) \\
s.t. \quad &\sum_{m=1}^{K_{co}} \text{Tr}\left(\mathbf{U}_{co,m,i}(\mathbf{T}_{co,m,i} - \gamma_{co,i}\sum_{n=1,n\neq i}^{M_{co}}\mathbf{T}_{co,m,n})\right) \geq \gamma_{co,i}\left(\text{Tr}(\mathbf{W}_{co}^{H}\mathbf{g}_{co,i}^{T}\mathbf{g}_{co,i}^{*}\mathbf{W}_{co})\sigma_{co,v}^{2} + \sigma_{co,n}^{2}\right) \\
&\qquad\qquad \text{for} \quad i = 1,\ldots,M_{co}, \\
&\qquad\qquad \mathbf{T}_{co,m,i} \succeq 0 \\
&\qquad\qquad \text{for} \quad m = 1,\ldots,K_{co} \quad \text{and} \quad i = 1,\ldots,M_{co}
\end{aligned} \tag{5.8}$$

where

$$\mathbf{U}_{co,j,k} = \mathbf{H}_{co,j}^{H}\mathbf{W}_{co}\mathbf{g}_{co,k}^{T}\mathbf{g}_{co,k}^{*}\mathbf{W}_{co}^{H}\mathbf{H}_{co,j}. \tag{5.9}$$

5.2.2.2 Relay Weights Optimization for BS Scenario

Semi-definite programming can be applied to solve (5.8). When the precoders at the multiple cooperating base stations are fixed, DRBF optimization over a multi-cell area can be achieved in a similar manner to that presented in Section 3.4.

Once the beamforming vectors are determined, the relay weights can be optimized. The iterative algorithm from Section 3.3 can be applied here to minimize the sum power at both base stations and relays.

5.2.3 IS scenario: one of multiple cells transmits to a specific user

This section considers the scenario that each subscriber only receives a signal from one of the K_{co} cells as shown in Fig. 5.1. In this scenario, there are K_{co} cells, and each cell is equipped with N_{co} antennas, where there are $M_{co,i}, i = 1,\ldots,K_{co}$ users in each cell and $M_{co,i} \leq N_{co}$, and n_R^{co} single antenna relays are shared by the K_{co} cells.

Let the $N_{co} \times 1$ vector $\mathbf{h}_{co,i,r}(i = 1,\ldots,K_{co})$, represent the link from the ith source to the rth relay, $1 \leq r \leq n_R^{co}$, which receives a symbol at rth relay is

$$x_{co,r} = \sum_{j=1}^{K_{co}} \mathbf{h}_{co,j,r}^T \sum_{i=1}^{M_{co,K}} \Omega_{co,j,i} s_{co,j,i} + \nu_{co,r} \tag{5.10}$$

where $\Omega_{co,j,i}$ denotes $N_{co} \times 1$ transmit beamforming vector corresponding to signal $s_{co,j,i}$ intended for the ith destination from the jth cell.

To model distributed beamforming, the rth relay multiplies its received signal by complex coefficient $w_{co,r}$. The vector $\mathbf{u}_{co}$ representing all signals transmitted from the relays to the destinations is

$$\mathbf{u}_{co} = \mathbf{W}_{co}^H \mathbf{x}_{co} \tag{5.11}$$

where diagonal DBRF matrix $\mathbf{W}_{co} = \text{diag}(w_{co,1}, w_{co,2}, \ldots, w_{co,n_R^{co}})$

and $\mathbf{x}_{co} = [x_{co,1}\ x_{co,2}\ \ldots\ x_{co,n_R^{co}}]^T$. Using (5.10), the received signal $y_{co,j,i}$ at the ith user of jth cell is

$$y_{co,j,i} = \mathbf{g}_{co,j,i}^T \mathbf{u}_{co} + n_{co,j,i}$$

$$= \underbrace{\mathbf{g}_{co,j,i}^T \mathbf{W}_{co}^H \mathbf{H}_{co,j} \Omega_{co,j,i} s_{co,j,i}}_{Desired\ Signal} + \underbrace{\mathbf{g}_{co,j,i}^T \mathbf{W}_{co}^H \nu_{co} + n_{co,j,i}}_{noise} \tag{5.12}$$

$$+ \underbrace{\mathbf{g}_{co,j,i}^T \mathbf{W}_{co}^H \mathbf{H}_{co,j} \sum_{k=1,k\neq i}^{M_{co,j}} \Omega_{j,k} s_{co,j,k} + \mathbf{g}_{co,j,i}^T \mathbf{W}_{co}^H \sum_{n=1,n\neq j}^{K_{co}} \mathbf{H}_{co,n} \sum_{l=1}^{M_{co,n}} \Omega_{n,l} s_{co,n,l}}_{interference}$$

where $n_R^{co} \times N_{co}$ matrix $\mathbf{H}_{co,j} = [\mathbf{h}_{co,j,1} \dots \mathbf{h}_{co,j,n_R^{co}}]^T$ represents the combined channel from the source to relays, $1 \times n_R^{co}$ row vector $\mathbf{g}_{co,j,i}^T$ represents the channel from the relays to the ith destination in jth cell, and $n_R^{co} \times 1$ vector $\nu = [\nu_{co,1}, \dots, \nu_{co,n_R^{co}}]^T$ represents noise at the relays and $n_{co,j,i}$ represents the receiver noise at the ith user of jth cell.

In the IS scenario as illustrated in Fig. 5.1, each user receives a signal from one of the cells through its relays, and base stations can coordinate their transmission to reduce interference to other cells by reducing their transmission power. In this scenario, each cell has a group of users and tries to reduce interference to other cells and it is an interference-limited system.

5.2.3.1 Transmit Precoder Optimization for IS Scenario

In this case, Eq. (3.10) generalizes to weighted sum power minimization

$$\min_{\Omega_{1,1},\dots,\Omega_{1,M_{co,1}},\dots,\Omega_{K_{co},1},\dots,\Omega_{K_{co},M_{co,K_{co}}}} \sum_{j=1}^{K_{co}} \sum_{i=1}^{M_{co,j}} \alpha_{j,i} \mathrm{Tr}\left(\Omega_{co,j,i} \Omega_{co,j,i}^H\right)$$

$$s.t. \quad \frac{\alpha_{j,i} \Omega_{co,j,i}^H \mathbf{H}_{co,j}^H \mathbf{W}_{co} \mathbf{g}_{co,j,i}^T \mathbf{g}_{co,j,i}^* \mathbf{W}_{co}^H \mathbf{H}_{co,j} \Omega_{co,j,i}}{\Upsilon + \mathrm{Tr}\{\mathbf{W}_{co}^H \mathbf{g}_{co,j,i}^T \mathbf{g}_{co,j,i}^* \mathbf{W}_{co} \sigma_{co,\nu}^2\} + \sigma_{co,n}^2} \geq \gamma_{co,j,i}$$

$$\text{for} \quad i = 1, \dots, M_{co,j}, j = 1, \dots, K_{co}, \tag{5.13}$$

where

$$\Upsilon = \sum_{k=1,k\neq i}^{M_{co,j}} \alpha_{j,k} \Omega_{j,k}^H \mathbf{H}_{co,j}^H \mathbf{W}_{co} \mathbf{g}_{co,j,i}^T \mathbf{g}_{co,j,i}^* \mathbf{W}_{co}^H \mathbf{H}_{co,j} \Omega_{j,k} \tag{5.14}$$

$$+ \sum_{n=1,n\neq j}^{K_{co}} \sum_{l=1}^{M_{co,n}} \alpha_{n,l} \Omega_{n,l}^H \mathbf{H}_{co,n}^H \mathbf{W}_{co} \mathbf{g}_{co,j,i}^T \mathbf{g}_{co,j,i}^* \mathbf{W}_{co}^H \mathbf{H}_{co,n} \Omega_{n,l}.$$

5.2.3.2 Solution using Semidefinite Relaxation

In (5.13), let

$$\mathbf{T}_{co,j,i} = \alpha_{j,i}\Omega_{co,j,i}\Omega_{co,j,i}^H, \quad \text{for} \quad j = 1,\ldots,K_{co} \quad \text{and} \quad i = 1,\ldots,M_{co,j}. \tag{5.15}$$

The weight factors $\alpha_{i,j}$ takes into account factors that include path loss from the base station to the relays, cell load, scheduling priority and other physical factors in the multicell scenario as the minimum power is not the only factor in the design of the transmit beamforming scheme. Apply semi-definite relaxation by similarly dropping constraints

$$\text{rank}(\mathbf{T}_{co,j,i}) = 1, \tag{5.16}$$

the optimization problem (3.12) generalizes to

$$\begin{aligned}
&\min_{\mathbf{T}_{co,1,1},\ldots,\mathbf{T}_{co,1,M_{co,1}},\ldots,\mathbf{T}_{co,K,1},\ldots,\mathbf{T}_{K_{co},M_{co,K_{co}}}} \sum_{j=1}^{K_{co}} \sum_{i=1}^{M_{co,K_{co}}} \text{Tr}\left(\mathbf{T}_{co,j,i}\right) \\
s.t. \quad &\text{Tr}\left(\mathbf{H}_{co,j}^H \mathbf{W}_{co}\mathbf{g}_{co,j,i}^T \mathbf{g}_{co,j,i}^* \mathbf{W}_{co}^H \mathbf{H}_{co,j}(\mathbf{T}_{co,j,i} - \gamma_{co,j,i}\sum_{k=1,k\neq i}^{M_{co,j}} \mathbf{T}_{co,j,k})\right) \\
&-\text{Tr}\left(\sum_{n=1,n\neq j}^{K_{co}} \sum_{l=1}^{M_{co,n}} \mathbf{H}_{co,n}^H \mathbf{W}_{co}\mathbf{g}_{co,j,i}^T \mathbf{g}_{co,j,i}^* \mathbf{W}_{co}^H \mathbf{H}_{co,n}\mathbf{T}_{co,n,l}\right) \\
&\geq \gamma_{co,j,i}\left(\text{Tr}(\mathbf{W}_{co}^H \mathbf{g}_{co,j,i}^T \mathbf{g}_{co,j,i}^* \mathbf{W}_{co})\sigma_{co,v}^2 + \sigma_{co,n}^2\right) \\
&\mathbf{T}_{co,j,i}, \mathbf{T}_{co,j,k}, \mathbf{T}_{co,n,l} \succeq 0 \qquad .
\end{aligned} \tag{5.17}$$

Semi-definite programming can be applied to solve (5.17). When the precoders at the multiple cooperating base stations are fixed, DRBF optimization over a multi-cell area can be achieved similarly to Section 3.4.

Similar to Chapter 3, the iterative algorithm can be applied to jointly optimize the precoders at the cells and the relays.

5.2.3.3 Solution of Transmit Precoder Optimization for IS Scenario Using Duality

In this subsection, transmit Precoder Optimization for IS Scenario is derived based on the duality relation of the uplink and downlink distributed beamforming. It is noted that the SINR constraints can be reformulated as a second-order coneprogramming problem as shown in [33]. The Lagrangian dual of (5.13) is

$$L(\Omega_{co,j,i},\lambda_{co,j,i}) = \sum_{co,j,i}\alpha_j\Omega^H_{co,j,i}\Omega_{co,j,i} - \sum_{co,j,i}\lambda_{co,j,i}(\frac{\Omega^H_{co,j,i}\mathbf{H}^H_{co,j}\mathbf{W}_{co}\mathbf{g}^T_{co,j,i}\mathbf{g}^*_{co,j,i}\mathbf{W}^H_{co}\mathbf{H}_{co,j}\Omega_{co,j,i}}{\gamma_{co,j,i}}$$
$$- \sum_{(n,l)\neq j,i}\Omega^H_{n,l}\mathbf{H}^H_{co,n}\mathbf{W}_{co}\mathbf{g}^T_{co,j,i}\mathbf{g}^*_{co,j,i}\mathbf{W}^H_{co}\mathbf{H}_{co,n}\Omega_{co,n,l} - \mathrm{Tr}(\mathbf{W}^H_{co}\mathbf{g}^T_{co,j,i}\mathbf{g}^*_{co,j,i}\mathbf{W}_{co}\sigma^2_{co,v}) - \sigma^2_{co,n}). \tag{5.18}$$

By rearranging (5.18), we get:

$$L(\Omega_{co,j,i},\lambda_{co,j,i}) = \sum_{j,i}\lambda_{co,j,i}\left(\mathrm{Tr}(\mathbf{W}^H_{co}\mathbf{g}^T_{co,j,i}\mathbf{g}^*_{co,j,i}\mathbf{W}_{co}\sigma^2_{co,v}) + \sigma^2_{co,n}\right) + \sum_{i,j}\Omega^H_{co,j,i}\Theta_{co,j,i}\Omega_{co,j,i}. \tag{5.19}$$

where

$$\Theta_{co,j,i} = \alpha_i\mathbf{I} + \sum_{n,l}\lambda_{n,l}\mathbf{H}^H_{co,j}\mathbf{W}_{co}\mathbf{g}^T_{co,j,i}\mathbf{g}^*_{co,j,i}\mathbf{W}^H_{co}\mathbf{H}_{co,j}$$
$$-(1+\frac{1}{\gamma_{co,i,j}})\lambda_{co,j,i}\mathbf{H}^H_{co,j}\mathbf{W}_{co}\mathbf{g}^T_{co,j,i}\mathbf{g}^*_{co,j,i}\mathbf{W}^H_{co}\mathbf{H}_{co,j}. \tag{5.20}$$

The dual objective is

$$g(\lambda_{co,j,i}) = \min_{\Omega_{co,j,i}} L(\Omega_{co,j,i},\lambda_{co,j,i}) \tag{5.21}$$

In (5.19), it can be seen that if $\Theta_{co,j,i}$ is not a positive definite matrix, then there exists $\Omega_{co,j,i}$ such that $L(\Omega_{co,j,i},\lambda_{co,j,i}) = -\infty$. Thus, the lagrangian dual of (5.18), which is the maximum of $g(\lambda_{co,j,i})$, is

$$\max_{\mathbf{W}_{co}}\sum_{i,j}\lambda_{co,j,i}\left(\mathrm{Tr}(\mathbf{W}^H_{co}\mathbf{g}^T_{co,j,i}\mathbf{g}^*_{co,j,i}\mathbf{W}_{co}\sigma^2_{co,v}) + \sigma^2_{co,n}\right)$$

$$
\begin{aligned}
s.t. \quad & \alpha_i \mathbf{I} + \sum_{n,l} \lambda_{co,n,l} \mathbf{H}_{co,j}^H \mathbf{W}_{co} \mathbf{g}_{co,j,i}^T \mathbf{g}_{co,j,i}^* \mathbf{W}_{co}^H \mathbf{H}_{co,j} \\
& \succeq \lambda_{co,j,i} (1 + \frac{1}{\gamma_{co,i,j}}) \mathbf{H}_{co,j}^H \mathbf{W}_{co} \mathbf{g}_{co,j,i}^T \mathbf{g}_{co,j,i}^* \mathbf{W}_{co}^H \mathbf{H}_{co,i} \\
& \qquad \text{for} \;\; j = 1, \ldots, K_{co}; i = 1, \ldots, M_j
\end{aligned} \tag{5.22}
$$

which can be reformulated as:

$$
\begin{aligned}
& \min_{\mathbf{W}_{co}} \sum_{i,j} \lambda_{co,j,i} \left(\mathrm{Tr}(\mathbf{W}_{co}^H \mathbf{g}_{co,j,i}^T \mathbf{g}_{co,j,i}^* \mathbf{W}_{co} \sigma_{co,v}^2) + \sigma_{co,n}^2 \right) \\
s.t. \;\; & \max_{\Omega_{co,j,i}} \quad \frac{\lambda_{co,j,i} \Omega_{co,j,i}^H \mathbf{H}_{co,j}^H \mathbf{W}_{co} \mathbf{g}_{co,j,i}^T \mathbf{g}_{co,j,i}^* \mathbf{W}_{co}^H \mathbf{H}_{co,j} \Omega_{co,j,i}}{\sum_{(m,n) \neq (j,i)} \lambda_{co,m,n} \Omega_{co,j,i}^H \mathbf{H}_{co,m}^H \mathbf{W}_{co} \mathbf{g}_{co,j,i}^T \mathbf{g}_{co,j,i}^* \mathbf{W}_{co}^H \mathbf{H}_{co,m} \Omega_{co,j,i} + \alpha_j \Omega_{co,j,i}^H \Omega_{co,j,i}} \\
& \qquad \geq \gamma_{co,i,j}.
\end{aligned} \tag{5.23}
$$

It has been shown [82] that the receive beamforming vector that maximize the SINR of the system is the principal eigenvector of (A_{co}, B_{co}),

$$
\hat{\Omega}_{co,j,i} = \wp(B_{co}^{-1} A_{co}), \tag{5.24}
$$

where $A_{co} = \mathbf{H}_{co,j}^H \mathbf{W}_{co} \mathbf{g}_{co,j,i}^T \mathbf{g}_{co,j,i}^* \mathbf{W}_{co}^H \mathbf{H}_{co,j}$,

$B_{co} = \sum_{(m,n) \neq (j,i)} \lambda_{m,n} \mathbf{H}_{co,m}^H \mathbf{W}_{co} \mathbf{g}_{co,j,i}^T \mathbf{g}_{co,j,i}^* \mathbf{W}_{co}^H \mathbf{H}_{co,m} + \alpha_j \mathbf{I}$. Here $\Omega_{co,j,i}$ and $\hat{\Omega}_{co,j,i}$ are scaled versions of each other. Thus, one would be able to find $\Omega_{co,j,i}$ by first finding $\hat{\Omega}_{co,j,i}$, then updating it through the scalar multiplications $\Omega_{co,j,i} = \sqrt{\delta_{co,j,i}} \hat{\Omega}_{co,j,i}$. The $\delta_{j,i}$ can be found through a matrix inversion using the fact that the SINR constraints in (5.13) are satisfied with equality.

Substituting (5.24) into SINR constraints of (5.13), the SINR constraints become

$$
\begin{aligned}
& \frac{1}{\gamma_{co,j,i}} \Omega_{co,j,i}^H \mathbf{H}_{co,j}^H \mathbf{W}_{co} \mathbf{g}_{co,j,i}^T \mathbf{g}_{co,j,i}^* \mathbf{W}_{co}^H \mathbf{H}_{co,j} \Omega_{co,j,i} \delta_{co,j,i} - \\
& \qquad \sum_{n \neq i} \Omega_{co,j,n}^H \mathbf{H}_{co,j}^H \mathbf{W}_{co} \mathbf{g}_{co,j,i}^T \mathbf{g}_{co,j,i}^* \mathbf{W}_{co}^H \mathbf{H}_{co,j} \Omega_{co,j,n} \delta_{j,n}
\end{aligned}
$$

$$- \sum_{m \neq j,l} \Omega^H_{co,m,l} \mathbf{H}^H_{co,m} \mathbf{W}_{co} \mathbf{g}^T_{co,j,i} \mathbf{g}^*_{co,j,i} \mathbf{W}^H_{co} \mathbf{H}_{co,m} \Omega_{co,m,l} \delta_{m,l}$$
$$= \mathrm{Tr}(\mathbf{W}^H_{co} \mathbf{g}^T_{co,j,i} \mathbf{g}^*_{co,j,i} \mathbf{W}_{co} \sigma^2_{co,v}) + \sigma^2_{co,n}. \tag{5.25}$$

Define $\delta_j \equiv [\delta_{j,1}, \ldots, \delta_{j,M_j}]^T$, $\delta \equiv [\delta_1^T, \ldots, \delta_K^T]^T$, $\eta \equiv [\eta_1^T, \ldots, \eta_K^T]^T$, and $\eta_j \equiv [\mathrm{Tr}(\mathbf{W}^H_{co} \mathbf{g}^T_{co,j,1} \mathbf{g}^*_{co,j,1} \mathbf{W}_{co} \sigma^2_{co,v}) + \sigma^2_{co,n}, \ldots, \mathrm{Tr}(\mathbf{W}^H_{co} \mathbf{g}^T_{co,j,M_j} \mathbf{g}^*_{co,j,M_j} \mathbf{W}_{co} \sigma^2_{co,v}) + \sigma^2_{co,n}]^T$. Based on this notation and (5.25), we can obtain $\delta_{co,j,i}$ by

$$\delta = \mathbf{F}^{-1}_{co} \eta$$

where $\mathbf{F}_{co}$ is the $K_{co}M_{co} \times N_{co}K_{co}$ matrix with the (j,n)-th entry of each $M_{co} \times M_{co}$ sub-matrix $\mathbf{F}^{im}_{co}$ defined as:

$$\mathbf{F}^{jm}_{co,in} = \begin{cases} \frac{1}{\gamma_{co,j,i}} \Omega^H_{co,j,i} \mathbf{H}^H_{co,j} \mathbf{W}_{co} \mathbf{g}^T_{co,j,i} \mathbf{g}^*_{co,j,i} \mathbf{W}^H_{co} \mathbf{H}_{co,j} \Omega_{co,j,i} & \text{if m=j, n=i} \\ -\Omega^H_{co,j,n} \mathbf{H}^H_{co,j} \mathbf{W}_{co} \mathbf{g}^T_{co,j,i} \mathbf{g}^*_{co,j,i} \mathbf{W}^H_{co} \mathbf{H}_{co,j} \Omega_{co,j,n} & \text{if m=j, n}\neq \text{ i} \\ \Omega^H_{co,m,n} \mathbf{H}^H_{co,m} \mathbf{W}_{co} \mathbf{g}^T_{co,j,i} \mathbf{g}^*_{co,j,i} \mathbf{W}^H_{co} \mathbf{H}_{co,m} \Omega_{co,m,n} & \text{if m}\neq \text{ j.} \end{cases}$$

We remark that for the multicell precoders optimization for the IS scenario, there are two methods to obtain the precoders, including the semidefinite relaxation method discussed in Section 5.2.3.1, as well as the duality method discussed in Section 5.2.3.3. While both methods can uniquely determine the optimal precoders, the duality method has lower computational complexity.

5.2.3.4 Relay weight optimization and iterative algorithm for IS scenario

When the precoders at the multiple cooperating base stations are fixed, DRBF optimization over a multi-cell area can be achieved in a similar manner to that presented in Section 3.4. The iterative algorithm from Section 3.3 can be applied here to minimize the sum power at both base stations and relays.

5.3 Numerical Results

To investigate multiple base station coordinated transmission, we assume that base stations are fiber-backbone-connected and a central controller collects information from the base stations and makes decisions as in industrial practice. We consider the scenario of three single-antenna mobile users (destinations) located in the coverage area of the relays as indicated in Fig. 5.1. This is typical of dense urban scenario where cells have overlapping coverage and where there is no indoor wireless as in the case of shopping malls which generally have poor indoor user cellular experiences. The relays deployed near the buildings could be used to enhance the indoor coverage. The proposed scheme in Section 5.2.2 is adopted. In this scenario, MS1, MS2 and MS3 are located in the coverage area of the relays but out of direct reach of Cell A and Cell B due to distance, shadowing effects and penetration loss due to indoor location. A group of 6 relays are located at the overlapping service areas of Cells A and B. Path loss from cell A and cell B are compensated by power control, so the channels from Cell A and Cell B to relays are Rayleigh flat-fading channels, following $\mathscr{CN}(0,\,1)$. For simplicity, here we also assume that the path loss from different base stations to the relays are the same, and that is $a_{i,1} = a_{i,2} = \ldots = a_{i,n_R}, i = 1,\ldots,K$. We also assume that the weight factors for the same base station to be the same, and that is $\alpha_{i,1} = \alpha_{i,2} = \ldots = \alpha_{i,M}, i = 1,\ldots,K$ and the path loss from different base station to relays are fully compensated by the weight factors as $|a_{i,r}|^2\alpha_{i,j} = 1, j = 1,\ldots,M$. In the scenario of Fig. 5.1, $M = 3, K = 2$, and $n_R = 6$. From Fig. 5.2, we can see that for a specific realization of the channels, the allocated power from Cell B to MS2 is about 30dB lower than power from the allocated power from Cell A to MS2 for different levels of SINR threshold. When the transmission power allocated by Cell B is 30dB lower than that of Cell A, Cell B should stop the data transmission to MS2. In this case, the beamforming algorithm in Section 5.2.2 allocated most of its power resources to a single cell, i.e., the best cell to serve a specific user can be found. The

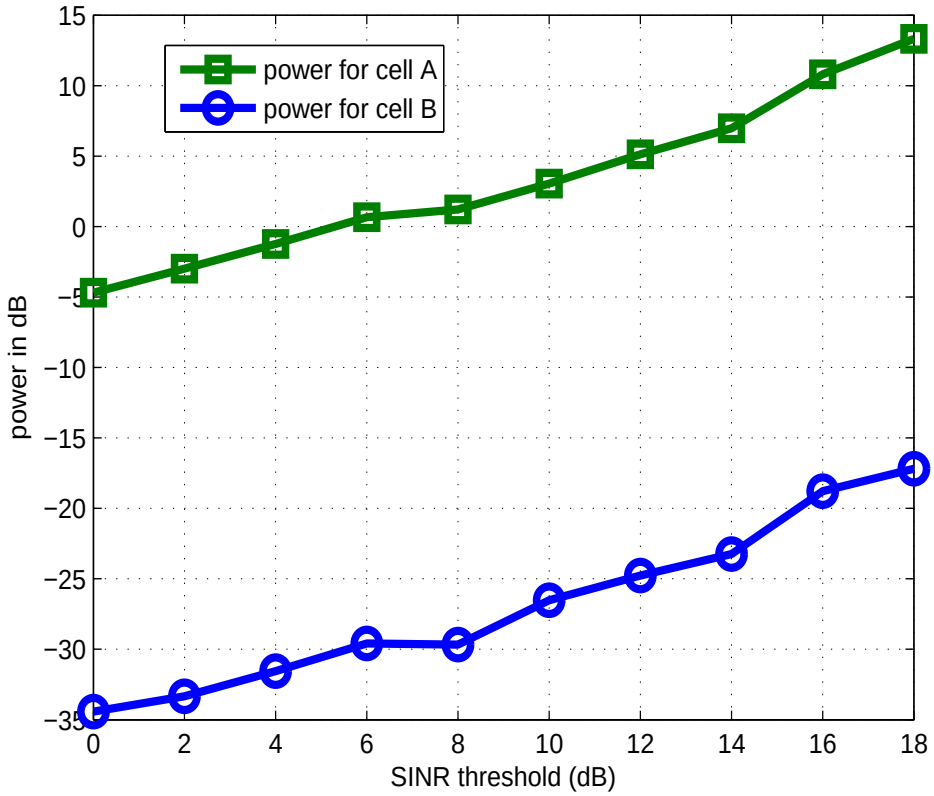

Figure 5.2. The comparison of the power allocation by Cell A to MS2 and Cell B to MS2

proposed algorithm may be combined with base station power control to assign an appropriate cell to transmit to a specific user, taking path loss, cell load, scheduling priority and other factors into account through the weight factor. We remark that in the process, the choice of the serving cell takes additional critical factors into account such as inter-cell interference, base station-relay alignment, and eigen-channels from relays to destination.

5.4 Summary

Wireless transmission from multiple multiple-antenna base station to multiple single-antenna destinations through a network of single-antenna relays is considered. Optimal precoding and distributed

relay beamforming solutions, in the sense of minimizing source and relay power, are formulated and computed. Two different scenarios are considered for coordinated beamforming, one is suitable for scenarios such as relays serving users located in overlapped areas (typical of dense urban scenarios) to select serving cell and another one is for users persists in specific cells to suppress inter-cell interference. Simulations show obvious gain for using coordinated beamforming compared with not using coordinated beamforming.

Chapter 6

Multi-antenna Relay Cooperative System Uplink

6.1 Uplink Cooperative System with Single Multi-antenna Relay

In previous chapters, we studied point-to-point cooperative systems, single cell downlink and uplink cooperative systems with single antenna relays as well as a multi-cell cooperative system with single antenna relays. In this chapter, we will extend the uplink scenario to cooperative multiple antenna relays that act as system access points, which is a scenario that is receiving increasing attention in emerging 3GPP LTE-Advanced [31]. In this scenario, the relay is targeted for the coverage of a hotspot and provides a high speed uplink for a group of users with high data rate terminals (equipped with multiple antennas). In this chapter, rather than power minimization used as an optimization criterion in previous Chapters 3-5, here the approach involves capacity optimization.

In the literature, multi-antenna relay systems have attracted strong interest. A cooperative system with a multiple antenna source, multiple multi-antenna relays and a single-antenna receiver is studied in [83]. However, the cooperative system is not efficient as multiple multi-antenna relays incur high system overhead for channel estimation and scheduling, and are very inefficient in scheduling just one user. For example, consider the case of source with M antennas, K relays each with N antennas and a single antenna destination, the overhead is a factor of $O(MNK)$ greater that of a cooperative system

with a single antenna at source, relay and destination. A cooperative scheme is proposed in [84] with a network of multi-antenna relays to serve a single user with AF or hybrid relaying. Similar to [83], this scheme proposed has high overhead and complexity but limited gain. For example, in the case of source with M antennas, K relays each with N antennas and a destination with L antennas, the overhead is about K times higher than a system with a M-antenna source, a N-antenna relay and a L-antenna destination. A cooperative scheme with a multi-antenna relay to serve a multi-antenna user is proposed in [46], where it is shown that the source and the relay should map their signals to the dominant right singular vectors of the source-relay and relay-destination channels. A cooperative scheme with a direct link from source to destination and an indirect link through a multi-antenna relay is proposed in [85], where a waterfilling algorithm in the spatial domain is proposed showing a gain in throughput. A cooperative system with a multi-antenna source, a multi-antenna relay and a multi-antenna destination is studied in [86], where an optimal solution was found when no direct link exists. For a multiple-antenna relay channel, the full-duplex cut-set capacity upper bound and decode-and-forward rate are formulated as convex optimization problems in [87]. For half-duplex relaying, bandwidth allocation and transmit signals are optimized jointly. The capacity and beamforming optimality of multi-antenna relaying systems was investigated in [88], where statistical channel information is assumed at the relay and source. The optimal transmission strategies at both the source and relay were developed and necessary and sufficient conditions for which beamforming achieves capacity were derived in [88]. A comprehensive analytical framework of dual-hop fixed decode-and-forward cooperative networks with multi-antenna relays and distributed spatial diversity is developed over generalized Nakagami-m fading channels [89]. The optimal linear beamforming matrix in closed form based on convex optimization techniques, aiming to minimize the weighted mean squared error (MSE) was developed in [90]. A multiuser multi-antenna downlink cooperative system was studied in [91], upper and lower bounds for sum rate was proposed.

An obvious trend in the communication industry is to increase spectrum efficiency deploying more antennas at the base station as well as at user terminals. However, spectrum efficiency decreases with the increase of distance between user terminals and the base station. To mitigate this effect, high transmission power is needed at user terminals. However, high transmission power is not achievable at user terminal due to radiation and battery life. In this chapter we propose the application of multiple antenna relays to draw the user terminals nearer to enable MIMO communication between user terminals and relays and between relays and the base station.

In this chapter, uplink cooperative system with multiple antennas at the relay is proposed. A specific schemes are studied: users access the base station through a single multi-antenna relay. In this chapter, full channel state information (CSI) from relays to the base station and full CSI from sources to relays are assumed at the base station is assumed at the base station. Perfect synchronization across the system is assumed [48] [49] [50].

The remainder of the chapter is organized as follows: in Section 6.2, system model for single multi-antenna relay system is presented, in Section 6.3 uplink system optimization with a multi-antenna relay is then developed. Numerical results are provided in Section 6.4, followed by a summary in Section 6.5.

6.2 System Model

We assume a single multi-antenna relay with $n_R^{ul,mu}$ antennas, with M_{ul} users each equipped with $N_{ul,ue}$ antennas and a base station with $N_{ul,ba}$ antennas. In order to communicate to the destination, each source transmits its data to the multi-antenna relay. The relay then delivers its data to the base station. The transmission from the users to the relay is represented, in matrix form, as

$$\mathbf{x}_{ul,mu} = \sum_{i=1}^{M_{ul}} \mathbf{B}_i \mathbf{S}_i \mathbf{s}_{ul,i} + \varsigma_{ul} \tag{6.1}$$

where $\mathbf{x}_{ul,mu}$ is the received signal at the relay, $\mathbf{B}_i$ is the channel from the ith source to the relay, $\mathbf{S}_i$ is the beamforming matrix for the ith user, and ς_{ul} is the noise vector at the relay with i.i.d. noise components. Each of the noise components has variance σ_ς^2. The relay multiplies its received signal by a complex weighting matrix $\mathbf{W}_{ul,mu}$. The vector of signals $\mathbf{u}_{ul,mu}$ transmitted from the relays is

$$\mathbf{u}_{ul,mu} = \mathbf{W}_{ul,mu}^H \mathbf{x}_{ul,mu}. \tag{6.2}$$

The received signal at the N_{ul}-antenna base station destination is expressed as

$$\mathbf{y}_{ul,mu} = \mathbf{J}_{ul,mu}\mathbf{u}_{ul,mu} + \vartheta_{ul} \tag{6.3}$$

where $\mathbf{J}_{ul,mu}$ is an $N_{ul,ba} \times n_R^{ul,mu}$ matrix representing the channel from the relay to the base station and ϑ_{ul} is the noise vector observed at the base station receiver. The variance of the i.i.d. noise terms at the base station receiver is σ_ϑ^2.

Using (6.1)-(6.3), the received signal at base station can be expressed as

$$\mathbf{y}_{ul,mu} = \mathbf{J}_{ul,mu}\mathbf{W}_{ul,mu}^H \sum_{i=1}^{M_{ul}} \mathbf{B}_i \mathbf{S}_i \mathbf{s}_{ul,i} + \mathbf{J}_{ul,mu}\mathbf{W}_{ul,mu}^H \varsigma_{ul} + \vartheta_{ul}. \tag{6.4}$$

Using the well-known results reviewed in Chapter 2, channel capacity of this uplink cooperative system can be expressed as

$$C_{ul,mu} = \frac{1}{2}\text{logdet}\left(\sum_{i=1}^{M_{ul}} \mathbf{H}_{ul,mu,i}\Gamma_i\mathbf{H}_{ul,mu,i}^H + \sigma_\varsigma^2\mathbf{H}_\varsigma\mathbf{H}_\varsigma^H + \sigma_\vartheta^2\mathbf{I}_{n_{ul,ba}}\right) - \frac{1}{2}\text{logdet}\left(\sigma_\varsigma^2\mathbf{H}_\varsigma\mathbf{H}_\varsigma^H + \sigma_\vartheta^2\mathbf{I}_{n_{ul,ba}}\right) \tag{6.5}$$

where

$$\mathbf{H}_{ul,mu,i} = \mathbf{J}_{ul,mu}\mathbf{W}_{ul,mu}^H\mathbf{B}_i,$$

$$\mathbf{H}_\varsigma = \mathbf{J}_{ul,mu}\mathbf{W}_{ul,mu}^H$$

$$\Gamma_i = \mathbf{S}_i\mathbf{S}_i^H.$$

The second term in (6.5) comes from amplified relay noise and receiver noise.

In the following subsections, we address the problem in three stages: 1) fix the relay beamforming matrix and maximize the channel capacity with the user beamforming matrices as variables, 2) fix the user beamforming matrices and maximize the channel capacity with relay beamforming matrix as variables, followed by 3) joint optimization of user transmit beamforming matrices and relay beamforming matrices.

6.3 Uplink Cooperative System with a Multi-antenna Relay

6.3.1 User beamformer optimization with fixed relay beamformer

Here we assume that the relay beamforming matrix is given and optimize the user beamforming matrices accordingly. Because $\mathbf{W}_{ul,mu}$ is given, the second terms $\frac{1}{2}\text{logdet}\left(\sigma_{\varsigma}^2\mathbf{H}_{\varsigma}\mathbf{H}_{\varsigma}^H+\sigma_{\vartheta}^2\mathbf{I}_{n_{ul,ba}}\right)$ in (6.5) is given, and we only need to maximize the first term in the channel capacity expression of this uplink cooperative system. The maximization of the capacity in (6.5) can be reformulated as

$$\begin{aligned}\min_{\Gamma_1,\ldots,\Gamma_{M_{ul}}} \quad & -\text{logdet}\Big(\sum_{i=1}^{M_{ul}}\mathbf{H}_{ul,mu,i}\Gamma_i\mathbf{H}_{ul,mu,i}^H+\mathbf{H}_{\varsigma}\mathbf{H}_{\varsigma}^H+\sigma_{\vartheta}^2\mathbf{I}_{n_{ul,ba}}\Big)\\ & s.t.\ \ \text{Tr}(\Gamma_i)\le P_{ul,i}\\ & \Gamma_i\succeq 0 \qquad i=1,\ldots,M_{ul}\\ & \text{and}\ \ \sum_{i=1}^{M_{ul}}\text{Tr}(\Gamma_i)\le P_{sum,ul}. \end{aligned} \tag{6.6}$$

Problem (6.6) becomes a colored-noise vector multiple access channel capacity maximization problem. After noise-whitening, this problem can be optimally solved by the multiple access iterative waterfilling algorithm proposed by Yu [92] [93] as follows:

Step 1: initialize $\mathbf{S}_i^{(1)}=0, i=1,\ldots,M_{ul}$.

Step 2: repeat for kth iteration, $k>1$

$$\Gamma_j^{(k)} = \arg\max_{\Gamma_j} \frac{1}{2}\log|\tilde{\mathbf{H}}_{ul,mu,j}\Gamma_j\tilde{\mathbf{H}}_{ul,mu,j}^H + \mathbf{I}|$$

$$\text{for} \quad j = 1,\ldots,M_{ul} \tag{6.7}$$

where

$$\tilde{\mathbf{H}}_{ul,mu,j} = \left(\sum_{i=1,i\neq j}^{M_{ul}} \mathbf{H}_{ul,mu,i}\Gamma_i^{(k-1)}\mathbf{H}_{ul,mu,i}^H + \mathbf{H}_\varsigma\mathbf{H}_\varsigma^H + \sigma_\vartheta^2\mathbf{I}_{n_{ul,ba}}\right)^{-1/2}\mathbf{H}_{ul,mu,j} \tag{6.8}$$

where $\Gamma_i^{(k-1)}$ is the beamforming matrix for ith user at the $(k-1)$th iteration. Repeat Step 2 until the desired accuracy is reached. In Step 2, waterfilling algorithm [92] [94] can be applied to obtain $\Gamma_j^{(k)}$.

6.3.2 Relay Beamforming Matrix Optimization With Fixed User Transmit Beamforming Matrices

In this part, we assume given a user transmit beamforming matrix and optimize the relay beamforming matrix. The problem can be formulated as follows:

$$\begin{aligned}\max_{\mathbf{W}_{ul,mu}} \frac{1}{2}\text{logdet}&\left(\mathbf{J}_{ul,mu}\mathbf{W}_{ul,mu}^H\sum_{i=1}^{M_{ul}}\left(\mathbf{B}_i\Gamma_i^H\mathbf{B}_i^H + \sigma_\varsigma^2\mathbf{I}_{n_{ul,ba}}\right)\mathbf{W}_{ul,mu}\mathbf{J}_{ul,mu} + \sigma_\vartheta^2\mathbf{I}_{n_{ul,ba}}\right)\\ &-\frac{1}{2}\text{logdet}\left(\sigma_\varsigma^2\mathbf{J}_{ul,mu}\mathbf{W}_{ul,mu}^H\mathbf{W}_{ul,mu}\mathbf{J}_{ul,mu} + \sigma_\vartheta^2\mathbf{I}_{n_{ul,ba}}\right)\\ s.t.\quad &\text{Tr}\left(\mathbf{W}_{ul,mu}\left(\mathbf{B}_i\Gamma_i^H\mathbf{B}_i^H + \sigma_\varsigma^2\mathbf{I}_{n_{ul,ba}}\right)\mathbf{W}_{ul,mu}^H\right) \leq P_{R,mu}.\end{aligned} \tag{6.9}$$

By applying singular value decomposition (SVD) to channel $\mathbf{J}_{ul,mu}$, i.e.,

$$\mathbf{J}_{ul,mu} = \mathbf{U}_{ul,mu}\mathbf{D}_{ul,mu}\mathbf{V}_{ul,mu}^H, \tag{6.10}$$

as well as to $\sum_{i=1}^{M_{ul}}\left(\mathbf{B}_i\mathbf{S}_i\mathbf{S}_i^H\mathbf{B}_i^H + \sigma_\varsigma^2\mathbf{I}_{n_R^{ul,mu}}\right)$,

$$\sum_{i=1}^{M_{ul}}\mathbf{B}_i\mathbf{S}_i\mathbf{S}_i^H\mathbf{B}_i^H + \sigma_\varsigma^2\mathbf{I}_{n_R^{ul,mu}} = \mathbf{O}_{ul}\left(\Sigma_{ul} + \sigma_\varsigma^2\mathbf{I}_{n_R^{ul,mu}}\right)\mathbf{O}_{ul}^H, \tag{6.11}$$

and finally to the user beamforming matrix sum,

$$\mathbf{W}_{ul,mu} = \mathbf{V}_{ul,mu}\Sigma_{\mathbf{W}_{ul,mu}}\mathbf{O}_{ul}^{H}. \tag{6.12}$$

By combining (6.5)(6.10)(6.11)(6.12), the uplink channel capacity can be calculated as follows:

$$\begin{aligned}
C_{ul,mu} &= \frac{1}{2}\text{logdet}\left(\mathbf{U}_{ul,mu}\mathbf{D}_{ul,mu}\Sigma_{\mathbf{W}_{ul,mu}}\left(\Sigma_{ul}+\sigma_{\varsigma}^{2}\mathbf{I}_{n_R^{ul,mu}}\right)\Sigma_{\mathbf{W}_{ul,mu}}^{H}\mathbf{D}_{ul,mu}^{H}\mathbf{U}_{ul,mu}^{H}+\sigma_{\vartheta}^{2}\mathbf{I}_{n_{ul,ba}}\right)\\
&-\frac{1}{2}\text{logdet}\left(\sigma_{\varsigma}^{2}\mathbf{U}_{ul,mu}\mathbf{D}_{ul,mu}\Sigma_{\mathbf{W}_{ul,mu}}\Sigma_{\mathbf{W}_{ul,mu}}^{H}\mathbf{D}_{ul,mu}^{H}\mathbf{U}_{ul,mu}^{H}+\sigma_{\vartheta}^{2}\mathbf{I}_{n_{ul,ba}}\right)\\
&=\frac{1}{2}\text{logdet}\left(\mathbf{D}_{ul,mu}\Sigma_{\mathbf{W}_{ul,mu}}\left(\Sigma_{ul}+\sigma_{\varsigma}^{2}\mathbf{I}_{n_R^{ul,mu}}\right)\Sigma_{\mathbf{W}_{ul,mu}}^{H}\mathbf{D}_{ul,mu}^{H}+\sigma_{\vartheta}^{2}\mathbf{I}_{n_{ul,ba}}\right)\\
&-\frac{1}{2}\text{logdet}\left(\sigma_{\varsigma}^{2}\mathbf{D}_{ul,mu}\Sigma_{\mathbf{W}_{ul,mu}}\Sigma_{\mathbf{W}_{ul,mu}}^{H}\mathbf{D}_{ul,mu}^{H}+\sigma_{\vartheta}^{2}\mathbf{I}_{n_{ul,ba}}\right)\\
&=\frac{1}{2}\text{logdet}\left(\mathbf{D}_{ul,mu}\left(\Sigma_{ul}+\sigma_{\varsigma}^{2}\mathbf{I}_{n_R^{ul,mu}}\right)\Sigma_{\mathbf{W}_{ul,mu}}^{2}\mathbf{D}_{ul,mu}^{H}+\sigma_{\vartheta}^{2}\mathbf{I}_{n_{ul,ba}}\right)\\
&-\frac{1}{2}\text{logdet}\left(\sigma_{\varsigma}^{2}\mathbf{D}_{ul,mu}\Sigma_{\mathbf{W}_{ul,mu}}^{2}\mathbf{D}_{ul,mu}^{H}+\sigma_{\vartheta}^{2}\mathbf{I}_{n_{ul,ba}}\right).
\end{aligned} \tag{6.13}$$

Assuming that there are enough users such that $n_R^{ul,mu} \leq M_{ul}N_{ul,ue}$, we consider the following two cases: 1) $n_R^{ul,mu} \leq N_{ul,ba}$ 2) $n_R^{ul,mu} > N_{ul,ba}$. In the first case, the effective uplink cooperative channel is a $n_R^{ul,mu}$ input, $N_{ul,ba}$ output MIMO channel with rank of $\min(n_R^{ul,mu}, N_{ul,ba}) = n_R^{ul,mu}$. The rank is limited by the number of relay antennas. In the second case, the effective uplink cooperative channel is a $n_R^{ul,mu}$ input, $N_{ul,ba}$ output MIMO channel with rank of $\min(n_R^{ul,mu}, N_{ul,ba}) = N_{ul,ba}$. The rank is limited by the number of base station antennas. Next we will study the channel capacity of the uplink cooperative channel with given user beamforming matrices corresponding to these two cases.

6.3.2.1 More Base Station Antennas than Relay Antennas $n_R^{ul,mu} \geq N_{ul,ba}$

In this case, we denote $\tilde{\Sigma}_{\mathbf{W}_{ul,mu}}$ as the upper triangular portion of $\Sigma_{\mathbf{W}_{ul,mu}}$ as follows:

$$(\tilde{\Sigma}_{\mathbf{W}_{ul,mu}})_{i,j} = \begin{cases} (\Sigma_{\mathbf{W}_{ul,mu}})_{i,j}, & i,j \leq N_{ul,ba} \\ 0, & \text{else.} \end{cases} \tag{6.14}$$

With (6.14), (6.13) can be rewritten as

$$\begin{aligned} C_{ul,mu} &= \frac{1}{2}\text{logdet}\left(\mathbf{I}_{n_{ul,ba}} + (\sigma_\varsigma^2 \mathbf{D}_{ul,mu}\Sigma^2_{\mathbf{W}_{ul,mu}}\mathbf{D}^H_{ul,mu} + \sigma_\vartheta^2 \mathbf{I}_{n_{ul,ba}})^{-1}\mathbf{D}_{ul,mu}\Sigma_{ul}\Sigma^2_{\mathbf{W}_{ul,mu}}\mathbf{D}^H_{ul,mu}\right) \\ &= \frac{1}{2}\text{logdet}\left(\left(\mathbf{D}_{ul,mu}\Sigma_{ul}\mathbf{D}^H_{ul,mu}\right)^{-1} + (\sigma_\varsigma^2 \mathbf{D}_{ul,mu}\mathbf{D}^H_{ul,mu}\tilde{\Sigma}^2_{\mathbf{W}_{ul,mu}} + \sigma_\vartheta^2 \mathbf{I}_{n_{ul,ba}})^{-1}\tilde{\Sigma}^2_{\mathbf{W}_{ul,mu}}\right) \\ &+ \frac{1}{2}\text{logdet}\left(\mathbf{D}_{ul,mu}\Sigma_{ul}\mathbf{D}^H_{ul,mu}\right). \end{aligned} \tag{6.15}$$

In this case, the rank of $\mathbf{W}_{ul,mu}$ is limited to $N_{ul,ba}$, which means that power will be only allocated to the eigenmodes up to rank $N_{ul,ba}$ due to the limitation from the number of base station antennas.

In (6.13), $\mathbf{D}_{ul,mu}\Sigma_{ul}\mathbf{D}^H_{ul,mu}$ is the eigen-matrix of the eigenvalue decomposition of the source-relay uplink channels. $\mathbf{D}_{ul,mu}$ is the eigen-matrix of singular vectors of the channel from relay to base station. Since Σ_{ul} are singular values of both user beamforming matrices and the channel from users to the relay, Σ_{ul} can be regarded as the eigenvalues of the aggregate channel from the users to the relay. The aim of the optimization of the user beamforming matrices is to make Σ_{ul} aligned with positive definite diagonal matrix $\mathbf{D}_{ul,mu}\mathbf{D}^H_{ul,mu}$ according to the waterfilling principle to maximize the capacity of the cooperative uplink channel, and $\left(\mathbf{D}_{ul,mu}\Sigma_{ul}\mathbf{D}^H_{ul,mu}\right)^{-1}$ is the effective noise level of the cooperative uplink channel. The problem of maximizing the uplink cooperative channel capacity with given user beamforming matrices can be rewritten to include a power constraint as follows:

$$\begin{aligned} \max_{\Sigma_{\mathbf{W}_{ul,mu}}} \frac{1}{2}\text{logdet}\left(\left(\mathbf{D}_{ul,mu}\Sigma_{ul}\mathbf{D}^H_{ul,mu}\right)^{-1} + (\mathbf{D}_{ul,mu}\mathbf{D}^H_{ul,mu}\tilde{\Sigma}^2_{\mathbf{W}_{ul,mu}} + \sigma_\vartheta^2 \mathbf{I}_{n_{ul,ba}})^{-1}\tilde{\Sigma}^2_{\mathbf{W}_{ul,mu}}\right) \\ s.t. \quad \text{Tr}\left(\tilde{\Sigma}^2_{\mathbf{W}_{ul,mu}}\left(\Sigma_{ul} + \sigma_\varsigma^2 \mathbf{I}_{n_R^{ul,mu}}\right)\right) \leq P_{\mathbf{W}}. \end{aligned} \tag{6.16}$$

By denoting the diagonal elements

$$\begin{aligned} z_j &:= (\tilde{\Sigma}^2_{\mathbf{W}_{ul,mu}})_{j,j}, j = 1,\ldots N_{ul,ba} \\ u_j &:= \left(\Sigma_{ul} + \sigma_\varsigma^2 \mathbf{I}_{n_R^{ul,mu}}\right)_{j,j}, \quad j = 1,\ldots,N_{ul,ba} \end{aligned} \tag{6.17}$$

the maximization in (6.16) can be written more explicitly as

$$\max_{\Sigma_{z_1,\ldots,z_{N_{ul,ba}}}} \frac{1}{2}\sum_{j=1}^{N_{ul,ba}} \log\left(\left(\mathbf{D}_{ul,mu}\Sigma_{ul}\mathbf{D}^H_{ul,mu}\right)^{-1}_{j,j} + \frac{z_j}{\sigma_\varsigma^2(\mathbf{D}_{ul,mu}\mathbf{D}^H_{ul,mu})_{j,j}z_j + \sigma_\vartheta^2}\right)$$

$$s.t. \quad \mathrm{Tr}\left(\sum_{1=1}^{N_{ul,ba}} z_j u_j\right) \leq P_{\mathbf{W}}. \tag{6.18}$$

In (6.18), define the objective function

$$f(z_1,\ldots,z_{N_{ul,ba}}) := \frac{1}{2}\sum_{j=1}^{N_{ul,ba}} \log\left(\left(\mathbf{D}_{ul,mu}\Sigma_{ul}\mathbf{D}_{ul,mu}^H\right)^{-1}_{j,j} + \frac{z_j}{\sigma_\varsigma^2(\mathbf{D}_{ul,mu}\mathbf{D}_{ul,mu}^H)_{j,j}z_j + \sigma_\vartheta^2}\right). \tag{6.19}$$

By differentiation, it can straightforwardly be shown that

$$\begin{aligned}
&\frac{\partial^2 f(z_1,\ldots,z_{N_{ul,ba}})}{\partial z_j \partial z_k} = 0, \quad \forall j \neq k \\
&\frac{\partial^2 f(z_1,\ldots,z_{N_{ul,ba}})}{\partial^2 z_j} < 0, \quad \text{for } \; j = 1,\ldots,N_{ul,ba},
\end{aligned} \tag{6.20}$$

which means that the Hessian matrix of function $f(z_1,\ldots,z_{N_{ul,ba}})$ is negative definite and $f(z_1,\ldots,z_{N_{ul,ba}})$ is concave in variables $z_j, j = 1,\ldots,N_{ul,ba}$. As $f(z_1,\ldots,z_{N_{ul,ba}})$ is concave in $z_j, j = 1\ldots,N_{ul,ba}$ and the constraint is linear in $z_j, j = 1,\ldots,N_{ul,ba}$, (6.18) is a convex optimization problem and the optimal solution can be obtained. For the details of the derivations in (6.20), please refer to Appendix F.

Since (6.18) is concave in $(z_1,\ldots,z_{N_{ul,ba}})$ with the constrained domain $z_j > 0, j = 1,\ldots,N_{ul,ba}$, $\mathrm{Tr}\left(\sum_{1=1}^{N_{ul,ba}} z_j u_j\right) \leq P_{\mathbf{W}}$, by solving KKT conditions of (6.18) [23], the numerical solution can be obtained. By applying (6.17) and (6.12), the optimal $\mathbf{W}_{ul,mu}$ can be obtained.

6.3.2.2 More Relay Antennas than Base Station Antennas $n_R^{ul,mu} < N_{ul,ba}$

In this case we denote $\tilde{\mathbf{D}}_{ul,mu}$ as the upper triangular portion of $\mathbf{D}_{ul,mu}$ as follows:

$$(\tilde{\mathbf{D}}_{ul,mu})_{i,j} = \begin{cases} (\mathbf{D}_{ul,mu})_{i,j}, & i,j \leq n_R^{ul,mu} \\ 0, & \text{else.} \end{cases} \tag{6.21}$$

With (6.21), (6.13) can be rewritten as

$$\begin{aligned}
C_{ul,mu} &= \frac{1}{2}\mathrm{logdet}\left(\mathbf{D}_{ul,mu}(\Sigma_{ul} + \sigma_\varsigma^2\mathbf{I}_{n_R^{ul,mu}})\Sigma^2_{\mathbf{W}_{ul,mu}}\mathbf{D}_{ul,mu}^H\right) - \frac{1}{2}\mathrm{logdet}\left(\sigma_\varsigma^2\mathbf{D}_{ul,mu}\Sigma^2_{\mathbf{W}_{ul,mu}}\mathbf{D}_{ul,mu}^H + \sigma_\vartheta^2\mathbf{I}_{ul,ba}\right) \\
&= \frac{1}{2}\mathrm{logdet}\left(\tilde{\mathbf{D}}_{ul,mu}(\Sigma_{ul} + \sigma_\varsigma^2\mathbf{I}_{n_R^{ul,mu}})\Sigma^2_{\mathbf{W}_{ul,mu}}\tilde{\mathbf{D}}_{ul,mu}^H\right) - \frac{1}{2}\mathrm{logdet}\left(\sigma_\varsigma^2\tilde{\mathbf{D}}_{ul,mu}\Sigma^2_{\mathbf{W}_{ul,mu}}\tilde{\mathbf{D}}_{ul,mu}^H + \sigma_\vartheta^2\mathbf{I}_{ul,ba}\right)
\end{aligned}$$

$$= \frac{1}{2}\text{logdet}\left(\mathbf{I}_{n_{ul,ba}} + (\tilde{\mathbf{D}}_{ul,mu}\Sigma^2_{\mathbf{W}_{ul,mu}}\tilde{\mathbf{D}}^H_{ul,mu} + \sigma^2_{\vartheta}\mathbf{I}_{n_{ul,ba}})^{-1}\tilde{\mathbf{D}}_{ul,mu}\Sigma_{ul}\Sigma^2_{\mathbf{W}_{ul,mu}}\tilde{\mathbf{D}}^H_{ul,mu}\right)$$
$$= \frac{1}{2}\text{logdet}\left(\left(\tilde{\mathbf{D}}_{ul,mu}\Sigma_{ul}\tilde{\mathbf{D}}^H_{ul,mu}\right)^{-1} + (\sigma^2_{\varsigma}\tilde{\mathbf{D}}_{ul,mu}\tilde{\mathbf{D}}^H_{ul,mu}\Sigma^2_{\mathbf{W}_{ul,mu}} + \sigma^2_{\vartheta}\mathbf{I}_{n_{ul,ba}})^{-1}\Sigma^2_{\mathbf{W}_{ul,mu}}\right)$$
$$+ \frac{1}{2}\text{logdet}\left(\tilde{\mathbf{D}}_{ul,mu}\Sigma_{ul}\tilde{\mathbf{D}}^H_{ul,mu}\right). \quad (6.22)$$

Similarly to Section 6.3.2.1, it can be shown that the capacity is a concave function which can be optimized in a similar manner.

6.3.3 Joint Optimization of User Transmit Beamformer and Relay Beamformer

In Section 6.3.1, we studied the optimization problem of the user beamforming matrices with fixed relay beamformer formulated as (6.6) and in Section 6.3.2, we studied the optimization problem of the relay beamformer with fixed user beamforming matrices formulated as (6.9). Here we study the multi-antenna relay uplink cooperative system capacity maximization problem in terms of the joint optimization problem of user transmit beamformer and relay beamformer formulated as

$$\begin{aligned}
&\arg\max_{\Gamma,\mathbf{W}} f(\Gamma,\mathbf{W}) \\
&\text{Tr}\left(\Gamma_j\right) \le P_u, \quad j = 1,\ldots,M_{ul} \\
&\text{Tr}\left(\sum_{j=1}^{M_{ul}}\Gamma_j\right) \le P_{sum,ul} \\
&\text{Tr}\left(\mathbf{W}\left(\mathbf{B}_i\Gamma_i^H\mathbf{B}_i^H + \sigma^2_{\varsigma}\mathbf{I}_{n_{ul,ba}}\right)\mathbf{W}^H\right) \le P_R. \\
&\Gamma_i \succeq 0, \quad i = 1,\ldots,M_{ul} \quad (6.23)
\end{aligned}$$

where

$$f(\Gamma,\mathbf{W}) = f(\Gamma_1,\Gamma_2,\ldots,\Gamma_{M_{ul}},\mathbf{W})$$
$$= \frac{1}{2}\text{logdet}\left(\sum_{i=1}^{M_{ul}}\mathbf{J}_{ul,mu}\mathbf{W}^H_{ul,mu}\mathbf{B}_i\Gamma_i^H\mathbf{B}_i^H\mathbf{W}_{ul,mu}\mathbf{J}^H_{ul,mu} + \sigma^2_{\varsigma}\mathbf{J}_{ul,mu}\mathbf{W}^H_{ul,mu}\mathbf{W}_{ul,mu}\mathbf{J}^H_{ul,mu} + \sigma^2_{\vartheta}\mathbf{I}_{n_R^{ul,mu}}\right)$$

$$-\frac{1}{2}\text{logdet}\left(\sigma_{\varsigma}^2\mathbf{J}_{ul,mu}\mathbf{W}_{ul,mu}^H\mathbf{W}_{ul,mu}\mathbf{J}_{ul,mu}^H+\sigma_{\vartheta}^2\mathbf{I}_{n_R^{ul,mu}}\right),$$

$$\Gamma=(\Gamma_1,\Gamma_2,\ldots,\Gamma_{M_{ul}}).$$

With the power constraints at the users and relay, the user transmit beamforming matrices and relay beamforming matrix can be jointly optimized using the following $Algorithm_1$:

Step 1. Initialize the relay beamforming matrix as $\mathbf{W}_{ul,mu}^{init}=\frac{P_{\mathbf{W}}}{n_R^{ul,mu}}\mathbf{I}_{n_R^{ul,mu}}$.

Step 2. Repeat: at ith iteration, with $\mathbf{W}_{ul,mu}^{(i)}$, optimize user transmit beamforming matrices to obtain $\Gamma_j^{(i)},\ \ j=1,\ldots,M_{ul}$ as in Section 6.3.1. Then with $\Gamma_j^{(i)},\ \ j=1,\ldots,M_{ul}$, optimize relay beamforming matrix to obtain $\mathbf{W}_{ul,mu}^{(i+1)}$ as in Section 6.3.2 until convergence.

Lemma 6.1: The iterative $Algorithm_1$ converges to a fixed point.

Proof:

Problem (6.24) can be reformulated as Eq. (2) in [92] with

$$\begin{aligned}\mathbf{Z}=\left(\sigma_{\varsigma}^2\mathbf{J}_{ul,mu}\mathbf{W}_{ul,mu}^H\mathbf{W}_{ul,mu}\mathbf{J}_{ul,mu}^H+\sigma_{\vartheta}^2\mathbf{I}_{n_R^{ul,mu}}\right)\quad &and\\ \mathbf{H}_i=\mathbf{J}_{ul,mu}\mathbf{W}_{ul,mu}^H\mathbf{B}_i\quad &and\\ S_j=\Gamma_j.\qquad (6.24)\end{aligned}$$

Since Eq. (2) is concave in S_j, the capacity function $f(\Gamma,\mathbf{W})$ in (6.24) is concave in Γ.

In $Algorithm_1$, assume that at the jth iteration, the relay beamforming matrix is $\mathbf{W}^{(j)}$. Applying Step 2 of $Algorithm_1$, there is

$$\Gamma^{(j)}=\arg\max_{\Gamma} f\left(\Gamma,\mathbf{W}^{(j)}\right)\qquad (6.25)$$

and because $f(\Gamma,\mathbf{W})$ is concave in Γ,

$$\forall\ \Gamma,\quad f\left(\Gamma^{(j)},\mathbf{W}^{(j)}\right)\geq f\left(\Gamma,\mathbf{W}^{(j)}\right).\qquad (6.26)$$

Compute

$$\mathbf{W}^{(j+1)} = \arg\max_{\mathbf{W}} f\left(\Gamma^{(j)}, \mathbf{W}\right). \tag{6.27}$$

As shown in Section 6.3.2, with given Γ, the optimum $\mathbf{W}$ can be obtained with the relay power constraint. Hence, there is

$$\begin{aligned} &\forall\ \mathbf{W}\quad f\left(\Gamma^{(j)}, \mathbf{W}^{(j+1)}\right) \geq f\left(\Gamma^{(j)}, \mathbf{W}\right) \\ &\Longrightarrow\quad f\left(\Gamma^{(j)}, \mathbf{W}^{(j+1)}\right) \geq f\left(\Gamma^{(j)}, \mathbf{W}^{(j)}\right). \end{aligned} \tag{6.28}$$

From (6.26), there is

$$\begin{aligned} &\forall\ \Gamma,\quad f\left(\Gamma^{(j+1)}, \mathbf{W}^{(j+1)}\right) \geq f\left(\Gamma, \mathbf{W}^{(j+1)}\right) \\ &\Longrightarrow\quad f\left(\Gamma^{(j+1)}, \mathbf{W}^{(j+1)}\right) \geq f\left(\Gamma^{(j)}, \mathbf{W}^{(j+1)}\right). \end{aligned} \tag{6.29}$$

Combining (6.28) and (6.29), there is

$$f\left(\Gamma^{(j+1)}, \mathbf{W}^{(j+1)}\right) \geq f\left(\Gamma^{(j)}, \mathbf{W}^{(j+1)}\right) \geq f\left(\Gamma^{(j)}, \mathbf{W}^{(j)}\right), \tag{6.30}$$

hence $f\left(\Gamma^{(j)}, \mathbf{W}^{(j)}\right)$ is a nondecreasing function for iteration j.

As the system is power constrained at the relay and users, $C_{ul,\Gamma,\mathbf{W}}$ is upper-bounded as indicated in [95], hence the iterative algorithm converges.

End of proof.

Lemma 6.2: The capacity of the uplink cooperative channel is upper-bounded by the minimum of the capacity of the multiple access channel from the users to the multi-antenna relay and the capacity of the MIMO channel from the multi-antenna relay to the base station.

Proof: It is an obvious cut-set upper bound so that it can be established from arguments similar to Corollary 1 in [96].

The joint optimization process can be intuitively interpreted as an iterative process of matched filtering plus waterfilling at the users and at the relay to align the users-to-relay and relay-to-base

station(BS) channels. When the relay beamforming matrix is fixed, optimization of the beamforming matrix considers the relay-amplified signal from other users, amplified relay noise, as well as receiver thermal noise as the effective noise as seen in (6.8). The design for optimizing user beamforming matrices is based on precoder matched filtering and waterfilling to the effective channel $\tilde{\mathbf{H}}_{ul,mu,j}$ in (6.8). When user beamforming matrices are fixed, relay beamforming matrix optimization can be interpreted in three stages: 1) $\mathbf{V}_{ul,mu}$ is the matched filter to the relay-to-BS channel seen in (6.10) and (6.12), 2) $\mathbf{O}_{ul}^{H}$ is the matched filter to the effective combined users-to-relay channel seen in (6.11) and (6.13), and 3) waterfilling to the effective cascaded channel by the relay to BS channel $\mathbf{J}_{ul,mu}$ in (6.10) and the effective user-relay channel $\mathbf{K}_{eff,mu,ul}$ in (6.12) considering the sum of amplified relay noise and BS receiver thermal noise as the effective noise. Since each step of the iterative algorithm achieves the optimum with either fixed user beamforming matrices or fixed relay beamforming matrix, the process can be seen as the alignment of the effective user-relay effective channel and the relay-BS channel until a good match is achieved. It is noted that successive interference cancelation is required to reach the capacity specified in the iterative algorithm in Section 6.3.3.

The iterative algorithm converges fast: on average, after 3 iterations, the difference in capacity between two adjacent iterations is less than 0.01b/Hz/s as shown in Figure 6.8.

In general, the joint optimization problem is not convex although it has the property that fixing a subset of the variables yields a sub-problem that is convex. However, we remark that in this specific problem (6.23), with different starting points (random initialization of user beamforming matrices and relay beamforming matrix satisfying power constraints), the convergence point appears to be the same in all cases tried and, in any case, the capacity achieved is very close to the cut-set upper bounds as determined in Lemma 6.2.

6.4 Numerical Results

In this section, the numerical results for the uplink cooperative system with users accessing the base station through a multi-antenna relay are presented. The numerical results are obtained using programs developed in [92] to obtain the user beamforming matrices and others in [23] to obtain the relay beamforming matrix.

6.4.1 Numerical Results for Multi-Antenna Multi-User Access through a Multi-antenna Relay

In this subsection, we present the numerical results of the uplink cooperative system with multi-antenna users that access the multi-antenna base station through a multi-antenna relay. We assume that a relay with $n_R^{ul,mu}$ antennas is located not very near the base station with $N_{ul,ba}$ directional antennas, and the users, each equipped with $N_{ul,ue}$ antennas are located around the relay and are served by the relay. Data is transmitted from users through relays to the base station over two time slots. We assume that full channel state information (CSI) of the user-relay and relay-BS channels are available to the base station. The channel from relay to BS is estimated at the BS and and the channels from users to relay are estimated at the relay and fed back to the BS. The iterative algorithm in Section 6.3.3 is used to obtain the numerical results. The user-relay and relay-BS channels are pseudo-randomly generated with i.i.d. unit variance complex Gaussian terms. In each figure, 500 monte carlo trials for each different combination of simulation variables are used and 0.002b/Hz/s is used as the convergence stopping criterion for the capacity computation (as described in $Algoritm_1$ in Section 6.3.3). On average, the algorithm was found to converge in fewer than 5 iteration. From all simulations performed, convergence was achieved, as expected from Lemma 6.1.

In Figures 6.1 to 6.7, we study the impact on the cooperative system capacity of the following

factors: 1) the number of users denoted as N_{user}, 2) the number of user antennas denoted as $N_{ul,ue}$, 3) the number of relay antennas denoted as $n_R^{ul,mu}$, 4) the sum power constraint at users denoted as $P_{sum,ul}$, and 5) the value of the power constraint at the relay denoted as P_R.

Numerical results in Figures 6.1 to 6.5 show that:

1) The system capacity increases with an increase in the sum transmission power of the users and the number of users, but as the number of users increases beyond 6, the capacity gain starts to saturate, as shown in Figure 6.1 (Simulation profile: $N_{ul,ba} = 6, n_R^{ul,mu} = 6, N_{ul,ue} = 2, P_R = 30dB$, $P_{sum,ul} \sim (0,25)\ dB, N_{user} \in \{2,4,6,8,10\}$),

2) The system capacity increases with an increase in the number of user antennas, and two user antennas obtains most of the capacity gain as shown in Figure 6.2 (Simulation profile: $N_{ul,ba} = 6, n_R^{ul,mu} = 6, N_{user} = 3, P_R = 30dB, P_{sum,ul} \sim (0,25)\ dB, N_{ul,ue} \in \{1,2,3,4\}$),

3) The system capacity increases with an increase in the number of relay antennas as shown in Figure 6.3 (Simulation profile: $N_{ul,ba} = 6, N_{user} = 3, P_R = 30dB, N_{ul,ue} = 2, P_{sum,ul} \sim (0,25)\ dB, n_R^{ul,mu} \in \{2,3,4,5,6\}$),

4) The system capacity increases with an increase in transmission power constraint of the relay as shown in Figure 6.4 (Simulation profile: $N_{ul,ba} = 6, n_R^{ul,mu} = 4, N_{user} = 3, N_{ul,ue} = 2, P_{sum,ul} \sim (0,25)\ dB, P_R \in \{0,5,10,15,20\}\ dB$),

5) The system capacity increases with an increase in the number of BS antennas as shown in Figure 6.5 (Simulation profile: $n_R^{ul,mu} = 6, N_{user} = 3, N_{ul,ue} = 2, P_{sum,ul} \sim (0,25)\ dB, P_R = 30dB, N_{ul,ba} \in \{2,3,4,5,6\}$),

We note that the cooperative uplink system is a cascade of a multi-access channel from the users to the relay and a MIMO channel from the relay to the base station. The overall uplink cooperative system capacity is upper-bounded by the cutset bound which is the minimum of the the relay-BS MIMO channel capacity (RBS-MIMO) and the user-relay multi-access channel capacity (UR-MU).

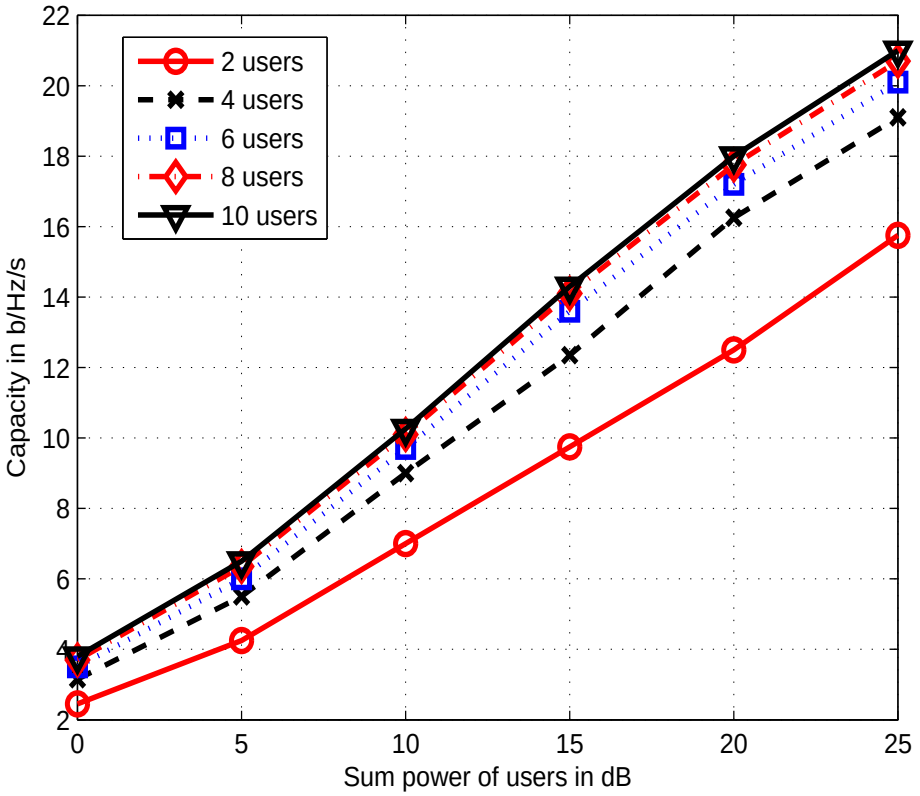

Figure 6.1. Cooperative system capacity with 6 base station antennas, 6 relay antennas, 30dB relay power, 2 user antennas and different numbers of users.

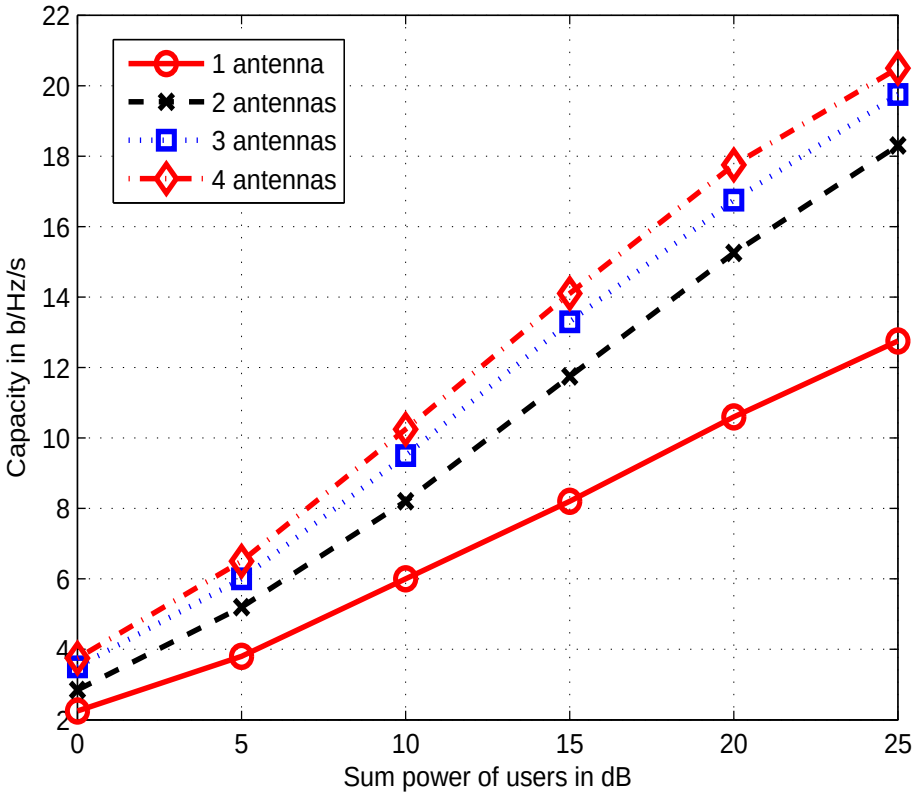

Figure 6.2. Cooperative system capacity with 6 base station antennas, 6 relay antennas, 30dB relay power, 3 users and different numbers of user antennas.

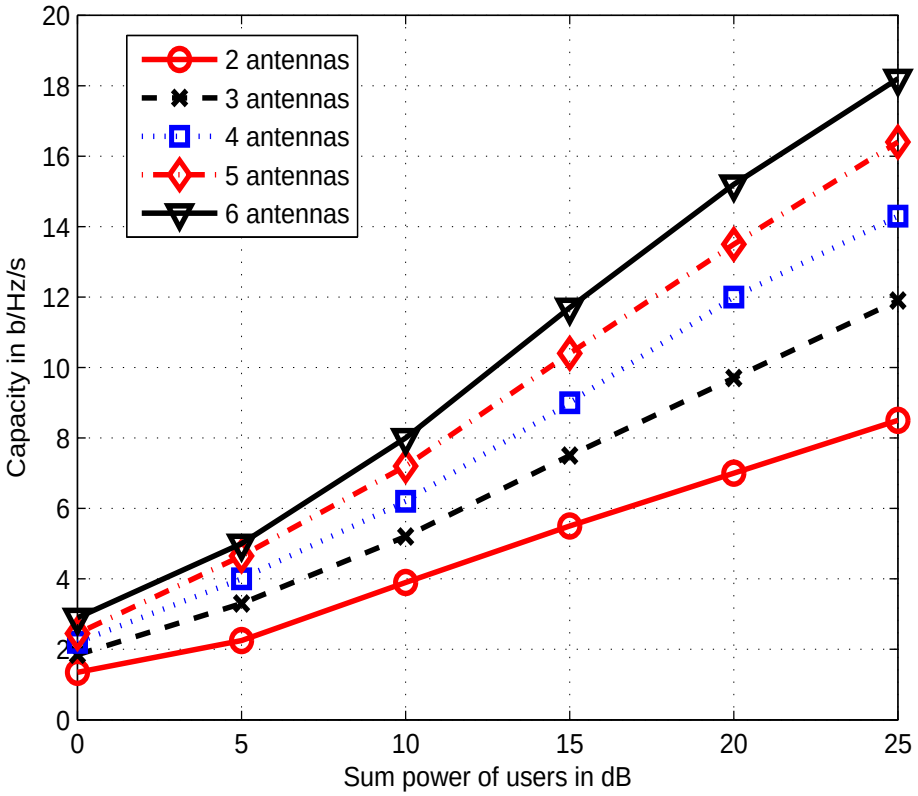

Figure 6.3. Cooperative system capacity with 6 base station antennas, 30dB relay power, 3 user each with 2 antennas and different numbers of relay antennas.

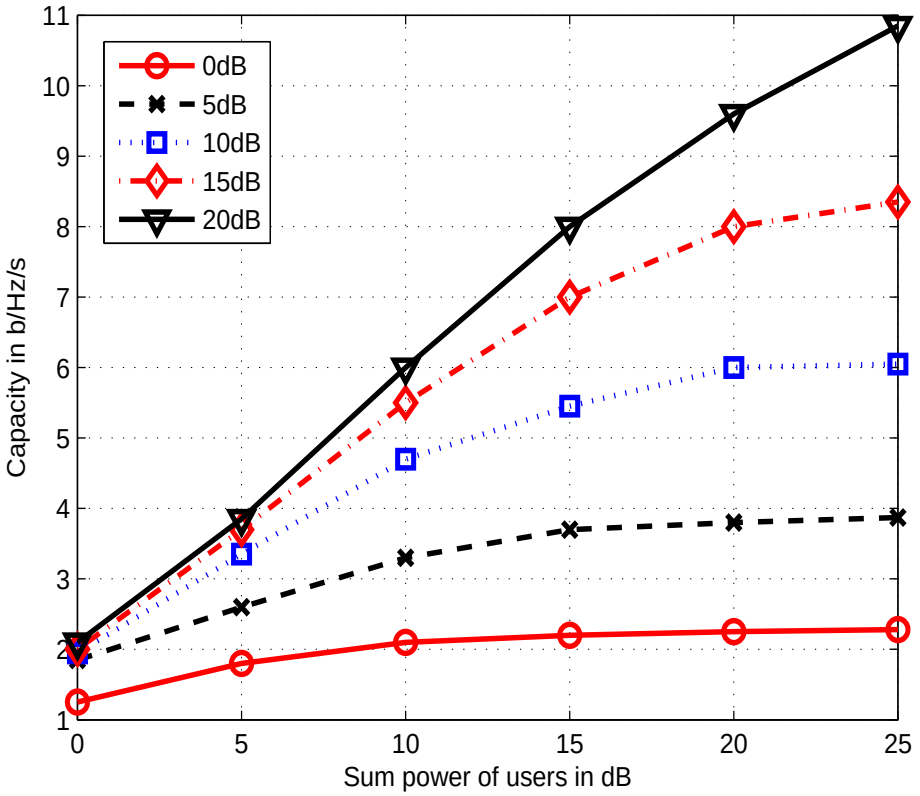

Figure 6.4. Cooperative system capacity with 6 base station antennas, 4 relay antennas, 3 user each with 2 antennas and different transmission power constraint at the relay.

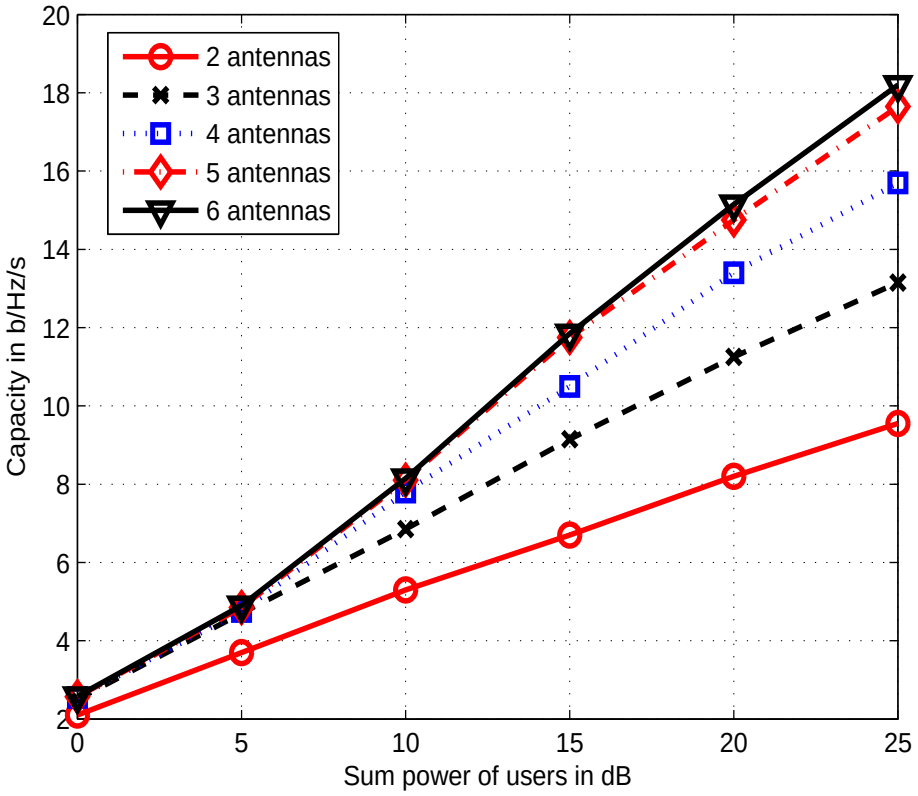

Figure 6.5. Cooperative system capacity with 6 relay antennas, 30dB relay power constraint, 3 user each with 2 antennas and different numbers of BS antennas.

We study the relationship between the uplink cooperative system capacity and UR-MU upper-bound In Figure 6.6 (Simulation profile: $N_{ul,ba} = 3, n_R^{ul,mu} = 5, N_{ul,ue} = 2, P_R = 30dB$, $P_{sum,ul} \sim (0,30)\ dB, N_{user} \in \{3,5,7,9,11\}$). Here the UR-MU upper bound is computed as the capacity of $N_{user} \in \{3,5,7,9,11\}$ accessing a source with 5 antennas and sum user transmission power ranging from 0 to 25dB. The relationship between the uplink cooperative system capacity and RBS-MIMO upper bound is shown in Figure 6.7 (Simulation profile: $n_R^{ul,mu} = 3, N_{ul,ue} = 2, P_{sum,ul} = 20dB, N_{user} = 3$, $P_R \sim (0,30)\ dB, N_{ul,ba} \in \{2,4,6,8\}$). The RBS upper-bound is computed as the capacity of a MIMO channel with 5 transmit antennas and 3 receive antennas with 25dB sum user transmission power.

The numerical results in Figure 6.6 and Figure 6.7 show that:

1) The system capacity also increases with an increase in the number of users and approaches the RBS-MIMO upperbound of the relay to base station channel capacity asymptotically (Figure 6.6),

2) The system capacity in Figure 6.7 shows that as the number of base station antennas increases, the system capacity increases and and approaches the UR-MU upperbound asymptotically.

Figure 6.8 compares algorithm performance as a function of the number of iterations in the iterative $Algorithm_1$ in Section 6.3.3 for the simulation profile $N_{ul,ba} = 6, n_R^{ul,mu} = 6, N_{ul,ue} = 2, P_R = 30dB$, $P_{sum,ul} \sim (0,25)\ dB, N_{user} = 4$. Note that that after about 3 iterations, a fixed point is approached, and that the first two iterations results in the largest gain.

When the MIMO channel is fixed (base station antenna number, relay antenna number and relay transmission power are fixed), the overall cooperative uplink system capacity is upper-bounded by RBS-MIMO. Before UR-MU is approaching RBS-MIMO, the uplink cooperative system capacity increases with the number of users, the number of user antennas and the sum transmission power of the users. It is noted that the gain is most significant when 1) the number of users increases from one to two, 2) the number of user antennas increases from one to two and 3) the user transmission power

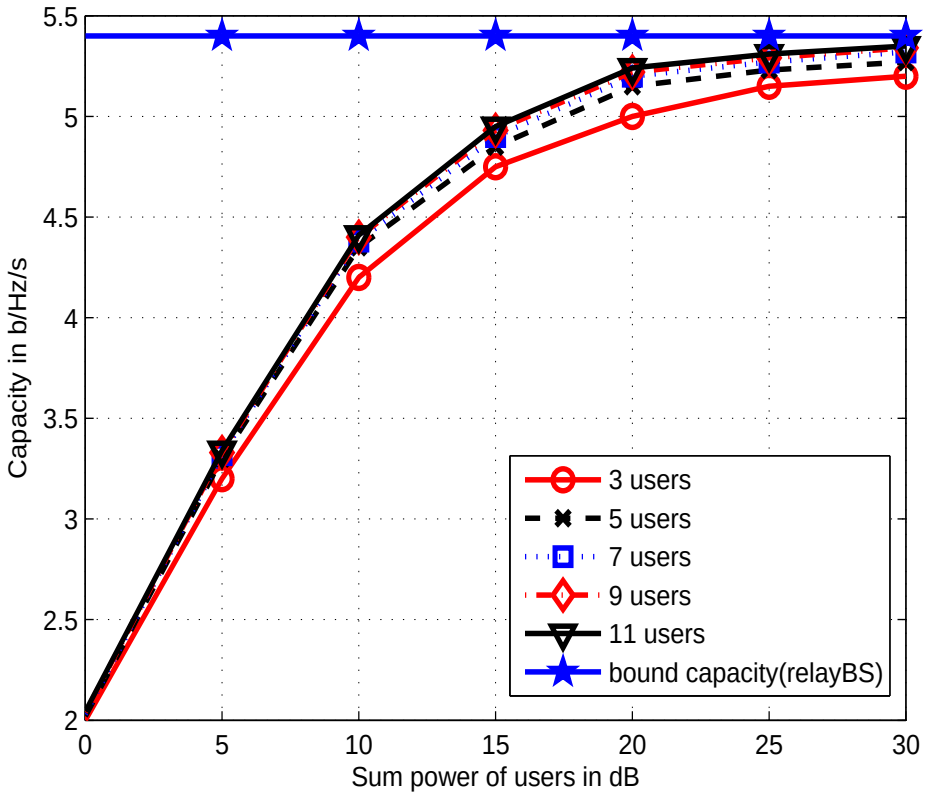

Figure 6.6. Cooperative system capacity with 3 base station antennas, 5 relay antennas, 30dB relay power, each user with 2 antennas and different number of users with a comparison with the relay-BS channel capacity bound.

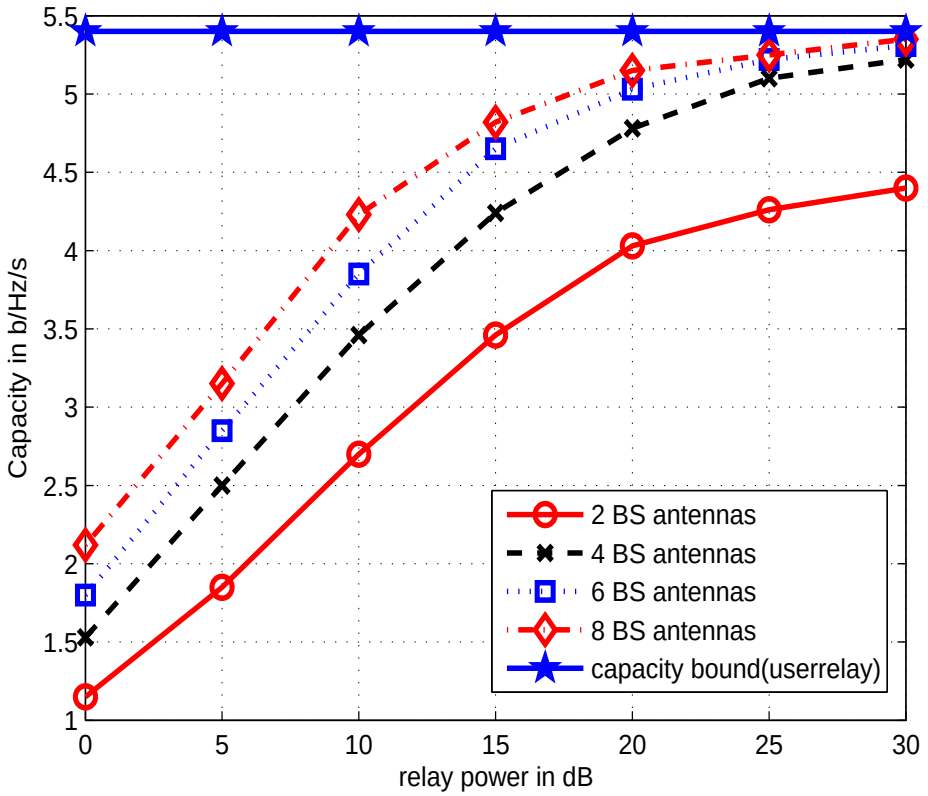

Figure 6.7. Cooperative system capacity with 3 relay antennas, 3 user with 2 antennas and different transmission power of the relay and base station antenna number from 2 to 8, and the comparison with the multiple access channel capacity bound from users to the relay.

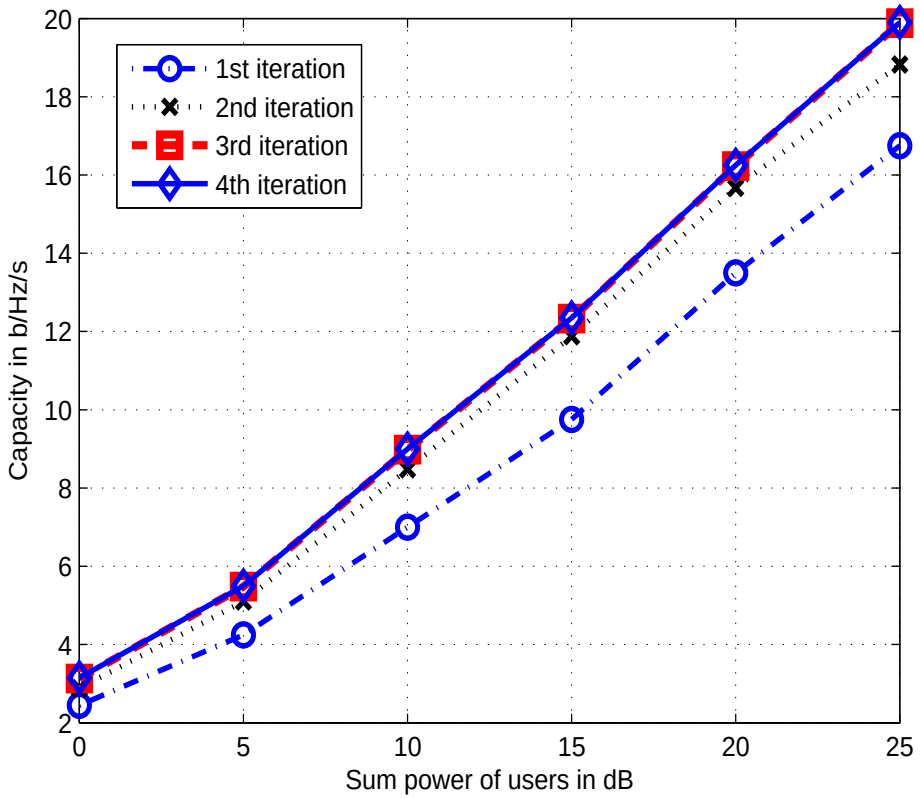

Figure 6.8. Cooperative system capacity with 6 base station antennas, 6 relay antennas, 30dB relay power, 2 user antennas, 4 users and different numbers of iterations.

increases from 0dB to 10dB. When UR-MU becomes larger than RBS-MIMO, further increase of these variables obtains less gain. When these variables become large, the capacity curves become saturated with almost no gain. It is also noted that when these variables become large, the overall uplink cooperative system capacity approaches RBS-MIMO or the cut-set upper-bound.

Similarly, when the multi-access channel is fixed (number of users, number of user antennas, user transmission power), the overall uplink cooperative system capacity is upper bounded by the UR-MU. When RBS-MIMO is smaller than UR-MU, the uplink cooperative system capacity increases with the relay transmission power and the number of base station antennas. When the number of base station antennas and the relay transmission power is small, the gain is significant. When RBS-MIMO becomes comparable or larger than UR-MU, the gain from the increase in base station antennas and relay transmission power diminishes. When RBS-MIMO becomes large, the capacity curve becomes saturated and approaches the UR-MU or the cut-set upper-bound.

From the perspective of the amplified relay noise, it can be regarded as an external interference for the system. When the received user signal energy is smaller than the relay noise energy, the relay noise becomes the bottleneck of the system capacity . When the received signal energy is comparable or larger than that of the relay noise, the system capacity is dependent on the relay transmission power. In other words, the system capacity is dependent on the SNR of the relay to the base station channel. When the relay transmission power is much larger than the receiver noise variance, the receiver noise is negligible compared with the relay noise. When the relay transmission power is small, the receiver noise becomes the dominant factor (compared with relay noise) to limit the overall system capacity.

6.5 Summary

In this chapter we study the scenario of a multi-access cooperative system. We proposed two schemes in the chapter. In the proposed scheme, multiple users access the BS through a multi-antenna relay. When relay beamformer is fixed, the optimal user beamformers are derived and when user beamformers are fixed, optimal relay beamformer is derived. An iterative algorithm to jointly optimize the user beamformers and relay beamformer is derived and proven to converge to a fixed point in about three iterations. Numerical results show that the performance of the iterative algorithm is very close to the user-relay MIMO-MAC channel upper bound and relay-BS MIMO upper bound.

Chapter 7

Conclusions and Future Work

In this chapter, we summarize the major contributions in this thesis and suggest several topics for future research.

7.1 Conclusions

In Chapter 3, a multi-antenna downlink distributed beamforming system is proposed. In this system, a multiple-antenna base station transmits to multiple destinations through multiple relays. The objective of system optimization is to minimize the sum power at the BS and the relays with quality of service (QoS) constraints. An iterative algorithm to jointly optimize the precoder and relay weights is developed and proven to converge locally. Imperfect CSI is taken into account into the design by using the statistical CSI information. The scheme is further extended to the case where the destinations have multi-antenna receivers. Numerical results show that ignoring the effects of imperfect CSI can result in a loss of performance of approximately 5dB over the range of target SINR QoS values from 0 to 14 dB. When channel estimation quality degrades substantially, the problem easily becomes infeasible.

In Chapter 4, an uplink distributed beamforming system is proposed. In this system, multiple

single-antenna sources access the multi-antenna BS through a group of single-antenna relays. The objective of system optimization is to minimize the relay power with QoS constraints. An iterative algorithm to jointly optimize the relay weights and the decoder at the base station is developed and proven to converge locally. When the CSI is not perfect, the design method takes into account the statistical information about CSI uncertainly and is evaluated by comparing the performance to that of a design that assumes perfect CSI. Numerical results show that the impact of individual power constraints is limited. Individual power constraints for a wide range of up to 15dB do not affect the performance of the scheme. Computationally, the proposed system is also less costly since it can support more users with fewer relays.

In Chapter 5, a novel multi-cell downlink cooperative system is proposed. In this system, multi-antenna BS coordinate data transmission to a group of users through single-antenna relays. Schemes are proposed for two different scenarios. In the first scenario, multiple cells that send the same signal to a specific user, with weighted sum power minimization as the objective with QoS constraints. In this case, the beamforming algorithm allocated most of its power resources to a single cell, i.e., the best cell to serve a specific user can be found. Numerical results also show that the power allocated to the best serving cell is 35dB higher than the other cells, which means only one cell should be transmitting to a given user.

In Chapter 6, a capacity maximization scheme for uplink cooperative system is proposed. In this scheme, multiple users access a BS through a multi-antenna relay. Optimal user beamformers are derived with a fixed relay beamformer and the optimal relay beamformer is derived with fixed user beamformers. An iterative algorithm is developed to jointly optimize the user beamformers and the relay beamformer and proven to converge to a fixed point. A number of insights have been provided for the design of the user beamformers and relay beamformer according to the numerical results. Numerical results show that iterative algorithm usually converges in 3 iterations to a difference of

less than 0.01b/Hz/s in capacity. It is observed from the numerical results that the performance of the iterative algorithm is very close to that of the user-relay MIMO-MAC upper bound and relay-BS MIMO upper bound. This shows that the cut-set upper-bounds are pretty tight and efficient in evaluate the performance of the algorithm. An interesting result is that we have observed that the performance of $Algorithm_1$ with multiple starting points is almost the same as that of the iterative algorithm with a single starting point. This is surprising since the problem is in general non-concave.

In this thesis, we proposed cooperative systems under different criteria: power and capacity. The advantage of the cooperative system design based on a power metric is targeted for reducing inter-cell interference, but is less flexible in user scheduling and evaluation of system throughput. In comparison, the system design based on capacity metric has the advantages of flexibility to dynamically adjust user throughput according to channel conditions, QoS requirements and fairness requirements and is of practical significance for operators. We note that currently in industry, capacity based design metrics are widely used. The capacity based design method in this thesis is more attractive from a practical standpoint.

7.2 Future Work

Here are some suggestions for future work.

- In Chapters 3 and 4, uplink and downlink distributed beamforming systems are studied. The beamforming at the multi-antenna relays can be designed to maximize the SINR at the end user or minimize the power to reduce interference to other cells.

- In Chapters 3 and 4, the uplink and downlink are studied separately. As seen in the literature, there is a duality relation between the uplink and downlink for multi-user systems. It would be interesting to study the duality relationship between the multiple antenna uplink and downlink

systems. If a duality relationship can be derived, a downlink distributed beamforming strategy may also be developed using the solution of the uplink distributed system.

- In Chapters 3 and 4, imperfect CSI for uplink and downlink distributed beamforming are studied based on average performance. Worst case performance due to imperfect CSI may be of interest for further study.

- In Chapters 3 and 4, distributed beamforming is studied in the framework of signal processing using SINR as criterion. Uplink and downlink distributed beamforming can also be studied using capacity as criterion as in Chapter 6. The relationship between capacity and SINR for the cooperative system can be of interest.

- In Chapter 5, multi-cell cooperative distributed beamforming system is studied using SINR as the criterion. As the cells are using the same frequency, it becomes an interference-limited system. It would be interesting to study the maximum weighted sum rate of the system and further study the performance under imperfect channel state information.

- In Chapter 6, perfect CSI was assumed. It would be worth investigating the imperfect CSI scenario.

Bibliography

[1] H. Bolcskei, R. U. Nabar, O. Oyman, and A. J. Paulraj, "Capacity scaling laws in MIMO relay networks," *IEEE Trans. Wireless Commun.*, pp. 1433–1444, June. 2006.

[2] A. J. Paulraj and C. B. Papadias, "Space-time processing for wireless communications," *IEEE Signal Processing Mag.*, pp. 49–83, Nov. 1997.

[3] A. Paulraj, R. Nabar, and D. Gore, *Introduction to Space-Time Wireless Communications*. Cambridge University Press, 2003.

[4] W. Jakes, *Microwave mobile communications*. Wiley Press, 1974.

[5] S. Alamouti, "A simple transmit diversity technique for wireless communications," *IEEE J. Select. Areas Commun.*, pp. 1451–1468, Feb. 1996.

[6] V. Tarokh, N. Seshadri, and A. Calderbank, "Space-time codes for high data rate wireless communication: performance criterion and code construction," *IEEE Trans. Inform. Theory*, pp. 744–765, Feb. 1998.

[7] J. N. Laneman, D. N. C. Tse, and G. W. Wornell, "Cooperative diversity in wireless networks: Efficient protocols and outage behavior," *IEEE Trans. Inform. Theory*, pp. 3062–3080, Sept. 2004.

[8] J. N. Laneman and G. W. Wornell, "Distributed Space-Time-Coded protocols for exploiting cooperative diversity in wireless networks," *IEEE Trans. Inform. Theory*, pp. 2415–2425, Oct. 2003.

[9] R. U. Nabar, H. Bolcskei, and F. W. Kneubuhler, "Fading relay channels: performance limits and space-time signal design," *IEEE J. Select. Areas Commun.*, pp. 1099–1109, Aug. 2004.

[10] M. Janani, A. Hedayat, T. E. Hunter, and A. Nosratinia, "Coded cooperation in wireless communications: space-time transmission and iterative decoding," *IEEE Trans. Signal Processing*, pp. 362–371, Feb. 2004.

[11] V. H. Nassab, S. Shahbazpanahi, A. Grami, and Z. Q. Luo, "Distributed beamforming for relay networks based on second-order statistics of the channel state information," *IEEE Trans. Signal Processing*, pp. 4306–4316, Sept. 2008.

[12] S. Fazeli-Dehkordy, S. Gazor, and S. Shahbazpanahi, "Distributed peer-to-peer multiplexing using ad hoc relay networks," in *IEEE International Conference on Acoustics, Speech and Signal Processing*, 2008, pp. 2373–2376.

[13] G. D. Golden, G. J. Foschini, R. A. Valenzuela, and P. W. Wolniansky, "Detection algorithm and initial laboratory results using the V-BLAST space-time communication architecture," *Electron. Lett.*, pp. 14–15, Jan. 1999.

[14] O. Damen, A. Chkeif, and J. Belfiore, "Lattice code decoder for space-time codes," *IEEE Commun. Lett.*, pp. 161–163, May. 2000.

[15] H. V. Poor, *An Introduction to Signal Detection and Estimation*. Springer, 1994.

[16] G. J. Foschini, G. D. Golden, R. A. Valenzuela, and P. W. Wolniansky, "Simplified processing for wireless communication at high spectral efficiency," *IEEE J. Select. Areas Commun.*, pp. 1841–1852, Nov. 1999.

[17] G. Ginis and J. M. Cioffi, "On the relation between V-BLAST and the GDFE," *IEEE Commun. Lett.*, pp. 364–366, Sept. 2001.

[18] R. A. Monzingo and T. W. Miller, *Introduction to Adaptive Arrays*. John Wiley, 1979.

[19] B. Hassibi, "A fast square-root implementation for BLAST," in *Proc. Asilomar Conf. on Signals, Systems, and Computers*, 2000.

[20] E. Telatar, "Capacity of multi-antenna Gaussian channels," *European Trans. Telecommun.*, pp. 585–595, Dec. 1999.

[21] R. A. Horn and C. R. Johnson, *Matrix Analysis*. Cambridge University Press, 1999.

[22] T. M. Cover and J. A. Thomas, *Elements of Information Theory*. John Wiley and Sons, 1991.

[23] S. Boyd, *Convex Optimization*. Cambridge University Press, 2004.

[24] F. Gao, T. Cui, and A. Nallanathan, "On channel estimation and optimal training design for amplify and forward relay networks," *IEEE Trans. Wireless Commun.*, pp. 1907–1916, Dec. 2008.

[25] B. Hassibi and B. M. Hochwald, "How much training is needed in multiple-antenna wireless links?" *IEEE Trans. Inform. Theory*, pp. 951–963, Apr. 2003.

[26] L. Musavian, M. R. Nakhai, M. Dohler, and A. H. Aghvami, "Effect of channel uncertainty on the mutual information of MIMO fading channels," *IEEE Trans. Veh. Technol.*, pp. 2798–2806, Sept. 2007.

[27] S. Serbetli and A. Yener, "Transceiver optimization for multiuser MIMO system," *IEEE Trans. Signal Processing*, pp. 214–226, Jan. 2004.

[28] T. Yoo, E. Yoon, and A. Goldsmith, "MIMO capacity with channel uncertainty: Does feedback help?" in *Proc. IEEE Global Telecommun. Conf.*, 2004, pp. 96–100.

[29] B. Wang, J. Zhang, and A. Host-Madsen, "On the capacity of MIMO relay channels," *IEEE Trans. Inform. Theory*, pp. 29–43, Jan. 2005.

[30] S. Sesia, I. Toufik, and M. Baker, *LTE-The UMTS Long Term Evolution From Theory to Practice*. Wiley Press., 2009.

[31] "Rp-090939 (3GPP submission package for IMT-advanced)," *http://www.3gpp.org/LTE-Advanced*, 2009.

[32] F. Khan, *LTE for 4G Mobile Broadband*. Cambridge University Press., 2009.

[33] A. Wiesel, Y. C. Eldar, and S. Shamai, "Linear precoding via conic optimization for fixed mimo receivers," *IEEE Trans. Signal Processing*, pp. 161–176, Jan. 2006.

[34] M. Schubert, S. Shi, E. A. Jorswieck, and H. Boche, "Downlink sum-MSE transceiver optimization for linear multi-user MIMO systems," in *Proc. Asilomar Conf. on Signals, Systems and Computers, Pacific Grove, CA*, 2005, pp. 1424–1428.

[35] J. Zhang, Y. Wu, S. Zhou, and J. Wang, "Joint linear transmitter and receiver design for the downlink of multiuser MIMO systems," *IEEE Commun. Lett.*, pp. 991–993, Nov. 2005.

[36] T. Weber, A. Sklavos, and M. Meurer, "Imperfect channel state information in MIMO transmission," *IEEE Trans. Commun.*, pp. 543–552, Mar. 2006.

[37] M. Ding and S. D. Blostein, "MIMO LMMSE transceiver design with imperfect CSI at both ends," *IEEE Trans. Signal Processing*, pp. 1141–1150, Mar. 2009.

[38] D. S. Michalopoulos, H. A. Suraweera, G. K. Karagiannidis, and R. Schober, "Amplify-and-foward relay selection with outdated channel estimates," *IEEE Trans. Commun.*, vol. 60, pp. 1278–1290, May. 2012.

[39] S. S. Soliman and N. C. Beaulieu, "Exact analysis of dual-hop AF maximum end-to-end SNR relay selection," *IEEE Trans. Commun.*, vol. 60, pp. 2135–2145, Aug. 2012.

[40] H. H. Kha, H. D. Tuan, H. H. Nguyen, and T. Pham, "Optimization of cooperative beamforming for SC-FDMA multi-user multi-relay networks by tractable D.C. programming," *IEEE Trans. Signal Processing*, vol. 61, pp. 467–479, Jan. 2013.

[41] G. Zheng, Y. Zhang, C. Li, and K.-K. Wong, "A stochastic optimization approach for joint relay assignment and power allocation in orthogonal amplify-and-forward cooperative wireless networks," *IEEE Trans. Wireless Commun.*, vol. 12, pp. 4091–4099, Dec. 2011.

[42] J. Yindi and H. Jafarkhani, "Network beamforming using relays with perfect channel information," *IEEE Trans. Inform. Theory*, pp. 473–476, Apr. 2007.

[43] K. S. Gomadam and S. A. Jafar, "Optimal distributed beamforming in relay networks with common interference," in *Proc. Globecom*, 2007, pp. 439–441.

[44] S. Fazeli-Dehkordy, S. Shahbazpanahi, and S. Gazor, "Multiple peer-to-peer communications using a network of relays," *IEEE Trans. Signal Processing*, pp. 3053–3062, Aug. 2009.

[45] Z. Ding, W. H. Chin, and K. K. Leung, "Distributed beamforming and power allocation for cooperative networks," *IEEE Trans. Inform. Theory*, pp. 1817–1822, May. 2008.

[46] B. Khoshnevis, W. Yu, and R. Adve, "Grassmannian beamforming for MIMO amplify-and-forward relaying," *IEEE J. Select. Areas Commun.*, pp. 1397–1407, Oct. 2008.

[47] A. Nasir, H. Mehrpouyan, S. Blostein, S. Durrani, and R. A. Kennedy, "Timing and carrier synchronization with channel estimation in multi-relay cooperative networks ieee transactions on signal processing," *IEEE Trans. Wireless Commun.*, pp. 793–811, Feb. 2012.

[48] "Evolved universal terrestrial radio access (E-UTRA); requirements for support of radio resource management," *http://www.3gpp.org/36.133*, 2012.

[49] "Evolved universal terrestrial radio access (E-UTRA); TDD home eNodeB (HeNB) radio frequency (RF) requirements analysis," *http://www.3gpp.org/36.922*, 2013.

[50] S. Ruffini, "Mobile standards and synchronization: 3gpp etc." in *International Telecom Sync Forum and Avren Events*, 2011.

[51] M. Bengtsson and B. Ottersten, *Optimal and Suboptimal transmit beamforming*. Handbook of Antennas in Wireless Communications, CRC Press, 2001.

[52] F. Rashid-Farrokhi, L. Tassiulas, and K. J. R. Liu, "Joint optimal power control and beamforming in wireless networks using antenna arrays," *IEEE Trans. Commun.*, pp. 1313–1323, Oct. 1998.

[53] M. Schubert and H. Boche, "Solution of the multiuser downlink beamforming problem with individual SINR constraints," *IEEE Trans. Veh. Technol.*, pp. 18–28, Jan. 2004.

[54] Y. Huang and S. Zhang, "Complex matrix decomposition and quadratic programming," *Mathematics of Operations Research*, pp. 758–765, 2007.

[55] N. D. Sidiropoulos, T. N. Davidson, and Z.-Q. Luo, "Transmit beamforming for physical-layer multicasting signal processing," *IEEE Trans. Signal Processing*, pp. 2239–2251, June. 2006.

[56] T. Rappaport, *Wireless Communications Principles and Practices*. Prentice Hall, 2002.

[57] Y. Jing and B. Hassibi, "Distributed space-time coding in wireless relay networks," *IEEE Trans. Wireless Commun.*, pp. 3524–3536, Dec. 2006.

[58] T. Kiran and B. S. Rajan, "Partial-coherent distributed space-time codes with differential encoder and decoder," *IEEE Trans. Inform. Theory*, pp. 1659–1874, Sept. 2004.

[59] Y. Rong and M. Khandaker, "On uplink-downlink duality of multi-hop MIMO relay channel," *IEEE Trans. Wireless Commun.*, vol. 61, pp. 1923–1931, Jun. 2011.

[60] R. Wang, M. X. Tao, and Y. W. Huang, "Linear precoding designs for amplify-and-forward multiuser two-way relay systems," *IEEE Trans. Wireless Commun.*, vol. 11, pp. 4457–4469, Dec. 2012.

[61] R. Wan, "Nonlinear precoding design for MIMO amplify-and-forward two-way relay systems," *IEEE Trans. Veh. Technol.*, vol. 61, pp. 3984–3995, Nov. 2012.

[62] Y. Jing and B. Hassibi, "Network beamforming using relays with perfect channel information," in *Int. Conf. Acoustics, Speech,Signal Processing (ICASSP)*, 2007, pp. 473–476.

[63] J. F. Sturm, "Using sedumi 1.02, a matlab toolbox for optimization over symmetric cones." *Technical report*, 1999.

[64] S. Zhang, "Quadratic maximization and semidefinite relaxation," *Math. Program.*, pp. 453–465, 2000.

[65] P. Tseng, "Further results on approximating nonconvex quadratic optimization by semidefinite programming relaxation," *SIAM J. Optim.*, pp. 268–283, Jul. 2003.

[66] O. Somekh, B. Zaidel, and S. Shamai, "Spectral efficiency of joint multiple cell-site processors for randomly spread DS-CDMA systems," *IEEE Trans. Inform. Theory*, pp. 2625–2637, Jul. 2007.

[67] M. Karakayali, G. J. Foschini, and R. A. Valenzuela, "Network coordination for spectrally efficient communications in cellular systems," *IEEE Trans. Wireless Commun.*, pp. 56–61, Aug. 2006.

[68] S. V. Hanly and P. A. Whiting, "Information-theoretic capacity of multi-receiver networks," *IEEE Trans. Inform. Theory*, pp. 1–42, Mar. 1993.

[69] A. D. Wyner, "Shannon-theoretic approach to a Gaussian cellular multiple-access channel," *IEEE Trans. Inform. Theory*, pp. 1713–1727, Nov. 1994.

[70] L. R. Welburn, J. K. Cavers, and K. W. Sowerby, "Multiuser macrodiversity detection in asynchronous DS-CDMA systems," *IEEE Trans. Wireless Commun.*, pp. 544–554, Mar. 2004.

[71] G. J. Foschini, M. Karakayali, and R. A. Valenzuela, "Coordinating multiple antenna cellular networks to achieve enormous spectral efficiency," in *Inst. Electr. Eng. Proc. Commun.*, 2006, pp. 548–555.

[72] H. Zhang and H. Dai, "Cochannel interference mitigation and cooperative processing in downlink multicell multiuser MIMO networks," *IEEE Trans. Wireless Commun.*, pp. 222–235, Jul. 2004.

[73] A. Vanelli-Coralli, R. Padovani, J. Hou, and J. E. Smee, "Capacity of cell clusters with coordinated processing," in *Proc. Inf. Theory Appl. Workshop, La Jolla, CA*, 2006.

[74] F. Verde, "Cooperative randomized MIMO-OFDM downlink for multicell networks: Design and analysis," *IEEE Trans. Signal Processing*, vol. 58, pp. 384–402, Nov. 2010.

[75] B. Clerckx, H. Lee, Y. Hong, and G. Kim, "A practical cooperative multicell MIMO-OFDMA network based on rank coordination," *IEEE Trans. Wireless Commun.*, vol. 99, pp. 1–11, Feb. 2013.

[76] G. Fettweis and J. N. Laneman, "Energy and cost efficient mobile communication using multi-cell MIMO and relaying," *IEEE Trans. Wireless Commun.*, vol. 11, pp. 3377–3387, Sept. 2012.

[77] J. H. Kim, J. Y. Hwang, and Y. Han, "Joint processing in multi-cell coordinated shared relay network," in *IEEE PIMRC International Symposium*, 2010, pp. 702–706.

[78] M. Salim, A. Adinoyi, M. Rahman, and H. Yanikomeroglu, "Fairness-aware radio resource management in downlink OFDMA cellular relay networks," *IEEE Trans. Wireless Commun.*, vol. 15, pp. 1536–1276, May. 2010.

[79] Y. C. Lin and W. Yu, "Fair scheduling and resource allocation for wireless cellular network with shared relays," in *Annual Conference on Information Sciences and Systems (CISS)*, 2012, pp. 1–6.

[80] Y. Liu, R. Hoshyar, X. Yang, and R. Tafazolli, "Integrated radio resource allocation for multihop cellular networks with fixed relay stations," *IEEE J. Select. Areas Commun.*, vol. 10, pp. 2137–2146, Nov. 2006.

[81] I. Hwang, C. B. Chae, J. Lee, and R. W. Heath, "Multicell cooperative systems with multiple receive antennas," *IEEE Trans. Wireless Commun.*, submitted.

[82] Y. Zheng and S. Blostein, "Optimization of power constrained multi-source uplink relay networks," in *Proc. IEEE Globecom*, 2009.

[83] Y. W. Liang and R. Schober, "Cooperative amplify-and-forward beamforming with multiple multi-antenna relays," *IEEE Trans. Commun.*, pp. 2605–2615, Sept. 2011.

[84] Y. Fan, C. Wang, H. V. Poor, and J. S. Thompson, "Cooperative multiplexing: Toward higher spectral efficiency in multiple-antenna relay networks," *IEEE Trans. Inform. Theory*, pp. 3909–3927, Sept. 2009.

[85] T. Kang and V. Rodoplu, "Algorithms for the MIMO single relay channel," *IEEE Trans. Wireless Commun.*, pp. 1596–1600, May. 2007.

[86] X. Tang and Y. Hua, "Optimal design of non-regenerative MIMO wireless relays," *IEEE Trans. Wireless Commun.*, pp. 3909–3927, Sept. 2009.

[87] C. T. K. Ng and G. J. Foschini, "Transmit signal and bandwidth optimization in multiple-antenna relay channels," *IEEE Trans. Inform. Theory*, pp. 2987–2993, Nov. 2011.

[88] P. Dharmawansa, M. R. McKay, R. K. Mallik, and K. B. Letaief, "Ergodic capacity and beamforming optimality for multi-antenna relaying with statistical CSI," *IEEE Trans. Commun.*, vol. 59, pp. 2119–2131, Aug. 2011.

[89] S. N. Datta, S. Chakrabarti, and R. Roy, "Comprehensive error analysis of multi-antenna decode-and-forward relay in fading channels," *IEEE Commun. Lett.*, vol. 16, pp. 47–49, Jan. 2012.

[90] G. Li, Y. Wang, and P. Zhang, "Optimal linear MMSE beamforming for two way multi-antenna relay systems," *IEEE Commun. Lett.*, vol. 15, pp. 47–49, May. 2011.

[91] C. B. Chae, T. Tang, R. W. Heath, and S. C. Cho, "MIMO relaying with linear processing for multiuser transmission in fixed relay networks," *IEEE Trans. Signal Processing*, pp. 727–738, Feb. 2008.

[92] W. Rhee, W. Yu, and J. M. Cioffi, "The optimality of beamforming in uplink multiuser wireless systems," *IEEE Trans. Wireless Commun.*, pp. 86–96, Jan. 2004.

[93] W. Yu, W. Rhee, S. Boyd, and J. Cioffi, "Iterative water-filling for vector multiple access channel," in *IEEE Intl. Symp. Inform. Theory, (ISIT)*, 2001, pp. 2605–2615.

[94] W. Yu, W. Rhee, S. Boyd, and J. M. Cioffi, "Iterative water-filling for Gaussian vector multiple access channels," in *Proc. Int. Symp. Information Theory (ISIT), Washington*, 2001, p. 322.

[95] A. Goldsmith, S. Jafar, N. Jindal, and S. Vishwanath, "Capacity limits of MIMO channels," *IEEE J. Select. Areas Commun.*, pp. 684–702, Jun. 2003.

[96] T. M. Cover and A. E. Gamal, "Capacity theorems for the relay channel," *IEEE Trans. Inform. Theory*, pp. 572–584, Sept. 1979.

Appendix A

Derivation of (2.26) (2.27):

Perform vectorization operation on (2.26) to obtain

$$vec(\hat{\mathbf{H}}_w) = vec(\mathbf{H}_w) + (\mathbf{I}_{n_T} \otimes \mathbf{R}_R^{-1/2}) vec(\mathbf{N}_0). \tag{A.1}$$

Then the MMSE estimate of $vec(\mathbf{H}_w)$ is given by

$$\begin{aligned} vec(\hat{\mathbf{H}}_w) &= \left[\mathbf{I}_{nTnR} + \mathbf{I}_{n_T} \otimes \mathbf{R}_R^{-1} \cdot \sigma_{ce}^2\right]^{-1} vec(\tilde{\mathbf{H}}_w) \\ &= \{\mathbf{I}_{n_T} \otimes [\mathbf{I}_{n_R} \otimes \mathbf{R}_R^{-1} \cdot \sigma_{ce}^2]^{-1}\} vec(\tilde{\mathbf{H}}_w). \end{aligned} \tag{A.2}$$

Then (2.27) is obtained by converting $vec(\tilde{\mathbf{H}}_w)$ back to its matrix version. The resulting estimation error covariance matrix is:

$$\begin{aligned} \Psi &= \mathbb{E}\left([vec(\mathbf{H}_w) - vec(\hat{\mathbf{H}}_w)][vec(\mathbf{H}_w) - vec(\hat{\mathbf{H}}_w)]^H\right) \\ &= \mathbf{I}_{n_T n_R} - [\mathbf{I}_{n_T n_R} + \sigma_{ce}^2 (\mathbf{I}_{n_T n_R} \otimes \mathbf{R}_R^{-1})]^{-1} \\ &= \mathbf{I}_{n_T} \otimes [\mathbf{I}_{n_R} - (\mathbf{I}_{n_R} + \sigma_{ce}^2 \mathbf{R}_R^{-1})^{-1}] \\ &= \sigma_{ce}^2 \underbrace{\cdot \mathbf{I}_{n_T} \otimes [\mathbf{R}_R^{-1} (\mathbf{I}_{n_R} + \sigma_{ce}^2 \mathbf{R}_R^{-1})^{-1}]}_{\Psi_0} \end{aligned} \tag{A.3}$$

The estimation error vector can be represented by $\Psi_0^{1/2} vec(\mathbf{E}_w)$ is given by $\mathbf{R}_R^{-1} (\mathbf{I}_{n_R} + \sigma_{ce}^2 \mathbf{R}_R^{-1})^{-1/2} \mathbf{E}_w$, and (2.27) follows.

Appendix B

Randomization method details:

Randomization method:

1. Assuming $\mathbf{Z}_{ul,opt}$ to be the solution obtained by solving (4.20), calculate the eigen-decomposition of $\mathbf{Z}_{ul,opt} = \beth_{ul}\Sigma_{ul}\beth_{ul}^H$ and choose $\chi_{ul,l} = \mathbf{D}_{ul}^{-1/2}\beth_{ul}\Sigma_{ul}^{1/2}\mathbf{e}_{ul,l}$, where the elements of $\mathbf{e}_l$ are independent random variables, chosen randomly with uniformly distributed on the unit circle in the complex plane: i.e., $[\mathbf{e}_{ul,l}]_i = e^{j\theta_{ul,l,i}}$, where $\theta_{ul,l,i}$ are independent and uniformly distributed on $[0, 2\pi)$. It is shown below that $\chi_{ul}^H\mathbf{D}_{ul}\chi_{ul} = \mathrm{Tr}(\mathbf{Z}_{ul,opt})$, i.e., the individual relay power and sum power is given irrespectively of the particular realization of $\mathbf{e}_{ul,l}$.

$$\begin{aligned}
\chi_l^H\mathbf{D}\chi_l &= \mathbf{e}_l^H\Sigma^{1/2}\beth_{dl}^H\mathbf{D}^{-1/2}\mathbf{D}\mathbf{D}^{-1/2}\beth_{dl}\Sigma^{1/2}\mathbf{e}_l \\
&= \mathbf{e}_l^H\Sigma\mathbf{e}_l \\
&= e^{-j\theta_{l,1}}\Sigma_{1,1}e^{j\theta_{l,1}} + \ldots + e^{-j\theta_{l,n_R^{ul}}}\Sigma_{n_R^{ul},n_R^{ul}}e^{j\theta_{l,n_R^{ul}}} \\
&= \Sigma_{1,1} + \ldots + \Sigma_{n_R^{ul},n_R^{ul}} \\
&= \mathrm{Tr}\left(\Sigma\right) \\
&= \mathrm{Tr}\left(\beth_{dl}\Sigma\beth_{dl}^H\right) \quad . \qquad \text{(B.1)}
\end{aligned}$$

2. A collection of χ_{ul} is then generated and each realization is scaled to satisfy the constraints. Only realizations that satisfy all the constraints are considered as candidates.

3. Among all candidates of χ_{ul} in Step 2, the one with minimum $\chi_{ul}^{H}\mathbf{D}_{ul}\chi_{ul}$ is chosen. This is a suboptimum solution.

Appendix C

Proof of the convergence of downlink iterative algorithm

Proof: It is clear that both the sum powers at the relays and the transmitter are larger than zero and lower bounded. It thus suffices to show that if the sum powers at the relays and transmitter are non-increasing, the iterative algorithm must converge. The DRBF vector at iteration k, denoted as $\mathbf{w}_{dl}^{k}$, is obtained from (3.20) with fixed linear precoder vectors for the $(k-1)$th iteration, denoted as $\mathbf{t}_{dl,1}^{k-1}, \mathbf{t}_{dl,2}^{k-1}, \ldots, \mathbf{t}_{dl,M_{dl}}^{k-1}$. So the following constraints are satisfied:

$$(\mathbf{w}_{dl}^{k})^{H}\left(\mathbf{E}_{dl,j}^{k-1}-\gamma_{dl,j}\mathbf{F}_{dl,j}^{k-1}\right)(\mathbf{w}_{dl})^{k} \geq \gamma_{dl,j}\sigma_{dl,n}^{2} \qquad \text{for} \quad j=1,2,\ldots,M_{dl} \tag{C.1}$$

where

$$\begin{aligned}\mathbf{E}_{dl,j}^{k-1} &= \mathrm{diag}(\mathbf{g}_{dl,k}^{T})\mathbf{H}_{dl}\mathbf{t}_{dl,j}^{k-1}(\mathbf{t}_{dl,j}^{k-1})^{H}\mathbf{H}_{dl}^{H}\mathrm{diag}(\mathbf{g}_{dl,k}^{*}) \\ \mathbf{F}_{dl,j}^{k-1} &= \mathrm{diag}(\mathbf{g}_{dl,k}^{T})\left(\mathbf{H}_{dl}(\sum_{j=1,j\neq k}^{M_{dl}}\mathbf{t}_{dl,j}^{k-1}(\mathbf{t}_{dl,j}^{k-1})^{H})\mathbf{H}_{dl}^{H}+\sigma_{dl,v}^{2}\mathbf{I}\right)\mathrm{diag}(\mathbf{g}_{dl,k}^{*}).\end{aligned} \tag{C.2}$$

Eq. (C.1) can be rewritten as

$$\frac{(\mathbf{t}_{dl,j}^{k-1})^{H}\mathbf{H}_{dl}^{H}\mathbf{W}_{dl}^{k}\mathbf{g}_{dl,i}^{*}\mathbf{g}_{dl,i}^{T}(\mathbf{W}_{dl}^{k})^{H}\mathbf{H}_{dl}\mathbf{t}_{dl,j}^{k-1}}{\sum_{i=1,i\neq j}^{M_{dl}}(\mathbf{t}_{dl,j}^{k-1})^{H}\mathbf{H}_{dl}^{H}\mathbf{W}_{dl}^{k}\mathbf{g}_{dl,i}^{*}\mathbf{g}_{dl,i}^{T}(\mathbf{W}_{dl}^{k})^{H}\mathbf{H}_{dl}\mathbf{t}_{dl,j}^{k-1}+P_{dl,n}^{j}}$$

$$\geq \gamma_{dl,j} \quad \text{for} \quad j = 1,2,\ldots,M_{dl}. \tag{C.3}$$

With fixed DRBF, $\mathbf{w}_{dl}^k$, optimum precoders $\mathbf{t}_{dl,1}^k, \mathbf{t}_{dl,2}^k, \ldots, \mathbf{t}_{dl,M_{dl}}^k$ satisfy

$$\frac{(\mathbf{t}_{dl,j}^k)^H \mathbf{H}_{dl}^H \mathbf{W}_{dl}^k \mathbf{g}_{dl,i}^* \mathbf{g}_{dl,i}^T (\mathbf{W}_{dl}^k)^H \mathbf{H}_{dl} \mathbf{t}_{dl,j}^k}{\sum_{i=1,i\neq j}^{M_{dl}} (\mathbf{t}_{dl,j}^k)^H \mathbf{H}_{dl}^H \mathbf{W}_{dl}^k \mathbf{g}_{dl,i}^* \mathbf{g}_{dl,i}^T (\mathbf{W}_{dl}^k)^H \mathbf{H}_{dl} \mathbf{t}_{dl,j}^k + P_{dl,n}^j}$$

$$\geq \gamma_{dl,j} \quad \text{for} \quad j = 1,2,\ldots,M_{dl} \text{ and} \tag{C.4}$$

$$\sum_{j=1}^{M_{dl}} (\mathbf{t}_{dl,j}^k)^H \mathbf{t}_{dl,j}^k \leq \sum_{j=1}^{M_{dl}} (\mathbf{t}_{dl,j}^{k-1})^H \mathbf{t}_{dl,j}^{k-1}, \tag{C.5}$$

i.e., the sum transmission power at the precoder is non-increasing.

Similarly, consider fixed precoders $\mathbf{t}_{dl,1}^k, \mathbf{t}_{dl,2}^k, \ldots, \mathbf{t}_{dl,M_{dl}}^k$, under DRBF optimization. The resulting $\mathbf{w}_{dl}^{k+1}$ satisfies

$$(\mathbf{w}_{dl}^{k+1})^H \left(\mathbf{E}_{dl,j}^k - \gamma_{dl,j} \mathbf{F}_{dl,j}^k \right) (\mathbf{w}_{dl})^{k+1} \geq \gamma_{dl,j} \sigma_{dl,n}^2 \tag{C.6}$$

$$\text{for} \quad j = 1,2,\ldots,M_{dl}, \text{ and}$$

$$(\mathbf{w}_{dl}^{k+1})^H \mathbf{D}_{dl} \mathbf{w}_{dl}^{k+1} \leq (\mathbf{w}_{dl}^k)^H \mathbf{D}_{dl} \mathbf{w}_{dl}^k. \tag{C.7}$$

Thus, the sum transmission power at the relays decreases or remains the same. From the above, we observe that since both the sum power at the transmitter and relays are non-increasing functions lower-bounded by a positive value, the iterative algorithm converges.

End of proof.

Appendix D

Derivation of the asymptotic upper bound of the achievable SINR at the kth user:

Proof: Assuming $\det(\mathbf{W}) \gg 0$, (4.11) can be simplified as

$$\mathrm{SINR}_{ul,k} = \frac{\mathbf{b}_k^T \left(P_k \mathbf{J}\mathbf{W}_{ul}^H \mathbf{f}_{ul,k}^* \mathbf{f}_{ul,k}^T \mathbf{W}_{ul} \mathbf{J}^H \right) \mathbf{b}_k^*}{\mathbf{b}_k^T \left(\mathbf{J}\mathbf{W}^H (\sum_{j=1,j\neq k}^{M_{ul}} P_j \mathbf{f}_{ul,j}^* \mathbf{f}_{ul,j}^T \mathbf{W}_{ul} \mathbf{J}^H + \sigma_{ul,v}^2 \mathbf{J}\mathbf{W}_{ul}^H \mathbf{W}_{ul} \mathbf{J}^H \right) \mathbf{b}_k^*}. \tag{D.1}$$

Denote $\mathbf{q}_{ul,k} = \mathbf{W}\mathbf{J}^H \mathbf{b}_k^*$, (D.1) can be rewritten as

$$\mathrm{SINR}_{\mathbf{q}_k} = \frac{P_k \mathbf{q}_{ul,k}^H \mathbf{f}_{ul,k}^* \mathbf{f}_{ul,k}^T \mathbf{q}_{ul,k}}{\mathbf{q}_{ul,k}^H \left(\sum_{j=1,j\neq k}^{M_{ul}} P_j \mathbf{f}_{ul,j}^* \mathbf{f}_{ul,j}^T + \sigma_{n,v}^2 \right) \mathbf{q}_{ul,k}}. \tag{D.2}$$

So the upper bound of the SINR for the kth source is $\lambda_{max} \left(P_k \mathbf{f}_{ul,k}^* \mathbf{f}_{ul,k}^T, \sum_{j=1,j\neq k}^{M_{ul}} P_j \mathbf{f}_{ul,j}^* \mathbf{f}_{ul,j}^T + \sigma_{n,v}^2 \right)$.

Here we denote

$$\begin{aligned}
O_{ul,1} &= P_k \mathbf{f}_{ul,k}^* \mathbf{f}_{ul,k}^T, \qquad (D.3)\\
O_{ul,2} &= \sum_{j=1,j\neq k}^{M_{ul}} P_j \mathbf{f}_{ul,j}^* \mathbf{f}_{ul,j}^T + \sigma_v^2,\\
O_{ul,3} &= P_k \mathbf{J}\mathbf{W}^H \mathbf{f}_{ul,j}^* \mathbf{f}_{ul,j}^T \mathbf{W}\mathbf{J}^H,\\
O_{ul,4} &= \mathbf{J}\mathbf{W}_{ul}^H \Big(\sum_{j=1,j\neq k}^{M_{ul}} P_j \mathbf{f}_{ul,j}^* \mathbf{f}_{ul,j}^T \Big) \mathbf{W}_{ul} \mathbf{J}^H + \sigma_{ul,v}^2 \mathbf{J}\mathbf{W}_{ul}^H \mathbf{W}_{ul} \mathbf{J}^H.
\end{aligned}$$

As in Chapter 4 we denote the number of relays as n_R^{ul} and the number of receive antennas at the base station as N_{ul}. If $N_{ul} = n_R^{ul}$, assuming $\mathbf{W}_{ul}\mathbf{J}^H$ is full rank, then $\mathbf{W}_{ul}\mathbf{J}^H$ is a square matrix, and

there is a unique $\mathbf{b}_k$ which satisfies $\mathbf{q}_{ul,k} = \mathbf{W}_{ul}\mathbf{J}^H\mathbf{b}_k^*$. So in this case the upper bound SINR of user k is $\lambda_{max}(O_{ul,1}, O_{ul,2})$.

If $N_{ul} > n_R^{ul}$, assuming $\mathbf{W}_{ul}\mathbf{J}^H$ is full rank, then $\mathbf{W}_{ul}\mathbf{J}^H$ is a flat matrix, there are an infinite number of vectors $\mathbf{b}_k$ which satisfy $\mathbf{q}_{ul,k} = \mathbf{W}_{ul}\mathbf{J}^H\mathbf{b}_k^*$. Thus each generalized eigenvector of $(O_{ul,1}, O_{ul,2})$, there exists a vector $\mathbf{b}_k$ to achieve the same generalized eigenvalue, so the generalized eigenvalues of $(O_{ul,1}, O_{ul,2})$ form a subset of the generalized eigenvalues of $(O_{ul,3}, O_{ul,4})$. However, because the rank of both $O_{ul,3}$ and $O_{ul,4}$ are the same as the number of relays, the number of generalized eigenvalues should also be the same as the number of relays. This implies that the generalized eigenvalues of $(O_{ul,3}, O_{ul,4})$ are exactly the same as the generalized eigenvalues of $(O_{ul,1}, O_{ul,2})$, and therefore the SINR upper bound in this case is $\lambda_{max}(O_{ul,1}, O_{ul,2})$.

note: $\gg$ stands for far greater than.

End of proof.

Appendix E

Proof of the convergence of uplink iterative algorithm

It is known that, the sum power at the relays is larger than zero and lower bounded, so if we can prove that for each iteration, the sum powers at the relays decrease, then the iterative algorithm must converge.

At the kth iteration, the relay weights, denoted as $\mathbf{w}_{ul}^{k}$, are obtained through (4.20) with fixed linear decoder vectors and for the $(k-1)$th iteration are denoted as $\mathbf{f}_{ul,1}^{k-1}, \mathbf{f}_{ul,2}^{k-1}, \ldots, \mathbf{f}_{ul,M_{ul}}^{k-1}$. With fixed relay weights $\mathbf{w}_{ul}^{k}$, we can obtain the optimum decoders as $\mathbf{f}_{ul,1}^{k}, \mathbf{f}_{ul,2}^{k}, \ldots, \mathbf{f}_{ul,M_{ul}}^{k}$ through (4.12). Then we have

$$\gamma_{ul,j}^{k} = \mathrm{SINR}_{ul,j}(\mathbf{f}_{ul,j}^{k}, \mathbf{w}_{ul}^{k}) \geq \mathrm{SINR}_{ul,j}(\mathbf{f}_{ul,j}^{k-1}, \mathbf{w}_{ul}^{k}) = \gamma_{ul,j}^{k-1},$$

$$j = 1, \ldots, M_{ul},$$

where

$$\mathrm{SINR}_{ul,j}(\mathbf{f}_{ul,j}^{k}, \mathbf{w}_{ul}^{k}) = \frac{(\mathbf{f}_{ul,j}^{k})^{T}(P_k \mathbf{J}(\mathbf{W}_{ul}^{k})^{H}\mathbf{b}_k\mathbf{b}_k^{H}(\mathbf{W}_{ul}^{k})\mathbf{J}^{H})(\mathbf{f}_{ul,j}^{k})^{*}}{(\mathbf{f}_{ul,j}^{k})^{T}\mathbf{L}_{ul}^{k}(\mathbf{f}_{ul,j}^{k})^{*}}$$

$$\mathbf{L}_{ul}^{k} = \mathbf{J}(\mathbf{W}_{ul}^{k})^{H}\left(\sum_{j=1, j\neq k}^{M_{ul}} P_j \mathbf{b}_j\mathbf{b}_j^{H} + \sigma_{ul,v}^{2}\mathbf{I}\right)(\mathbf{W}_{ul}^{k})\mathbf{J}^{H} + \sigma_{ul,n}^{2}\mathbf{I}$$

$$\mathbf{W}_{ul}^{k} = \mathrm{diag}\{\mathbf{w}_{ul}^{k}\}. \tag{E.1}$$

On the other hand, according to (E.2), $\mathrm{SINR}_{ul,j}(\mathbf{f}_{ul,j}^k, \mathbf{w}_{ul}^k)$ can also be written as

$$\mathrm{SINR}_{ul,j}(\mathbf{f}_{ul,j}^k, \mathbf{w}_{ul}^k) = \frac{(\mathbf{w}_{ul}^k)^H \mathrm{diag}((\mathbf{f}_{ul,j}^k)^T \mathbf{J}) \left(P_k \mathbf{b}_k \mathbf{b}_k^H\right) \mathrm{diag}((\mathbf{f}_{ul,j}^k)^T \mathbf{J})^H \mathbf{w}_{ul}^k}{(\mathbf{w}_{ul}^k)^H \mathbf{M}_j^k \mathbf{w}_{ul}^k + \sigma_{ul,n}^2 (\mathbf{f}_{ul,j}^k)^T (\mathbf{f}_{ul,j}^k)^*}$$

$$j = 1, \ldots, M_{ul} \tag{E.2}$$

where

$$\mathbf{M}_j^k = \mathrm{diag}((\mathbf{f}_{ul,j}^k)^T \mathbf{J}) \left(\sum_{j=1, j\neq k}^{M_{ul}} P_j \mathbf{b}_j \mathbf{b}_j^H + \sigma_{ul,v}^2 \mathbf{I} \right) \mathrm{diag}((\mathbf{f}_{ul,j}^k)^T \mathbf{J})^H. \tag{E.3}$$

Denote

$$\beta_{ul}^k = \min \left(\frac{\gamma_{ul,1}^k}{\gamma_{ul,1}^{k-1}}, \ldots, \frac{\gamma_{ul,M_{ul}}^k}{\gamma_{ul,M_{ul}}^{k-1}} \right). \tag{E.4}$$

Combining (E.1) and (E.4), we have

$$\begin{aligned} &\frac{1}{\beta_{ul}^k} (\mathbf{w}_{ul}^k)^H \mathrm{diag}((\mathbf{f}_{ul,j}^k)^T \mathbf{J}) \left(P_k \mathbf{b}_k \mathbf{b}_k^H\right) \mathrm{diag}((\mathbf{f}_{ul,j}^k)^T \mathbf{J})^H \mathbf{w}_{ul}^k = \\ &\qquad \frac{\gamma_{ul,j}^k}{\beta_{ul}^k} (\mathbf{w}_{ul}^k)^H \mathbf{M}_j^k \mathbf{w}_{ul}^k + \frac{\gamma_{ul,j}^k}{\beta_{ul}^k} \sigma_{ul,n}^2 (\mathbf{f}_{ul,j}^k)^T (\mathbf{f}_{ul,j}^k)^* \geq \\ &\qquad \gamma_{ul,j}^{k-1} (\mathbf{w}_{ul}^k)^H \mathbf{M}_j^k \mathbf{w}_{ul}^k + \gamma_{ul,j}^{k-1} \sigma_{ul,n}^2 (\mathbf{f}_{ul,j}^k)^T (\mathbf{f}_{ul,j}^k)^* \end{aligned} \tag{E.5}$$

so the relay weight vector $\mathbf{w}_{ul}^{k+1} = \frac{1}{\sqrt{\beta_{ul}^k}} \mathbf{w}_{ul}^k$ satisfies all the SINR constraints and has lower power, which means in each iteration the power consumption reduces or is the same since $\beta_{ul}^k \geq 1$. As the power consumption is lower bounded by a positive value, the iterative algorithm must converge.

End of proof.

Appendix F

Derivation of Second Derivatives

As in (6.18),

$$f(z_1,\ldots,z_{N_{ul,ba}}) := \frac{1}{2}\sum_{j=1}^{N_{ul,ba}} \log\left(\left(\mathbf{D}_{ul,mu}\Sigma_{ul}\mathbf{D}_{ul,mu}^H\right)_{j,j}^{-1} + \frac{z_j}{\sigma_\varsigma^2(\mathbf{D}_{ul,mu}\mathbf{D}_{ul,mu}^H)_{j,j}z_j + \sigma_\vartheta^2}\right). \tag{F.1}$$

Define

$$\begin{aligned} a_j &= \left(\mathbf{D}_{ul,mu}\Sigma_{ul}\mathbf{D}_{ul,mu}^H\right)_{j,j}^{-1} \\ b_j &= \sigma_\varsigma^2(\mathbf{D}_{ul,mu}\mathbf{D}_{ul,mu}^H)_{j,j}. \end{aligned} \tag{F.2}$$

The first derivative of $f(z_1,\ldots,z_{N_{ul,ba}})$ in z_j is

$$\begin{aligned} \frac{\partial f(z_1,\ldots,z_{N_{ul,ba}})}{\partial z_j} &= \frac{\frac{\partial(a_j+\frac{z_j}{bz_j+\sigma_\vartheta^2})}{\partial z_j}}{a_j+\frac{z_j}{bz_j+\sigma_\vartheta^2}} \\ &= \frac{\sigma_\varsigma^2}{(b_jz_j+\sigma_\varsigma^2)\left((a_jb_j+1)z_j+a_j\sigma_\varsigma^2\right)}. \end{aligned} \tag{F.3}$$

The second derivatives are

$$\begin{aligned} \frac{\partial^2 f(z_1,\ldots,z_{N_{ul,ba}})}{\partial z_j\partial z_k} &= 0, \quad \forall\ j\neq k \\ \frac{\partial^2 f(z_1,\ldots,z_{N_{ul,ba}})}{\partial^2 z_j} &= -\frac{b_j\left((a_jb_j+1)z_j+a_j\sigma_\varsigma^2\right)+(a_jb_j+1)(b_jz_j+\sigma_\varsigma^2)}{(b_jz_j+\sigma_\varsigma^2)^2\left((a_jb_j+1)z_j+a_j\sigma_\varsigma^2\right)^2}. \end{aligned} \tag{F.4}$$

Because $a_j \geq 0, b_j \geq 0, j = 1 \ldots, N_{ul,ba}$ and $\sigma_\xi^2 > 0$, $\frac{\partial^2 f(z_1,\ldots,z_{N_{ul,ba}})}{\partial^2 z_j} < 0, \ \forall j = 1, \ldots, N_{ul,ba}$. Hence the Hessian matrix of $f(z_1, \ldots, z_{N_{ul,ba}})$ is negative definite.